University of Padua PhD Courses Medical and Biomedical Sciences



UNIVERSITÀ DEGLI STUDI DI PADOVA

### PhD STUDENT RESEARCH PROJECT DAY MEDICAL AND BIOMEDICAL SCIENCES (XXXVII Cycle)

Thursday, September 7, 2023

Old University Aula Magna - Archivio Antico Palazzo del Bo Via 8 Febbraio, 2 - 35122 Padova

Organized by: **Alessandra Cervellin** Department of Cardiac Thoracic Vascular Sciences And Public Health Tel 049/8272288 – Fax 049/8272294 e-mail: <u>alessandra.cervellin@unipd.it</u>

> A.R.C.A. Associazione Ricerche Cardiopatie Aritmiche Via A. Gabelli, 86 35121 Padova sito web: http://www.arca-cuore.it/



#### INDEX

# PHD COURSEpage7"ARTERIAL HYPERTENSION AND VASCULAR BIOLOGY"page7KOHLSCHEEN Evapage9PINTUS Giovannipage10

#### PHD COURSE "BIOMEDICAL SCIENCE"

|                   | page | 11 |
|-------------------|------|----|
| FIETTA Anna       | page | 13 |
| FRIGO Elena       | page | 14 |
| GIACCHIN Giacomo  | page | 15 |
| MORBIDELLI Maria  | page | 16 |
| MORO Nicola       | page | 17 |
| TOMMASIN Ludovica | page | 18 |
|                   |      |    |

#### PHD COURSE "CLINICAL AND EXPERIMENTAL ONCOLOGY AND IMMUNOLOGY"

|                              | page | 19 |
|------------------------------|------|----|
| CASARIN Martina              | page | 21 |
| D'ACCARDIO Giulia            | page | 22 |
| DEBIASI Giulia               | page | 23 |
| GENOVA Beatrice              | page | 24 |
| JAFARNEZHAD ANSARIHA Fahimeh | page | 25 |
| MADDALENA Giulia             | page | 26 |
| MARANGIO Asia                | page | 27 |
| PADOVAN Marta                | page | 28 |
| SACCHI Diana                 | page | 29 |

#### PhD COURSE "CLINICAL AND EXPERIMENTAL SCIENCES"

| > Curriculum: CLINICAL METHODOLOGY, METABOLISM, ENDOCRINOLO |                         |      | Υ, |
|-------------------------------------------------------------|-------------------------|------|----|
|                                                             | NEPHROLOGY AND EXERCISE | page | 31 |
|                                                             | BORTOLETTO Alessandro   | page | 33 |
|                                                             | FAGGIAN Sara            | page | 34 |
|                                                             | LIEVORE Nicole          | page | 35 |
|                                                             | QUINTO Giulia           | page | 36 |
|                                                             | VECCHIATO Marco         | page | 37 |

| $\triangleright$ | <i>Curriculum: HEMATOLOGICAL AND GERIATRIC SCIEN</i><br>TONIAZZO Silvia | <b>CES</b><br>page | page  | <b>39</b><br>41 |
|------------------|-------------------------------------------------------------------------|--------------------|-------|-----------------|
| $\triangleright$ | Curriculum: HEPATOLOGY AND TRANSPLANTATION SC                           | IENCE              | 5     |                 |
|                  |                                                                         |                    | page  | 43              |
|                  | MANGINI Chiara                                                          | page               |       | 45              |
| $\triangleright$ | Curriculum: MULTIDISCIPLINARY APPROACH TO RAR                           | RE DIS             | EASES |                 |
|                  |                                                                         |                    | page  | 47              |
|                  | ARCIDIACONO Gaetano Paride                                              | page               |       | 49              |
|                  | CECCATO Jessica                                                         | page               |       | 50              |
| $\triangleright$ | <b>Curriculum:</b> RHEUMATOLOGICAL AND LABORATORY S                     |                    | CES   |                 |
|                  |                                                                         |                    | page  | 51              |
|                  | GASPAROTTO Michela                                                      | page               |       | 53              |

#### PhD COURSE "DEVELOPMENTAL MEDICINE AND HEALTH PLANNING SCIENCES"

| $\triangleright$ | Curriculum: ONCOHEMATOLOGY, MEDICAL GENETICS, | RARE | DISEASES / | 4 <i>ND</i> |
|------------------|-----------------------------------------------|------|------------|-------------|
|                  | PREDICTIVE MEDICINE                           |      | page       | 55          |
|                  | BRIGADOI Giulia                               | page |            | 57          |
|                  | BUCCIARELLI Linda                             | page |            | 58          |
|                  | DUCI Miriam                                   | page |            | 59          |
|                  | FAVARO Jacopo                                 | page |            | 60          |
|                  | FICHERA Giulia                                | page |            | 61          |
|                  | FUMANELLI Jennifer                            | page |            | 62          |
|                  | GUIDUCCI Silvia                               | page |            | 63          |
|                  | LONGO Giorgia                                 | page |            | 64          |
|                  | MANFREDA Lorenzo                              | page |            | 65          |
|                  | MARCHIORO Chiara                              | page |            | 66          |
|                  | MENEGHELLI Marta                              | page |            | 67          |
|                  | REGGIANI Giulia                               | page |            | 68          |
|                  | ROSSI Bartolomeo                              | page |            | 69          |
|                  | SARTORI Anna                                  | page |            | 70          |
|                  | TACCHETTO Elena                               | page |            | 71          |
|                  | TOSATO Anna                                   | page |            | 72          |
|                  | VALENTINO Agata                               | page |            | 73          |
| ~                |                                               |      |            |             |
|                  | Curriculum: HEALTH PLANNING SCIENCES          | -    | page       | 75          |
|                  | CATTAPAN Irene                                | page |            | 77          |
|                  | GUTIERREZ DE RUBALCAVA DOBLAS Joaquin         | page |            | 78          |

#### PhD COURSE "MOLECULAR MEDICINE"

| > Curriculum: BIOMEDICINE | page | 79 |
|---------------------------|------|----|
| BADO Martina              | page | 81 |
| DAL MOLIN Emanuela        | page | 82 |
| DONATO Alice Cristina     | page | 83 |
| ISPANO Emilio             | page | 84 |
| RUBIN Michela             | page | 85 |
| TANCREDI Giuditta         | page | 86 |
| TERRERI Marianna          | page | 87 |
| VICCO Anna                | page | 88 |
| ZATTA Veronica            | page | 89 |

| Curriculum: REC | GENERATIVE MEDICINE | page | 91 |
|-----------------|---------------------|------|----|
| RUSSO Loris     |                     | page | 93 |
| SAYAF Katia     |                     | page | 94 |
| SULI Ambela     |                     | page | 95 |

#### PhD COURSE "PHARMACOLOGICAL SCIENCES"

| > Curriculum: PHARMACOLOGY, TOXICOLOGY AN | D THERAPY pag | e 97 |
|-------------------------------------------|---------------|------|
| CAMPARA Benedetta                         | page          | 99   |
| FERRARESE Irene                           | page          | 100  |
| HAZIZAJ Enidia                            | page          | 101  |
| LINASSI Federico                          | page          | 102  |

#### PhD COURSE "TRANSLATIONAL SPECIALISTIC MEDICINE G.B. MORGAGNI"

| <i>Curriculum: BIOSTATISTICS AND CLINIC EPIDEMIOLO</i><br>AHSANI-NASAB Sara<br>BATZELLA Erich<br>SALARIS Silvano<br>URRU Sara                        | page<br>page<br>page<br>page<br>page | page | <b>103</b><br>105<br>106<br>107<br>108        |
|------------------------------------------------------------------------------------------------------------------------------------------------------|--------------------------------------|------|-----------------------------------------------|
| <i>Curriculum: CARDIOVASCULAR SCIENCES</i><br>BARISON Ilaria<br>BECK DE LOTTO Michael Allen<br>BERNAVA Giacomo<br>CIBIN Giorgia<br>DE GASPARI Monica | page<br>page<br>page<br>page<br>page | page | <b>109</b><br>111<br>112<br>113<br>114<br>115 |

| Curriculum: CLINICAL AND TRANSLATIONAL NEUROSCIENCES page<br>GORGOGLIONE Domenico page |      |      | <b>117</b><br>119 |
|----------------------------------------------------------------------------------------|------|------|-------------------|
| <i>Curriculum: ENDOCRINE AND METABOLIC SCIENCES</i><br>RODELLA Anna                    | page | page | <b>121</b><br>123 |
| <i>Curriculum: THORACIC AND PULMONARY SCIENCES</i><br>CASARA Alvise                    | page | page | <b>125</b><br>127 |

### **AUTHOR'S INDEX**

page 129



University of Padua PhD Courses Medical and Biomedical Sciences

## PhD COURSE "ARTERIAL HYPERTENSION AND VASCULAR BIOLOGY" COORDINATOR: PROF. GIAN PAOLO ROSSI

#### DOES ALDOSTERONE DIRECTLY INDUCE CHANGES IN TONEBP EXPRESSION?

Ph.D. Student: Dr. Eva KOHLSCHEEN TUTOR: Prof. Gian Paolo ROSSI – CO-TUTOR: Prof. Teresa SECCIA Ph.D. Course "Arterial Hypertension and Vascular Biology

#### Background

Mononuclear phagocyte system (MPS) cells are recruited to the skin, sense the hypertonic electrolyte accumulation in skin, and activate the tonicity-responsive enhancer-binding protein (TONEBP, also known as NFAT5) to initiate expression and secretion of VEGFC, which enhances electrolyte clearance via cutaneous lymph vessels and increases eNOS expression in blood vessels. It is unclear whether this local MPS response to osmotic stress is important to systemic blood pressure control. The skin contains a hypertonic interstitial fluid compartment in which MPS cells exert homeostatic and blood pressure-regulatory control by local organization of interstitial electrolyte clearance via TONEBP and VEGFC/VEGFR3-mediated modification of cutaneous lymphatic capillary function. Previously, we measured *NFAT5* gene expression in the skin biopsies obtained by APA patients or controls (CTR), founding that *NFAT5* is expressed at higher levels in APA patients skin compared to control.

#### **Material and Methods**

Patients who will undergo abdominal surgery will be recruited (Abdominoplasty). This approach is chosen to limit possible biases given by a different anatomical area of the biopsy.

These patients should have been at a stable weight for approximately one year with a non-obesity BMI. Besides the routine laboratory tests further biochemical analysis will be performed : 24h urine collector, for the measurement of urinary sodium, potassium, creatinine, urea, osmolality, and microalbuminuria. Skin biopsies, containing both epidermal and dermal tissue, will be obtained in the abdominal region, using a disposable sterile biopsy Punch.

Whole skin biopsies will be divided in smaller pieces and cultured in vitro.

#### Results

TonEBP is a central regulator of macrophages, which are involved in both innate and adaptive immunity against infections caused by bacteria and other pathogens.

We want to isolate primary monocytes from buffycoat and stimulated with GM-CSF for 7days.M1 macrophages will be stimulated with Aldosterone alone of after pre-treatment with the MRA Canrenone for 12 h - 24 h to evaluate *NFAT5* gene expression via ddPCR.

As preliminary data, we aim to stimulate with Aldosterone, analyzing 4 different time points (12h - 24h - 48h - 72h) for *NFAT5* expression.

#### Conclusions

Our previous study results suggest that aldosteronism is associated with a prominent increase in the skin expression of the TonEBP, causing enhanced lymphoangiogenesis and tissue Na+, and water drainage. We want therefore determinate that Aldosterone directly induces changes in TonEBP expression through Mononuclear phagocyte system.

#### FEASIBILITY OF PRIMARY ALDOSTERONISM SUBTYPING BY ADRENAL VEIN SAMPLING DURING MINERALOCORTICOID RECEPTOR ANTAGONISTS TREATMENT

#### Ph.D. Student: Dr. Giovanni PINTUS TUTOR: Prof. Gian Paolo ROSSI – CO-TUTOR: Prof. Teresa SECCIA Ph.D. Course "Arterial Hypertension and Vascular Biology

#### Background

Guidelines suggest withdrawal of mineralocorticoid receptor antagonists (MRAs) before subtyping primary aldosteronism (PA) by adrenal venous sampling (AVS) to avoid minimization of the Lateralization Index (LI), but this practice can cause severe hypokalemia and/or uncontrolled blood pressure. The objective of this study is to investigate the feasibility of performing AVS in patients undergoing MRA treatment.

#### **Material and Methods**

We analyzed two large databases of patients who underwent AVS from 2000 to 2022. After exclusion of patients on renin-angiotensin-aldosterone system interfering drugs, the rate of unilateral PA (uPA) identification between patients submitted to AVS with and without MRA treatment was compared. Differences in the AVS indexes used to identify uPA (Relative Aldosterone Secretion Index RASI, Contralateral Suppression Index CSLI, LI) between the two groups were also analyzed.

#### Results

At baseline total daily drug dose, rate of adrenalectomies and imaging positive for nodules were higher in the MRA group (p < 0.001, p 0.003, p 0.024, respectively), thus reflecting a more florid PA phenotype in these patients. No significant differences in direct renin concentration, plasma aldosterone levels, systolic and diastolic blood pressure were found. The ROC curves did not differ significantly groups (at baseline: AUROC 0.885 vs 0.950, p 0.311; after cosyntropin: AUROC 0.914 vs 0.941, p 0.716). No significant differences in the AVS indexes at baseline were observed.

#### Conclusions

Administration of MRAs at doses that controlled blood pressure and potassium levels, in florid PA phenotype patients, did not preclude diagnosis of uPA.



University of Padua PhD Courses Medical and Biomedical Sciences

### PhD COURSE "BIOMEDICAL SCIENCE" COORDINATOR: PROF. FABIO DI LISA

#### BONE MARROW ON A CHIP AND ZEBRAFISH EMBRYO AS TOOLS TO STUDY THE ROLE OF HYPOXIC EXTRACELLULAR VESICLES IN NEUROBLASTOMA METASTATIC DISSEMINATION

#### Ph.D. Student: Dr. Anna FIETTA TUTOR: Prof. Elisa CIMETTA – CO-TUTOR: Prof. Barbara MOLON Ph.D. Course Biomedical Sciences

#### Background

Neuroblastoma (NB) is a pediatric solid tumor of neural crest origin in which bone marrow (BM) is one of the main metastatic sites. Extracellular vesicles (EVs), a heterogeneous family of vesicles released into the extracellular space, have lately emerged as potential mediators of the premetastatic niche formation. The zebrafish is a valuable model organism for studying human malignancies and EVs intravascular injection within it allows a non-invasive visualization of their dispersion, uptake, and interactions with host cells. Organs-on-chips (OOCs) instead, are systems containing engineered or natural miniature tissues grown inside microfluidic chips that mimic human physiology and diseases and allow the study of cells interactions in a *in vivo*-like system.

#### **Material and Methods**

To study the effects of hypoxic NB-derived EVs on the metastatic process, we cultured NB cells at  $37^{\circ}$ C with 5% CO<sub>2</sub> and 1.5% O<sub>2</sub> and isolated the EVs from conditioned media by ultrafiltration. For the zebrafish studies, we used the *Casper* strain and three transgenic lines: *Tg(fli1:EGFP)*, *Tg(mpeg1:mCherry)* and the *Tg(gata1:dsRed)*. We injected labeled EVs in the zebrafish embryo at 48 hours post fertilization and studied the interactions between exogenous EVs and host cells via confocal imaging. For the OOC studies we created a bone marrow on a chip composed by (i) a lower polydimethylsiloxane (PDMS) 6-chambers layer where we seeded BM cells derived from patients, (ii) a porous 5µm membrane and (iii) an upper PDMS layer housing the endothelial cells monolayer and NB-derived EVs and NB cells in perfusion.

#### Results

We demonstrated that the injection of hypoxic NB-derived EVs in the zebrafish embryos induced changes in the recipient cells by increasing angiogenesis and macrophages recruitment; qPCR analyses also proved that EVs affected the expression of *mmp-9* and *cxcl8b*. Furthermore, we demonstrated that the pre-conditioning with hypoxic EVs of the caudal hematopoietic tissues, as a potential metastatic site, promoted the proliferation of NB cells. By creating a bone marrow on a chip stable up to three days, we showed for the first time the possibility to seed and culture patient-specific BM aspirates on chip. To mimic the *in vivo* endothelial barrier, we created a cell monolayer composed by microvascular endothelial cells isolated from patients' skin. Furthermore, we demonstrated that the perfusion of hypoxic EVs inhibited the ability of perfused-NB cells to invade the BM chambers and increased the release of IL-6.

#### Conclusions

Our data demonstrate that hypoxic EVs promote the proliferation of NB cells and modify the behavior of recipient cells in the zebrafish embryo. Furthermore, we developed a bone marrow on a chip that replicates the *in vivo* metastatic process thanks to the interactions between NB cells, their derived hypoxic EVs, endothelial cells and patients-derived BM cells.

#### EXPLORING THE FUNCTIONS OF ATP SYNTHASE DIMERIZATION SUBUNITS e AND g THROUGH GENETIC MANIPULATION OF Drosophila melanogaster

Ph.D. Student: Dr. Elena FRIGO TUTOR: Prof. Paolo BERNARDI – CO-TUTOR: Dr. Michele BRISCHIGLIARO Ph.D. Course Biomedical Sciences

#### Background

The permeability transition pore (PTP) is a  $Ca^{2+}$ -activated, unselective channel that induces an increase in the permeability of the inner mitochondrial membrane to ions and solutes up to 1.5 kDa. This channel is involved in both physiological  $Ca^{2+}$  homeostasis and cell death. The molecular identity of the PTP is still not completely elucidated, but the ATP synthase is one of the key candidates, as it mediates the permeability transition in mammals and yeast. Concerning *Drosophila melanogaster*, the PTP appears to operate as a selective  $Ca^{2+}$ -activated  $Ca^{2+}$ -release pathway, which does not allow K<sup>+</sup> diffusion and matrix swelling, a typical feature of cell death induction. Like in mammals and yeast, also *Drosophila* ATP synthase dimers can generate  $Ca^{2+}$ -activated channels which, at variance from the nS conductance of the former species, have a conductance of 53 pS, indicating a much smaller channel size. Recently, it has been shown that the ablation of the so-called 'dimerization subunits' e and g of ATP synthase impairs PTP formation in yeast and mammalian cells. The role that these two subunits can have *in vivo* and how they relate to PTP formation and function in a multicellular organism has not been studied yet.

#### **Material and Methods**

Fruit fly ubiquitous knock-down (KD) individuals for subunits e and g were generated exploiting the yeast-derived binary system *GAL4/UAS*. Initially, we evaluated the silencing efficiency of the *GAL4/UAS* system through real-time PCR. To biochemically characterize these models, we performed BN-PAGEs in isolated mitochondria, to assess the oligomerization state of ATP synthase and the relative abundance of the different multimeric forms. Mitochondrial respiration was evaluated in total tissue homogenates, which were also used to carry out ATP measurements through a luciferase assay. Lastly,  $Ca^{2+}$  retention capacity (CRC) experiments were performed in isolated the Ca<sup>2+</sup> dependence of *Drosophila* channel opening.

#### Results

Ubiquitous downregulation of subunit e or g (about 80% and 60%, respectively) leads to a dramatic arrest in fly development at larval stage, impairs the dimerization and oligomerization states of ATP synthase (as revealed by BN-PAGE experiments) and decreases mitochondrial respiration, yet the total amount of tissue ATP is unaltered. Strikingly, the CRC is increased in both subunit e and subunit g KD mitochondria (about 1.5-fold and 3-fold, respectively), indicating that the channel is less sensitive to  $Ca^{2+}$ .

#### Conclusions

Our results suggest that the arrest in development of ubiquitously knocked-down flies is not entirely due to bioenergetic defects, but may also arise from PTP-related, dysregulated  $Ca^{2+}$  homeostasis, in line with previous studies demonstrating that also in *Drosophila* ATP synthase has other functions besides ATP production. Considering  $Ca^{2+}$  homeostasis, it is already known that PTP flickering is important for synaptic transmission *in vivo* in a mouse model of spastic paraplegia. Moreover, in *Drosophila* it was demonstrated that the release of ecdysone, a steroid hormone necessary to trigger metamorphosis, *i.e.* the transition from larvae to pupae, occurs through  $Ca^{2+}$ -dependent exocytosis, highlighting the importance of  $Ca^{2+}$  dynamics during fly development.

#### A HIGH-CONTENT IN VITRO SCREENING TO IDENTIFY NEW MITOPHAGY-ACTIVATING COMPOUNDS

#### Ph.D. Student: Dr. Giacomo GIACCHIN TUTOR: Prof. Carlo Fiore VISCOMI Ph.D. Course Biomedical Sciences

#### Background

Mitochondrial diseases (MD) are a group of clinically heterogeneous and untreatable hereditary disorders caused by faulty oxidative phosphorylation (OXPHOS), a process carried out by five enzymatic complexes (cI-V) of the inner mitochondrial membrane.

The aim of my project is to explore the possibility of exploiting mitophagy, the cellular process responsible for the selective degradation of dysfunctional mitochondria, to improve mitochondrial myopathies. My goal is to identify new mitophagy-inducing compounds, whose mechanism of action is mediated by the activation of Transcription Factor EB (TFEB), the main transcription factor involved in autophagy and lysosomal biogenesis. Therefore, I carried out a two-step screening of an FDA-approved drug library to identify compounds able to induce (i) the translocation to the nucleus of TFEB, and (ii) the activation of mitophagy.

#### **Material and Methods**

I isolated and immortalized mouse adult fibroblasts (MAFs) from wild-type animals and infected them with a lentiviral vector expressing a tagged TFEB-GFP protein. TFEB-GFP overexpressing MAFs were treated with a library of 1971 FDA-approved drugs (DiscoverProbe<sup>TM</sup> FDA-approved Drug Library, ApexBio). Each compound was tested in quadruplicate at 125nM for 24 hours. Cells were then fixed and imaging was performed using the Operetta CLS High-Content Analysis System (PerkinElmer). An automated and unbiased quantification of GFP-positive nuclei was performed by the Harmony High-Content Analysis Software (PerkinElmer).

The "lead" compounds were screened in wildtype MAFs expressing the MitoQC (MQC) transgene, which encodes a pH-sensitive fluorescent reporter based on the expression of the mCherry-GFP proteins, allowing the evaluation of mitochondrial architecture and mitophagic flux. Each compound was tested at three different concentrations, chosen according to the cell survival observed during the primary screening. An automated quantification protocol was employed to measure (i) mitolysosome number per cell and (ii) mitochondrial morphology.

#### Results

TFEB-GFP overexpressing cells were validated by treatment with known mitophagy inducers. Among the tested drugs, Torin 1 caused the highest rate of TFEB translocation in the nucleus (89% vs 14% in DMSO-treated cells). In addition, MQC-expressing MAFs showed a strong activation of mitophagy upon Torin 1 administration (up to 3 times more mitolysosomes than DMSO-treated cells). Thus, Torin 1 was chosen as positive control in the following screening experiments.

The primary screening identified 294 putative TFEB activators, that were grouped into three classes based on cell survival; drugs with a low survival rate were excluded from further analyses. The remaining 147 drugs were selected for the secondary screening to assess mitophagy induction on MQC-expressing immortalized MAFs. MQC quantification identified 8 drugs causing a significant increase in mitophagy, but no significant fragmentation of the mitochondrial network.

#### Conclusions

My two-step high-throughput screening identified 8 compounds, which induced the translocation of TFEB and the induction of mitophagy without toxic effects on mitochondria. These compounds will be validated in cellular and animal models of MD for their capacity to improve OXPHOS defects through mitophagy activation.

### THE IMPORTANCE OF NANOPARTICLE COATING STRUCTURAL DESIGN IN THE DEVELOPMENT OF NANOVACCINES

Ph.D. Student: Dr. Maria MORBIDELLI TUTOR: Prof. Emanuele PAPINI– CO-TUTOR: Prof. Regina TAVANO Ph.D. Course Biomedical Sciences

#### Background

Homogeneity/dis-homogeneity of the nanoparticle surface may deeply influence the formation of the protein corona, defined by serum proteins that recognize and bind the surface of a nanoparticle. Innate immunity may intercept nanoparticles whose coating mimic Pathogen Associated Molecular Patterns (PAMP) or Damage Associated Molecular Patterns (DAMP), leading to Antigen Presenting Cells (APC) targeting. Knowing this, we decided to characterize the effect of different types of -COOH or -OH terminated polyetilenglycol (PEG) coatings, that differ in length and charge, with the aim of finding candidates for the design of an anti-cancer nanovaccine.

#### **Material and Methods**

The safety and biocompatibility of nanoparticles were tested through cytotoxicity and coagulation assay. Biochemical techniques, proteomic approaches and cell capture experiments using primary derived human and mouse macrophages and dendritic cells were used to characterize these nanosystems. Induced coupled plasma mass spectrometry (ICP-MS) was used to measure the amount of gold inside each cell and also to perform biodistribution studies. The induced activation of dendritic cells and splenocytes and the antibody titer were tested with FACS and ELISA. *In vivo* studies were performed in the CIC bioGUNE (Bilbao, ES) animal facility.

#### Results

We found an impressive difference in the protein corona composition of these systems: the differential presence of opsonins, like Platelet Factor 4 (PF4) and Serum Amyloid P (SAP) and complement cascade proteins translates in a different recognition and uptake by phagocytic cells. Since the nanoparticle coated with the shorter PEG and all negatively charged (100EG) showed the best behavior in terms of uptake and immune recognition, we decided to functionalize it with cancer MUC1 peptide, generating a potential therapeutic anti-cancer nanovaccine. This nanosystem was tested in comparison with the nanoparticle coated with the 100PEG (longer PEG and negatively charged) conjugated with cancer MUC1. Cell capture experiments and proteomic characterization of the protein corona revealed that the addition of the peptide to the coatings modifies the protein corona composition, inducing a reduction in the capture by phagocytic cells *in vitro*. Nonetheless, we decided to move *in vivo*. To test the antibody production induced, an immunization campaign using C57BL/6 female mice was performed; we found that he 100EG nanovaccine induces a lower antibody titer compared to the 100PEG based nanovaccine.

#### Conclusions

According to what observed *in vitro*, the 100EG nanovaccine induces a lower antibody titer compared to the positive control. For this reason, we plan to change the core of the nanovaccine to add the MUC1 peptide inside the nanosystem. In this way we intent to preserve the surface properties of the 100EG nanoparticle, and therefore the preferable uptake, to induce an augmentation in the antibody titers against MUC1.

#### MUSCLE RING fiNGER-1 IS REQUIRED TO PREVENT AGE-RELATED MYOCARDIAL HYPERTROPHY AND INTERSTITIAL REMODELLING

#### Ph.D. Student: Nicola MORO TUTOR: Prof. Marco MONGILLO – CO-TUTOR: Prof. Tania ZAGLIA Ph.D. Course Biomedical Sciences

#### Background

The Ubiquitin Proteasome System (UPS) is a selective degradation system mediating the removal of intracellular unfolded/misfolded proteins and is essential for cardiomyocyte (CM) health. Substrate specificity and ubiquitination rate are mediated by E3 ubiquitin-ligases, i.e. Atrogin1 and MuRF1, which are specifically expressed in muscle cells. Perturbation of protein quality control leads to CM proteotoxicity. UPS dysfunction occurs in ageing, a risk factor for cardiac hypertrophy and HF. We have demonstrated that Atrogin-1 is essential to maintain CM health during ageing. Whether MuRF1 plays similar roles in heart adaptation to ageing is still debated and is the object of this study.

#### **Material and Methods**

To assess the role of MuRF1 in heart homeostasis, we combined echocardiography, histology, IF, TUNEL assay and EM on heart sections from MuRF1 knock-out (KO) mice, and littermate controls, at 3, 10 and 24 mo. RTqPCR and WB assessed markers of UPS and extracellular matrix (ECM). Isolated CMs and cardiac fibroblasts were analyzed. Molecular and IF analyses were performed in heart samples from patients affected by aortic stenosis.

#### Results

MuRF1 ablation leads to cardiac hypertrophy, progressing during ageing (LV CM areas: 3 mo., KO: 329.14±10.66 vs Ctrl: 296.25±5.43; 10mo., KO: 399.73±7.64 vs Ctrl: 247.49±3.67; 24 mo., KO: 418.90±11.10 vs. Ctrl: 209.93±4.48, in µm<sup>2</sup>). The hypertrophic remodelling was accompanied by diastolic-, in adult, and, systolic- dysfunction in aged mice (EF, 24 mo., KO: 29.55±8.82 vs Ctrl: 51.23±6.56, in %). Loss of MuRF1 increased interstitial collagen -I and -VI deposition and activation of Matrix MetalloProteinases (MMP), even before the onset of contractile dysfunction, suggesting that such alterations may be responsible for decreased cardiac performance. Interestingly, collagen established rings enveloping MuRF1 KO CMs, and such fibrotic remodelling was not accompanied by increased CM apoptosis, nor myofibroblast activation. Such peculiar remodelling, called peri-endomysial fibrosis, was detected in hearts from patients with aortic stenosis, a condition in which MuRF1 levels decrease. Our data supports that MuRF1 has a role in CM- dependent regulation of the ECM dynamics. Consistently, MuRF1 downregulation in normal cultured CMs demonstrated that such ubiquitin ligase impacts on ECM homeostasis. Consistently, fibroblasts, treated with culture medium conditioned by MuRF1 KO CMs, display increased collagen and MMP expression.

#### Conclusions

We identify a novel role of MuRF1 in the control of CM proteostasis and unveil that, in addition to cardiac fibroblasts, CMs may directly regulate ECM dynamics, indicating that MuRF1 is essential for heart adaptation to ageing.

#### ASSESSING THE RELATIVE CONTRIBUTION OF ATP SYNTHASE AND ADENINE NUCLEOTIDE TRANSLOCATOR IN THE MITOCHONDRIAL PERMEABILITY TRANSITION

#### Ph.D. Student: Dr. Ludovica TOMMASIN TUTOR: Prof. Paolo BERNARDI – CO-TUTOR: Dr. Michela CARRARO Ph.D. Course Biomedical Sciences

#### Background

The Permeability Transition (PT) is as an increased permeability of the inner mitochondrial membrane which allows the diffusion of solutes and ions with a molecular mass up to 1.5 kDa. This phenomenon is due to opening of the Permeability Transition Pore (PTP), a  $Ca^{2+}$ -activated channel that causes matrix swelling. The modulators of PTP include cyclophilin D and thiol reagents (like phenylarsine oxide, PAO), which favor opening; and acidic pH, cyclosporin A and adenine nucleotides, which act as inhibitors. The nature of the PTP has been a matter of debate for decades, but recent advances suggest that the ATP synthase is the main candidate for PTP formation and that the Adenine Nucleotide Translocator (ANT) may also contribute, indicating that different permeability pathways coexist. To assess their relative role, we evaluated the effect of the ANT specific ligands bongkrekic acid (BKA, which inhibits opening of the ANT channel) and atractylate (ATR, which facilitates opening of the ANT channel), on  $Ca^{2+}$ -dependent swelling of non-respiring mouse liver mitochondria at pH 7.4 (a condition that allows opening of both channels) and at pH 6.5 (which selectively inhibits ATP synthase channel).

#### **Material and Methods**

Experiments were performed using non-respiring mouse liver mitochondria (MLM). MLM were resuspended in KSCN which allows  $Ca^{2+}$  uptake driven by the SCN<sup>-</sup> diffusion potential within the matrix, which is followed by swelling due to PTP opening. A remarkable feature of this method is that  $Ca^{2+}$  fluxes are not matched by H<sup>+</sup> movements, allowing to maintain stable the matrix pH during the experiments. To induce swelling,  $Ca^{2+}$  was added and absorbance changes were measured at 540 nm. We also tested the propensity of pore opening in MEF wild-type cells and after ablation of all ANT murine isoforms. Finally, to investigate a possible physical interaction between ANT and ATP synthase, co-migration and co-immunoprecipitation assays were performed.

#### Results

BKA exerted a partial inhibition of  $Ca^{2+}$ -dependent swelling of MLM at pH 7.4, suggesting that ANT is not primarily involved in the PT. At pH 6.5  $Ca^{2+}$  induced swelling only in presence of ATR and was fully prevented by BKA, suggesting that the ANT pore opens in this condition. The PTP inducer PAO was also tested in presence of  $Ca^{2+}$ . PAO-dependent swelling was detectable but insensitive to BKA. Consistently, PAO was fully effective in ANT KO cells indicating that ANT is not its target. We believe that there is a reciprocal modulation between ATP synthase and ANT, which is supported by their co-migration and co-immunoprecipitation, suggesting their physical interaction through specific ATP synthase subunits.

#### Conclusions

Our hypothesis is that PTP channel formation by ATP synthase predominates in response to  $Ca^{2+}$  and PAO, and that ANT participates in PTP formation when the ATP synthase channel cannot open. We suggest that a reciprocal modulation exists through the physical interaction of ANT and ATP synthase, through subunits g and c of the latter.



University of Padua PhD Courses Medical and Biomedical Sciences

### PhD COURSE "CLINICAL AND EXPERIMENTAL ONCOLOGY AND IMMUNOLOGY" COORDINATOR: PROF. STEFANO INDRACCOLO

#### URINARY DIVERSIONS AFTER RADICAL CYSTECTOMY: REALIZATION OF CONDUITS AND BLADDER REPLACEMENT USING TISSUE ENGINEERING TECHNIQUES

#### Ph.D. Student: Dr. Martina CASARIN TUTOR: Prof. Fabrizio DAL MORO – CO-TUTOR: Dr. Alessandro MORLACCO Ph.D. Course Clinical and Experimental Oncology and Immunology

#### Background

In case of radical cystectomy, urine flow is restored through the creation of a urinary diversion using an autologous segment of the small intestine, which is unfortunately related to high risk of complications. Thus, the present project focused on the realization of an alternative urinary diversion starting from porcine small intestinal submucosa (SIS) and on ureter substitution using decellularized porcine ureter. In order to improve decellularized SIS impermeability and patency, it was thought to couple it with two alternative commercially available polycarbonate urethanes and the challenge consists in the realization of a conduit with appropriate dimensions.

#### **Material and Methods**

For the preparation of the flat hybrid membrane, polycarbonate urethanes (Chronoflex AR and Chronoflex AR-LT) were poured on decellularized SIS and dried at 38°C for 3 days. The hybrid membranes were then morphologically and mechanically characterized before performing the cytocompatibility assessments. Subsequentially, the work has been focused on the preservation of the SIS conduit-shape to create a hybrid conduit.

Regarding engineered ureter, different decellularization procedures based on the use of protease inhibitors, hypo- and hyper-tonic solutions and detergents were compared on the basis of histology.

#### Results

SIS remained preserved after hybrid membranes realization and tightly fitted to the polymers as suggested by the immunofluorescence and the two-photon analysis, with a higher penetration of Chronoflex AR-LT than Chronoflex AR. Moreover, FTIR-ATR analysis suggested the maintenance of tissue composition. In addition, mechanical uniaxial tests assessed a decreasing in stiffness and an increasing in isotropic behavior. *In vitro* cytotoxicity assays demonstrated a significant improvement of human bone marrow stem cells growth in comparison with decellularized SIS or polymers alone. Further efforts have been done in order to create a tubular hybrid membrane starting from decellularized SIS conduit, but still the best setup has to be found.

Regarding ureter decellularization, histology showed effective nuclei removal and ECM preservation, but still not optimal muscular fibers removal in all the tested decellularization protocols.

Besides the publication related to hybrid membranes [https://doi.org/10.3390/jfb13040222], a paper related to descending aorta decellularization for the urinary diversions application was published [https://doi.org/10.3390/jfb14030141] and a review [https://doi.org/10.3390/pr11072013]. Finally, two posters have been presented in the VIII National Congress of Bioengineering in Padua.

#### Conclusions

SIS-based hybrid membranes have shown to be promising for urinary diversions due to the increased mechanical resistance and cells growth. The first efforts allow to create cylindrical hybrid membranes as well, but still further analyses are necessary to characterize them. Regarding ureters decellularization, further efforts must be done in order to effectively remove muscle fibres from the tissue.

#### TARGETING THE EXTRACELLULAR MATRIX TO IMPROVE CAR-T CELL THERAPY AGAINST SOLID TUMORS

#### Ph.D. Student: Dr. Giulia D'ACCARDIO TUTOR: Prof. Antonio ROSATO – CO-TUTOR: Dr. Emilia VIGOLO, PhD Ph.D. Course Clinical and Experimental Oncology and Immunology

Background: Adoptive cell therapy (ACT) with T lymphocytes expressing Chimeric Antigen Receptors (CAR-T) has emerged as a promising immunotherapy to treat hematological malignancies. However, CAR-T cell therapy in solid tumors remains challenging, mainly because the immunosuppressive tumor microenvironment (TME) limits proper T cells functionality. In particular, the tumor extracellular matrix (ECM), which is rich in collagen and hyaluronic acid (HA), blocks the infiltration of immune cells. Hence, we aim to improve the efficacy of CAR-T cells in those solid tumors characterized by a dense ECM and mostly unresponsive to ACT, such as prostate and pancreatic cancer. In this study, we engineered T cells to co-express the CAR molecule and either a collagenase (MMP8 and MMP14) or a hyaluronidase (PH20), in order to dismantle the tumor ECM and therefore to improve the CAR-T cells' infiltration and invasion. Since the ECM actively regulates the immune cell motility and functionality, its disruption during CAR-T cell therapy could alter the interactions between the effector and immune cells of the TME. Therefore, we aim to gain a deep understanding of the immune cells' interactions affected by ECM remodeling. Material and Methods: First, we cloned the ECM-degrading enzyme downstream of the human prostate-specific membrane antigen (PSMA) CAR transgene into a clinically relevant lentiviral vector. Thus, we transduced either Jurkat (PSMA CAR.E-J cells) or primary T cells (PSMA CAR.E-T cells) with a MOI of 5 and 30, respectively. The co-expression of transgenes was assessed by flow cytometry and Western blotting analysis. The PSMA CAR.E-T cells' cytotoxic activity was evaluated by in vitro Calcein-AM assay. Lastly, we assessed the enzyme functionality by in vitro assays. The PH20 activity was evaluated by particle exclusion assay, which allows us to measure the pericellular HA deposition by PC3 cells and its subsequent degradation upon PSMA CAR.PH20-J cells co-culture. Meanwhile, the MMP14 activity was assessed by Transwell cells invasion assay in Matrigel, followed by z-stack 3D confocal imaging analysis of PSMA CAR.MMP14-J cells migrating through the Matrigel layer. To investigate the effects on the TME induced by the ECM remodeling fully immunocompetent mice will be used to model the ECM-rich pancreatic cancer and its immunosuppressive TME. Murine Mesothelin (mMSLN) CAR-T cells expressing either MMPs or PH20 will be produced, and finally whole transcriptomic analysis at single cell level will be performed on tumors undergoing therapy.

**Results:** Two days following transduction, we observed a high percentage of Jurkat cells positive for both PSMA-CAR (85.7%), and PH20 (39%) or MMP14 (74.3%) molecules, as confirmed by Western blotting analysis. On day 9 after transduction, PSMA CAR.E-T cells co-cultured with PSMA-positive PC3-PiP cells showed higher cytotoxicity ( $34.5\pm3.00\%$ , 1:25 T:E ratio), when compared to the PSMA CAR.E-T cells co-cultured with PSMA-negative PC3 cells ( $12.36\pm1.37\%$ , 1:25 T:E ratio). Lastly, preliminary results showed a remarkable difference in the infiltration capacity of PSMA CAR.MMP14-J cells ( $230 \mu m$  in depth) when compared to non-transduced Jurkat cells ( $60 \mu m$  in depth). Concerning the mMSLN CAR-T cells production, we successfully optimized a protocol to retrovirally transduce murine CD8+ T cells.

**Conclusions:** Here, we present a promising strategy to enhance CAR-T cells' therapeutic efficacy in solid tumors. Indeed, we observed that the PSMA CAR.E-J cells are endowed with high invasion capacity thanks to the efficient expression of ECM-degrading enzymes. In parallel, a deep characterization of the TME during the therapy in a fully preserved immune system will entangle unknown immune cells relationship, allowing for a better tumor therapy design.

#### **NEUROAID: NEUROIMAGING OF GLIOMAS FROM DIAGNOSIS TO TREATMENT**

Ph.D. Student: Giulia DEBIASI TUTOR: Dr. Giuseppe LOMBARDI - CO-TUTOR: Prof. Alessandra BERTOLDO Ph.D. Course Clinical and Experimental Oncology and Immunology

#### Background

Gliomas are a heterogeneous group of primary brain tumors with glioblastoma being the most aggressive type, with poor prognosis and a median overall survival of 14.6 months. The standard protocol for newly diagnosed glioblastoma is maximal safe resection, followed by concomitant chemotherapy with temozolomide and radiotherapy. Despite treatments, a recurrence of the disease occurs in almost all patients after an average of 6-9 months. In this scenario, neuroimaging plays a pivotal role in several stages of the pathology. Standard structural Magnetic Resonance (MR) sequences, advanced MR techniques as well as Positron Emission Tomography (PET) give insights about the disease and its progression. This project poses itself at different level of intervention within the course of the pathology and therefore seek to achieve multiple aims. First, we want to investigate the added value of Quantitative Susceptibility Mapping (QSM) in differentiating glioma grades and predicting patient outcome at diagnosis. Then, we aim to identify edema sub-regions to address the hypothesis of its heterogeneity and finally, we want to study the predictive role of imaging features related to the use of regorafenib as treatment in recurrent glioblastoma patients.

#### **Material and Methods**

A different glioma dataset is used for each objective comprising both MR and PET acquisitions. For the first aim, a multi-echo gradient echo MR sequence acquired on newly diagnosed gliomas is used to derive QSM maps, thus obtaining information about tissue susceptibility in the brain and in the tumor tissues. Distribution of values from different areas will be compared with statistical analysis and a model will be tested to assess QSM capability of predicting patient outcome. For the second aim, given edema fluid composition, diffusion MRI was exploited to investigate the edema heterogeneity in a cohort of glioblastoma patients. Value distributions were inspected for each parameter map to identify the most promising in terms of tumoral tissue differentiation and then a clustering analysis was performed. For the third aim, the dataset is composed of recurrent glioblastoma patient treated with regorafenib, a multi kinase inhibitor with several molecular targets involved in angiogenesis, oncogenesis, and maintenance of the tumoral microenvironment. Imaging data comprises both MR and PET acquisitions with a specific tracer (i.e., O-(2-<sup>18</sup>F-fluoroethyl)-Ltyrosine (<sup>18</sup>F–FET), an amino acid tracer). Data were processed and the analysis will investigate the relationship between the imaging features and the given treatment.

#### Results

As regards the characterization of gliomas by means of QSM, different methods for its quantification were tested and distribution of susceptibility values of the tumoral tissues were obtained. As for the objective of edema tissues differentiation, it was successfully addressed with clustering analysis providing two spatially separated clusters that show similarity with the contralateral normal appearing white matter and another tumoral tissue, respectively. Finally, considering the third aim, several processing stages were tackled, and an automatic pipeline was developed.

#### Conclusions

Gliomas are associated to poor prognosis and no efficient treatment is currently available, especially when exhibiting the most aggressive type (i.e., the glioblastoma). Neuroimaging techniques contribute to study and monitoring pathological mechanisms and changes, and my research project aim at providing support at different level of the disease progression.

#### HYALURONIC ACID AS AN IMMUNOLOGICAL ADJUVANT FOR PROTEIN-BASED **VACCINATION STRATEGIES**

#### Ph.D. Student: Dr. Beatrice GENOVA TUTOR: Prof. Antonio ROSATO - CO-TUTOR: Dr. Anna DALLA PIETA' Ph.D. Course Clinical and Experimental Oncology and Immunology

#### Background

In the last years, the scientific community has been focused on developing suitable therapies to counteract the COVID-19 pandemic. Although the currently approved vaccines are mainly based on RNA platforms, they still rise concernment. Therefore, protein-based vaccination strategies are intensively investigated and consequently, the study of effective adjuvants is fundamental. The natural polymer hyaluronan (HA) can stimulate robust and long-lasting humoral responses when chemically conjugated with a protein antigen, acting as an effective adjuvant without the addition of other immunostimulatory compounds. In this project, HA was covalently conjugated to the receptor binding domain (RBD) of SARS-CoV-2 Spike (S) protein.

#### **Material and Methods**

Immunization experiments were carried out in BALB/c and K18-hACE2 mice, a transgenic strain characterized by the expression of human angiotensin enzyme 2 (hACE2) receptor, which was monitored through Real-Time PCR.

Mice were immunized by intramuscular injection with 10 µg of RBD, conjugated with HA (HA-RBD) or properly mixed with other commercial adjuvants (i.e. Quil-A and Addavax), with different immunization schedules: three doses at day 0, 14 and 21 and two doses at day 0 and 21. Inflammation at the injection site was evaluated through staining with Haematoxylin and Eosin.

Sera were collected at different time points and titrated for RBD-specific IgGs by enzyme-linked immunosorbent assay (ELISA), while neutralizing antibodies (nAbs) were titrated by evaluating the cytopathogenic effect on Vero-E6 cells infected with SARS-CoV-2.

Single-cell suspensions of lymph nodes and bone marrow collected at different time points from immunized mice, were stained and analysed by flow cytometry for the detection of germinal centre (GC) B cells and long-lived plasma cells (LLPCs) respectively.

After vaccination, K18-hACE2 mice were infected via intranasal route with 1x10<sup>5</sup> TCID<sub>50</sub> of SARS-CoV-2 and the disease progression was assessed by daily monitoring weight loss, clinical score and survival. Same experiments were performed using Delta and Omega variants of the virus. Results

Data obtained from vaccination of mice showed that the HA-RBD bioconjugate elicited a robust humoral response in all mouse strains inducing the generation of RBD-specific GC B cells and the consequent production of an amount of RBD-specific IgGs that is higher that elicited by other commercial adjuvants. HA-induced anti-RBD IgGs peaked one week after the end of the immunization schedule, remaining detectable one year after priming. Moreover, their presence correlated to the detection of LLPCs in the bone marrow, which supports the development of longlasting immunity.

Importantly, RBD-specific IgGs displayed neutralizing activity against SARS-CoV-2 in vitro and vaccination of K18-hACE2 mice showed to protect animals from developing COVID-19 disease and prevent their death after infection with SARS-CoV-2, also in the case of two consequent infections driven by different variants, and even a long time after the immunization.

#### Conclusions

Overall, these data demonstrate the efficacy of HA-based vaccination against COVID-19 disease and supports the promising use of the biocompatible polymer HA as an efficient and well tolerated adjuvant for protein-based vaccination strategies.

#### PRELIMINARY CLINICAL EXOME ASSESSMENTS OF INTRADUCTAL PAPILLARY MUCINOUS NEOPLASM PATIENTS BY NEXT GENERATION SEQUENCING

#### Ph.D. Student: Dr. Fahimeh JAFARNEZHAD ANSARIHA TUTOR: Prof. Daniela BASSO Ph.D. Course Clinical and Experimental Oncology and Immunology

#### Background

Intraductal papillary mucinous neoplasm (IPMN) of the pancreas is a distinct type of precursor lesions originating from pancreatic intraductal epithelial cells and characterized by duct dilatation, mucin overproduction, and potential progression to invasive pancreatic ductal adenocarcinomas (PDACs). The estimated incidence of IPMN in individuals is approximately 0.001% to 0.002%. Despite extensive research and significant improvements in management of IPMN, there is little information about its specific genetic landscape and evolutions. The value of genomic screening by next-generation sequencing (NGS) in IPMN patients has not been well-studied yet. The objective of the current study was to verify whether clinical exome sequencing by NGS could aid in identifying IPMN genetic predispositions especially in high-risk populations.

#### **Material and Methods**

Eight IPMN patients (mean age  $68.6 \pm 11.4$  years; 3 males) were enrolled. Whole blood was used for clinical exome sequencing analysis. Library preparation and sequencing were performed using Clinical Exome Solution v2 (Sophia Genetics) and MiSeq platform (Illumina). The clinical exome panel comprised the coding regions and  $\pm$ 5bp of exome flanking regions of 4490 genes. Alignment, annotation, and variant filtering (MAF <0.05 and coding sequences) were carried out with Sophia DDM software (v. 5.10.32).

#### Results

Considering all patients, an average of 73588 retained variants were found, focusing our analysis on virtual panels. According to the literature and Gene Ontology (GO), virtual panels related to inflammation (204 genes), obesity (38 genes), diabetes (170 genes), pancreatic cancer susceptibility (51 genes) and clinical exome (4490 genes) were designed. Interestingly, in each panel, rare variants with ACMG>3 and common in 11 patients were identified. Protein kinase, DNA-activated, catalytic subunit (PRKDC), protein tyrosine phosphatase non-receptor type 22 (PTPN22) and activating transcription factor 6(ATF6) in inflammation panel were detected. For obesity panel cadherin related 23 (CDH23), HPS4 biogenesis of lysosomal organelles complex 3 subunit 2 (HPS4), phosphodiesterase 11A (PDE11A) and for diabetes panel alpha-methylacyl-CoA racemase (AMACR), glycerol-3-phosphate dehydrogenase 2 (GPD2), lipase C hepatic type (LIPC), phosphodiesterase 11A (PDE11A), and protein O-linked mannose N-acetylglucosaminyltransferase 1 (POMGNT1) were identified. Additionally, for pancreatic cancer susceptibility panel polycystin 1, transient receptor potential channel interacting (PKD1), ciliary IPT domain containing fibrocystin/polyductin (PKHD1), and transmembrane protein 216 (TMEM216) were detected. Moreover, for clinical exome 4 different variants in potassium inwardly rectifying channel subfamily J member 12 (KCNJ12) and one variant of ovochymase 2 (OVCH2), golgi associated secretory pathway kinase (FAM20C) and SH3 and multiple ankyrin repeat domains 3 (SHANK3) were found.

#### Conclusions

This study introduced the preliminary concepts about the application of NGS to reveal various types of germline genetic alterations in IPMN patients. The comprehensive analyses of IPMN genomic characteristics underlie its complicated dynamics, providing a critical strategy to better understand the earliest steps in pancreatic tumorigenesis, and as a result, insight into the discovery of early detections and interventions.

#### COMPREHENSIVE LIST OF LOSS OF PROOFREADING MUTATIONS IN POLYMERASE EPSILON (POLE) IDENTIFY IMMUNOTHERAPY RESPONDER AND REFRACTORY PATIENTS

#### Ph.D. Student: Dr. Giulia MADDALENA TUTOR: Dr. Sara LONARDI - CO TUTOR: Dr. Scott KOPETZ Ph.D. Course Clinical and Experimental Oncology and Immunology

#### Background

*POLE* mutation has been proposed as a biomarker for immune therapy response; however, most *POLE* mutations are passenger and not associated with a hypermutated phenotype. Current classifications of *POLE* mutations are limited in both accuracy and completeness with important implications for patient treatment decisions and subsequent outcomes.

#### **Material and Methods**

Starting from WES data, we average together the mutational signature from a curated list of 19 known loss of proof-reading (LOP) *POLE* mutations. The resulting signature was used to screen 46,332 patients from Natera and define a comprehensive LOP *POLE* mutation list, validated in 69,223 patients data from cBioportal. Additionally, a retrospective analysis of 41 metastatic CRC patients with *POLE* mutation treated with immune checkpoint inhibitors was performed to assess therapeutic response.

#### Results

A total of 2581 (5.6%) patients with unique *POLE* mutations were identified from the exploratory cohort, 153 carrying LOP POLE mutations (6%) based on mutational signature correlation. A total of 31 LOP *POLE* mutations were listed, some not located in the exonuclease region. Data were confirmed in cBioportal validation cohort. Endometrial and colorectal cancer were confirmed to be the cancers with the high incidence of LOP mutations within the overall *POLE* mutations (28.69% and 18.15% respectively). In the clinical cohort all 9 pts with *POLE* LOP achieved clinical benefit (ORR 88.9%, DCR 100%) with mPFS and mOS not yet reached at 48 months. In contrast, none of the 9 MSS pts with Non-LOP POLE mut achieved an objective response to IO therapy, and had disease progression with median PFS of 3.7 months (log-rank p<0.0001). We also investigated 1st line cytotoxic agents, significantly shorter for LOP *POLE* mutated subgroup (log-rank p=0.021).

#### Conclusions

Identifying the subset of *POLE* mutations that cause LOP is critical to distinguish those patients likely to respond to immunotherapy. Patients with CRC tumors containingLOP *POLE* mutation were found to have deep, sustained response to IO therapy but were resistant to standard cytotoxic chemotherapy, in stark contrast to those with non-LOP *POLE* mutations. These data suggest that front line immunotherapy is the best treatment option for CRC tumors with LOP *POLE* mutation.

#### DESIGN IN PATIENT SPECIFIC HYDROGEL-BASED MODEL FOR TAILORED COLORECTAL CANCER MEDICINE

#### Ph.D. Student: Dr. Asia MARANGIO TUTOR: Prof. Marco AGOSTINI Ph.D. Course Clinical and Experimental Oncology and Immunology

Colorectal cancer (CRC) is one of the most lethal malignancies worldwide with high mortality rate. Despite the great insights obtained with the use of monolayer cultures in vitro, the 2D cultures entail several limitations such as the lack of cancer-cell heterogeneity and, mostly, the absence of the tumor microenvironment. In view of overcoming these limitations, modeling CRC using patient derived organoids (PDOs) has emerged as in vitro tool to predict the patient sensitivity to treatments, providing hopeful insights to personalize medicine. PDOs culture are usually relied on commercial matrix that still need improvements to fully reconstitute the biochemical extracellular matrix (ECM) composition of native tissue.

Here we develop a PDOs culture platform using patient-derived decellularized ECM to obtain ECM Hydrogel (HydrogEM). Then, we culture CRC PDOs in our HydrogEM obtaining a 3D enriched model (HyDEM) of CRC.

Surgically resected healthy colon mucosa from CRC patient were decellularized by a detergentenzymatic treatment (DET). Decellularized samples were then lyophilized and reduced to powder. The obtained powder was pepsin-digested for 72h to produce HydrogEM. At the end of digestion the pH was neutralized to pH=7.4 on ice. To characterize and compare decellularized matrix and HydrogEM immunofluorescence (IF), immunohistochemistry (IHC), scanning electron microscopy (SEM) analysis and DNA quantification were performed on decellularized matrix after 2 DET cycle and on HydrogEM.

In parallel, we developed a specific mechanical and enzymatic digestion protocol for PDOs derivation from CRC samples. Finally, to develop our HydEM, we seeded isolated organoids in HydrogEM.

HydrogEM maintains the structural environment of native tumoral tissue as demonstrated by IHC and SEM analysis. CRC PDOs concordance with the native tumoral tissue was evaluated through IHC analysis for the diagnostics biomarkers, CDX2, MSH6 and MSH2 with an index of 91.33%, 94% and 81% respectively, suggesting that PDOs maintain the patient mutational profile. PDO IF analysis confirmed the expression of epithelial marker E-cadherin. F-actin and  $\beta$ -catenin markers were investigated to study cellular morphology and polarization. Finally, PDOs expression of intestinal stem cells marker LGR5 was also confirmed.

We explored HydrogEM biocompatibility cultivating PDOs. After 7 days of culture IF analysis confirmed the presence of proliferative nuclei engrafted in HydrogEM and linked to the basement memebrane. The quantification of viable PDOs through Live and Dead assay, indicated that HydrogEM offers a proper environment for PDOs culture.

These data indicate that the proposed HydrogEM is suitable platform for CRC PDOs viability and growth. Further, the developed HydEM, could represent a repeatable and scalable 3D enriched model of CRC since it recapitulates important tumour microenvironment features and could potentially promote discovery and development of chemotropic drug for cancer treatment.

#### DRUGGABLE MOLECULAR ALTERATIONS AND THERAPEUTIC IMPLICATIONS IN PATIENTS WITH RECURRENT *IDH1/2* WILDTYPE GLIOBLASTOMA: A REAL-LIFE COHORT ANALYSIS

#### Ph.D. Student: Dr. Marta PADOVAN TUTOR: Dr. Giuseppe LOMBARDI Ph.D. Course Clinical and Experimental Oncology and Immunology

#### Background

Next-generation sequencing (NGS) enables the identification of patient subgroups that may respond to targeted therapies (TT), thus guiding a molecularly targeted treatment strategy for glioblastoma (GBM).

#### Material and methods

We retrospectively analyzed a large cohort of *IDH1/2* wildtype GBM. NGS profile was obtained with FoundationOne®CDx on formalin-fixed paraffin-embedded tissue samples. We aimed to 1) identify potentially actionable molecular alterations at diagnosis and/or recurrence based on ESCAT (ESMO Scale for Clinical Actionability of Molecular Targets) defined categories of targetability, 2) understand the clinical implications of NGS in terms of access to and effectiveness of targeted therapies (TT). We identified 7 relevant alterations, categorized according to ESCAT as follows: *BRAF V600E* mutation (IB), *NTRK 1-3* fusions (IC), *FGFR1-3* alterations (IIB), *ROS1* fusions, *MET* amplification/fusions, *PIK3CA* mutations, and *PTEN* loss/mutations (IIIA).

#### Results

In 442 samples, NGS profile was available in 98.2% of cases. Although approximately half of the patients had at least one druggable molecular alteration, only 3.4% of them were classified as ESCAT IB-IC, and 6.7% as ESCAT IIB.

37 patients (8.9%) received personalized treatment in clinical trials or as off-label or compassionate use. Out of the 37 patients who received TT, 21 were male; ECOG performance status was  $\leq 1$  in 31 patients. The median line of therapy with TT was 3 (range 2-7). TT agents included dabrafenib/trametinib (9 patients), larotrectinib (2 patients), erdafitinib (4 patients), entrectinib (1 patient), vebreltinib (2 patients), capmatinib (1 patient), alpelisib (6 patients), and ipatasertib+/-atezolizumab (12 patients). At the cut-off date (August 2023), 26 patients had died, and 35 patients had a progressive disease. In the entire cohort, the median overall survival and progression-free survival (PFS) after starting TT were 8.06 (95% CI: 6.48-15.92) and 2.17 months (95% CI: 1.94-3.68), respectively. The dabrafenib/trametinib subgroup had the longest median PFS (5.23 months), a disease control rate of 77%, an objective response rate of 22%, and a median duration of response of 27.35 months. Seven out of nine patients had died, and two patients were continuing dabrafenib/trametinib. A multifocal GBM patient with a *PTPRZ1-MET* fusion achieved an impressive partial response with vebreltinib in the third-line, but duration of response was only 3.68 months. Among the others, no complete or partial responses were detected.

#### Conclusions

Our study has showcased the feasibility of utilizing NGS on GBM samples. Given the restricted count of clinically relevant targets and the small subset of GBM patients who underwent targeted therapy, conducting NGS testing should ideally be carried out within the framework of clinical trials. Our findings endorse the efficacy of anti-BRAF/anti-MEK treatments, while for the remaining agents, solid conclusions necessitate prospective study outcomes.

#### BILIARY TRACT CANCERS: A LARGE RETROSPECTIVE PROGNOSTIC AND PREDICTIVE MOLECULAR ANALYSIS

#### Ph.D. Student: Dr. Diana SACCHI TUTOR: Prof. Matteo FASSAN – CO-TUTOR: Prof. Maria GUIDO Ph.D. Course Clinical and Experimental Oncology and Immunology

**Background:** Biliary tract cancers, including intrahepatic, perihilar, and distal cholangiocarcinoma as well as gallbladder cancer, are low-incidence malignancies, but they represent a health problem that often present as advanced, unresectable, or metastatic disease, which limits the number of available treatment options. In recent years, next-generation sequencing technology have identified genetic differences between these biliary cancers and molecular subgroups. Indeed, the identification of distinct molecular subgroups with corresponding targeted therapies (such as, *IDH1* mutations and *FGFR2/3* fusions in intrahepatic cholangiocarcinoma) is changing the treatment scenario. However, reliable prevalence estimates of these molecular alterations, their prognostic role and the feasibility of molecular analysis in the routinely pathological diagnosis in biliary tract cancers (for which the specimens are usually limited to small biopsies) and the possible role of the liquid biopsy have not been fully elucidated.

**Material and Methods:** Medical records of 590 patients affected by advanced biliary tract carcinomas were retrospectively collected from January 2008 to July 2023 and prospectively followed. All patients are followed in Veneto Institute of Oncology (IOV, Padua). Due to the lack of clinical information and/or no availability of tissue samples, 155 patients have been excluded.

A clinical dataset about 435 patients eligible has been provided and all the pathologic samples has been re-evaluated by GI pathologist (MF, SB, DS) and the pathological prognostic features were collected. 115 patients were immediately excluded because of insufficient quantity or quality of the tissue samples. Therefore, 320 patients were considered eligible for the molecular analysis. Among these we focus our attention on 151 patients with advanced intrahepatic cholangiocarcinoma. 16 cases have been excluded because of specimen's inadequacy for the molecular analysis. A final series of 135 tumors is profiled by kit Fusion Plex Research (Archer) in platform next-generation sequencing (Illumina), comprehensive Genomic Profiling by FoundationOne®CDx, Fluorescence *in situ* analysis and immunohistochemistry for *FGFR2/3*, *ERBB2*, *NTRK* alterations, *IDH1/2* and *BRAF* mutations and DNA mismatch repair complex proteins alterations/microsatellite instability. In 22/135 patients, the liquid biopsy has also been collected in order to compare the results with those obtained from the tissue samples.

**Results (on going):** From a preliminary analysis, *FGFR2* rearrangements, amplifications and point mutations were detected in 5.2%; *FGFR3* alterations were observed in 1.7% cases; *IDH1/2* were mutated in 15.7%; *ERBB2* and *BRAF* gene mutation were observed in 3,5% and 2,3%, respectively. Two cases had *NTRK1* amplifications but no rearrangement was found. A deficit of mismatch repair protein expression was identified in 3.8%. At multivariate analysis, age, ECOG performance status, number of metastatic sites, tumour stage, *FGFR2/3* alterations and *IDH1/2* mutations were prognostic factors of overall survival. Data on a final series of 250 intrahepatic cholangiocarcinoma will be collected by the end of the PhD program.

**Conclusions:** As known in Literature, among the biliary tract cancers, intrahepatic cholangiocarcinoma is related to specific alterations in *FGFR2*, *IDH1/2* and *ERBB2*. In particular, from this preliminary analysis, *FGFR2/3* aberrations and *IDH1/2* mutations seem to be prognostic for better overall survival.



Università degli Studi di Padova University of Padua PhD Courses Medical and Biomedical Sciences

### PhD COURSE "CLINICAL AND EXPERIMENTAL SCIENCES" COORDINATOR: PROF. ALBERTO FERLIN

Curriculum "CLINICAL METHODOLOGY, METABOLISM, ENDOCRINOLOGY, NEPHROLOGY AND EXPERIMENTAL EXERCISE"

#### HYDRO-N-OMICS (IMPROVING ERGONOMICS IN THE HYDROPONIC AGRICULTURAL INDUSTRY TO FACILITATE ENVIRONMENTAL SUSTAINABILITY)

#### Ph.D. Student: Dr. Alessandro BORTOLETTO TUTOR: Prof. Marco BERGAMIN Ph.D. Course Clinical and Experimental Sciences Curriculum "Clinical Methodology, Metabolism, Endocrinology, Nephrology and Exercise"

#### Background

"Above-ground" crops represent a significant innovation in modern agriculture, driven by population growth, resource scarcity, climate change, and pollution concerns. Hydroponics, a soilless farming technique, is a promising sustainable alternative to traditional agriculture, offering reduced pollutant use and water consumption. However, workers in this system may still face ergonomic risks during various manual activities, including assembling modular architectures and tanks. This study aims to assess work-related musculoskeletal disorder risks in upper limbs using the Occupational Repetitive Actions (OCRA) method, comparing different screwdrivers: Electric drive (ET), and Pneumatic drive (15C) adopted in assembly activities with different working setups: Balanced Screwdriver (BS), Telescopic arm (BT), Cartesian arm (BC9, Articulated cartesian arm (BCA), and Cartesian arm with push-off assistance (BC25PK).

#### **Material and Methods**

Five male participants, aged 18-65 years, engaged in manual activities, were recruited and informed about the experimental purpose. Approval from the ethical committee and written consent from each participant was obtained before testing. Each participant performed one assembly task for each of the ten screwdriver / support arm combination, captured by a webcam. The OCRA checklist was computed for each condition to assess upper limb risk.

Due to non-normal data distribution, Kruskal-Wallis and Mann-Whitney U tests were used to infer significant differences ( $\alpha = 0.05$ ).

#### Results

Mann-Whitney U test showed no statistically significant differences in the use of two types of screwdrivers (ET and 15C) for both right and left upper limbs. However, Kruskal-Wallis test revealed significant differences in the risk index for the right upper limb ( $\chi^2 = 49.0$ , p < 0.05). Posthoc Dwass-Steel-Critchlow-Flinger test was performed to compare individual screwdriver usage:

a) BC25PK showed significant differences compared to all other conditions (p < 0.05), suggesting its suitability for specific assembly activities, as no muscular force was declared by participants.

b) BS (absence of support arm) showed significant differences compared to all other conditions (p < 0.05), indicating increased risk due to wrist joint recoil, recognized by the OCRA checklist as an additional risk factor.

#### Conclusions

Those are preliminary findings, based on the first 5 recruited subjects from an expected complete sample of 40 participants. The current promising results may be reinforced and confirmed with a larger sample. Nevertheless, the significant differences observed in screwdrivers support arms usage provide valuable insights for reducing ergonomic risks in hydroponic tank assembly and emphasize the need for personalized approaches to optimize ergonomics in this specific work setting.

#### THE ATAEXER PROJECT: PROTOCOL FOR A SELF-CONTROLLED CLINICAL TRIAL OF A MULTICOMPONENT HOME-BASED EXERCISE PROGRAM FOR PEOPLE LIVING WITH ATAXIA

#### Ph.D. Student: Dr. Sara FAGGIAN TUTOR: Prof. Andrea ERMOLAO Ph.D. Course Clinical and Experimental Sciences Curriculum "Clinical Methodology, Metabolism, Endocrinology, Nephrology and Exercise"

#### Background

Exercise prescription for people living with cerebellar ataxia suggests improvements in balance, limb coordination and gait, with an overall increase in function, although no evidence-based exercise guidelines are currently available. Home-based programs require fewer resources than centre-based programs and may facilitate participation, as exercise should be performed daily. The ATAEXER project aims to explore the feasibility and effectiveness of a multicomponent home-based exercise program for people with cerebellar ataxia on disease severity, balance, walking efficiency, muscle strength, fall risk and quality of life.

#### **Material and Methods**

A self-controlled clinical trial of an 8-week multicomponent home-based exercise training program (5 days/week, 45 min/day) and 2-month follow-up period will be applied in 15 adults with ataxia (Fragile X-associated tremor and ataxia syndrome or spinocerebellar ataxia type 1). Before the intervention, participants will perform an 8-week control period of usual care. Participants will be assessed at baseline (T<sub>0</sub>), before the exercise period (T<sub>1</sub>), immediately after the last training (T<sub>2</sub>) and at the end of a 2-month period as a follow-up measurement (T<sub>3</sub>). The individualised exercise program, delivered with demonstration videos, will include training of balance, gait, and strength, flexibility and coordination of lower limbs using simple equipment.

The primary outcome will be the walking efficiency assessed by performing the 10-meter walking test and the cardiopulmonary exercise test combined with gait analysis. Secondary outcomes will be: the disease severity assessed using the Scale for Assessment and Rating of Ataxia, balance assessed as the centre of mass, the Berg Balance Scale and the Timed-Up and Go test, gait kinematics using gait analysis, muscle strength using the handgrip test and 30-second chair stand test, and quality of life and fear of falling by administering specific questionnaires. Comparisons between and within groups for primary and secondary outcomes will be conducted. The local Ethical Committee for Clinical Research has approved this study (protocol code AOP2938).

#### Results

Currently, feasibility trials with a healthy subject and a patient with ataxia have been conducted. The recruitment is ongoing, the evaluation of healthy subjects for a case-control comparison will start in October, while the  $T_0$  for patients with ataxia is scheduled in January.

#### Conclusions

The feasibility of the ATAEXER Project and improvements in the evaluated aspects are expected after the intervention period compared to the control period. The protocol will provide a model for a clinical pathway and real-life exercise prescription for people living with ataxia.

#### ROLE OF AN ECO-SUSTAINABLE SUPPLY CHAIN IN THE WORLD OF DIETARY SUPPLEMENTS: GREEN TEA EXTRACT IN OVERWEIGHT AND OBESE POST-MENOPAUSAL WOMEN

#### Ph.D. Student: Dott.ssa. Nicole LIEVORE TUTOR: Prof. Valérie TIKHONOFF Ph.D. Course Clinical and Experimental Sciences Curriculum "Clinical Methodology, Metabolism, Endocrinology, Nephrology and Exercise"

**Background:** The GTEPOWER (Green Tea Extract in Postmenopausal Obese Women: Environmentally sustainable Randomized trial) study aims to develop an environmentally sustainable green tea extract supplement and to evaluate its impact on the lipid profile and on the body composition in overweight and obese post-menopausal women (PMW). With the onset of menopause loss of the protective effect of estrogen and changes in body fat distribution with increased abdominal obesity and dyslipidemia might be observed. Those metabolic and anthropometric modifications underlie the possible acceleration of cardiovascular disease observed in women after menopause.

Material and Methods: Based on preliminar power analysis, a single-blind randomized controlled intervention trial will recruit 80 PMW (naturally or surgical, excluding those on hormone replacement therapy or those on prior chemo or radiation therapy) aged between 40 and 65 years, with BMI between 24 and 38 kg/m<sup>2</sup> and following the exclusion criteria (active neoplastic disease, decompensated thyroid disease, autoimmune diseases undergoing specific pharmacological treatment, evident psychiatric disorders and advanced cardiovascular, hepatic and renal pathologies). Each randomly recruited PMW will sign an informed consent and will undergo a onemonth Mediterranean diet (run-in phase) to homogenize the sample. Then they will be randomly assigned to one of two groups: intervention group (n = 40) with green tea extract capsule for 3 months and placebo group (n = 40). Each PMW will be followed-up for 6 months (including the run-in phase) with monthly outpatient reassessments for the first 4 months and the last visit 2 months after the last supplement intake. A detailed questionnaire on lifestyle, medical history and physical activity, IPAQ (Physical Activity Questionnaire), Food Frequency Questionnaire will be administered at each visit. The outpatient assessment will include anthropometric measurements, detection of vital parameters such as systolic and diastolic blood pressure, heart rate, body composition, subclinical atherosclerosis assessment with tonometry, performance test (Gait Speed and timed up and go), and hand grip strength test with dynamometer. At each visit, blood samples for biochemical measurements will be taken. A weekly food diary will be provided. Green tea extract capsule was obtained from thirty kilo of Mao Feng green tea leaves coming from a sustainable plantation in Yunnan, China. The tea leaves were dried by dry heat without any oxidation and extracted with 60% etanol (D:S 1:10 V/V) at 60°C for 60 min in an Italian specialized firm. The extract was processed through filter press, concentrated at 40°C under vacuum, pasteurized at 80°C and dried in spray dried pilot with 30% maltodextrin added. Placebo capsules contain inert substances and look similar to green tea capsules. The packaging is environmentally sustainable, packaged in biodegradable bottles derived from corn.

**Results:** The all procedure is ongoing. So far, the obtained dry extract has a weight yield of 20-24%, EGCG concentration of 17.1% and Caffeine concentration of 19.5%. The General Directorate for Hygiene and Food Safety and Nutrition of the Ministry of Health has set the maximum daily intakes of caffeine (Prot. 6191-P-22/02/2017) and of EGCG (Reg. (UE) 2022/2340) with food supplements at 200 mg and 800 mg, respectively. In compliance with the legislation, a total of 175 mg of EGCG and 200 mg of Caffeine will be administered daily to each participant for 3 months.

**Conclusions:** This project is designed to promote the safety of dietary supplements in the face of climate change and biodiversity loss to improve people's health, quality of life and care for nature.

#### HEART FAILURE WITH PRESERVED EJECTION FRACTION IN PATIENTS WITH OBESITY: ROLE OF CARDIOPULMONARY EXERCISE TESTING

Ph.D. Student: Dr. Giulia QUINTO TUTOR: Prof. Roberto VETTOR – CO-TUTOR: Andrea ERMOLAO Ph.D. Course Clinical and Experimental Sciences Curriculum "Clinical Methodology, Metabolism, Endocrinology, Nephrology and Exercise"

#### Background

Heart failure (HF) with preserved ejection fraction (HFpEF) accounts more than 50% of HF, and in the last few years an obesity-specific phenotype of HFpEF has been proposed. Despite the numerous studies, its diagnostic and therapeutic approaches in practice are complex. Cardiopulmonary exercise testing (CPET) is a robust albeit underutilized prognostic and diagnostic tool in obesity and heart failure, and a recent clinical consensus statement shows its the important role in the diagnostic algorithm of HFpEF. Furthermore, a study show that peak VO2 reduction is sensitive but not specific and it can discriminate HFpEF from non-cardiac causes of dyspnea. Focusing on obesity-related HFpEF, the primary aim of this study is to investigate whether a specific CPET pattern can be identified in patients with obesity and HFpEF, which might allow screening of patients with obesity for HFpEF as related comorbidity.

#### Material and Methods

Patients with obesity were recruited at obesity dedicated outpatient clinic. Anthropometric measurements, clinical history and medical examination have been collected. All obesity related complications have been diagnosed using recent guidelines. Moreover, patients perform clinical examinations indicated to make a diagnosis of HFpEF, applying the current diagnostic algorithm (HFA-PEFF score, H2FPEF score), and they underwent CPET. No invasive haemodynamic stress test has been done. At the end, patients have been divided into 3 groups: low probability of HFpEF, intermediate probability of HFpEF and high probability of HFpEF.

#### Results

Forty patients were evaluated (age 48,86±12,67 years; BMI 44,94±7,78 kg/m<sup>2</sup>). Using score system, probability of HFpEF has been established: 11 patients with low probability, 23 patients with intermediate probability and 6 patients with high probability of HFpEF. Echocardiographic characteristics show averagely a cardiac concentric remodeling (LVMI 86,53±18,01 g/m<sup>2</sup>, RWT 0,46±0,09) without severe diastolic dysfunction (E/A 1,04±0,33; E/e' 10,07±3,89). All patients have a reduction in maximal and submaximal functional capacity (VO<sub>2</sub> peak/kg 17,60±4,0 mL/min kg; OUES 2314,86±677,8 mL/logL) without indirect sign of exercise induced pulmonary hypertension (VEVCO2 slope 26,51±4,68; PETCO2 increase 7,4±3,1 mmHg).

#### Conclusions

Patients with high probability of HFpEF are older and all affected by hypertension, both condition typically associated with HFpEF also in patients without obesity. Average BMI was similar between groups, but patients with higher HFpEF probability seems to have a lower maximal and submaximal functional capacity, expressed as VO2 peak/kg and OUES. Moreover, absolute value of oxygen pulse, and its predicted, seems to be lower in patients with high probability of HFpEF. Due to small sample size, no inference can be done, but preliminary analysis seems to show especially peripheral exercise limitation, with a normal/high respiratory reserve, and a high reduction of VO<sub>2</sub> peak also in patients with obesity-related HFpEF.

#### SOFTWARE FOR MOUNTAIN AREA ENHANCEMENT THROUGH SUSTAINABLE, PERSONALIZED AND CONSCIOUS HIKING

Ph.D. Student: Dr. Marco VECCHIATO TUTOR: Prof. Andrea ERMOLAO Ph.D. Course Clinical and Experimental Sciences Curriculum "Clinical Methodology, Metabolism, Endocrinology, Nephrology and Exercise"

#### Background

Recent years have seen a real growth in mountain tourism. This has also generated an increase in rescue calls with a record of more than 10000 calls per year in 2020-2022 period in Italy. The increase in rescue services can be substantially attributed to the increase in mountain tourists and to the superficiality of people approaching the mountains without adequate physical and/or technical preparation. The mountain signage provides hiking times calculated for an average person without considering the specific individual, who may have an indefinite number of different biological variables. The project aims to create a tool providing indications of personalized hiking times, speed and caloric consumption considering the specific physical characteristics of the trail and the individual in every aspect. The idea of the project joins the need to increase the safety profile of hikers with the promotion of sustainable tourism, which guarantees a tailored experience respecting the mountain environment.

#### **Material and Methods**

The PhD project consists of different steps for its realization:

Analysis and collection of supporting evidence for the formulation of the algorithm: the most recent data regarding functional capacity and the impact of altitude on performance were examined.
Algorithm validation – Digital data: this study aims to compare the algorithm's current outcomes with online data uploaded by real users from different open-free platforms as Wikiloc or Komoot.
Algorithm validation - Prospective study: healthy subjects and patient affected by chronic diseases will perform hiking on a selected trail with a portable gas analyzer and other wearables in order to verify the accuracy of the algorithm prediction.

4) Software development

#### Results

- Relevant literature has been used to create an algorithm useful to predict different personalized outputs that consider the hiker's biologic parameters and the physical characteristics of the trail. The extended algorithm cannot be totally disclosed as it is covered by the patent application.

- The digital validation study on a sample of 530 subjects is currently being finalised.

- The validation field study on a sample of about 60 subjects is awaiting approval by the Local Ethics Committee.

- A demo version of the software has been created, called **MOVE**. The recommended exercise time, calorie consumption, hydrosaline loss and replenishment, and health precautions for populations affected by chronic diseases are the main outputs. The software also allows the user to know whether or not the chosen trail is appropriate for his/her physical characteristics and health status.

#### Conclusions

The PhD project is advancing, and the software needs validation before it can be used by the general population, specially by subjects affected by chronic diseases. This project has won individual and collective awards and this year received funding from the European Space Agency. Future goals include the software optimisation and the extension to other movement modalities (running, cycling) and interaction with wearables.



### **University of Padua PhD Courses Medical and Biomedical Sciences**

## **PhD COURSE "CLINICAL AND EXPERIMENTAL SCIENCES**" **COORDINATOR: PROF. ALBERTO FERLIN**

## **Curriculum "HEMATOLOGICAL AND GERIATRIC** SCIENCES"

#### DIET- PREVENTION OF SARCOPENIA AND PRESERVATION OF SKELETAL MUSCLE MASS IN THE ELDERLY: PRELIMINARY DATA

#### Ph.D. Student: Dr. Silvia TONIAZZO TUTOR: Prof. Paolo SPINELLA Ph.D. Course Clinical and Experimental Sciences Curriculum "Hematological and Geriatric Sciences"

**Background** Sarcopenia and frailty syndrome correlate with poor clinical outcomes, increased morbidity and mortality. The Mediterranean Diet has favorable effects on health, helping to prevent sarcopenia. An adequate energy-protein intake and a greater BCAA (branched-chain amino acids) bioavailability can help to preserve skeletal muscle mass even in the elderly.

**Material and Methods** Elderly ( $\geq$ 65 years) with BMI (Body Mass Index) value of 20-30 kg/m<sup>2</sup>, free from uncontrolled chronic pathologies and physical-cognitive-neurological disabilities are recruited. The Mediterranean Diet intervention provides for 25-30 Kcal/kg/day and 1-1.2 g of protein/kg/day, with protein-dietary intake redistribution in daily meals, an increased fiber, vegetable proteins and BCAA intake. For each outpatient, eating habits are investigated and Barthel's index, anthropometric and bioimpedance measurements, handgrip, Short Physical Performance Battery (SPPB) are collected. Sarcopenia is assessed according to EWGSOP2 criteria. Outpatients are followed up with a reassessment of the same protocol every 3 months, for 12 months. Biochemical tests are checked every 6 months.

**Results** We enrolled 74 patients (mean age  $71\pm5$  years, male 36.5%); none were malnourished or sarcopenic at baseline. We observed a reduction in weight, BMI, waist circumference, with lean mass maintenance and faster walking pace (Table 1).

Daily protein intake, particularly breakfast protein intake, and BCAA are positively associated with greater lean mass, handgrip strenght and faster walking pace (Table 2).

**Conclusions** By these preliminary results, a healthy weight and a balanced dietary intervention with protein intake redistribution to daily meals and a sufficient BCAA intake, could be useful in skeletal muscle mass preservation in the elderly.

| W                        | BMI                                     | WC                                                                                                 | PA                                                                                                                                                  | FFM                                                                                                                                                    | FFMI                                                                                                                                                                                                                                        | ASM                                                                                                                                                                                                                                                                                      | SMI                                                                                                                                                                                                                                                                                                                                   | HG                                                                                                                                                                                                                           | WS                                                                                                                                                                                                                                                                                                                                                                                                                         |  |  |
|--------------------------|-----------------------------------------|----------------------------------------------------------------------------------------------------|-----------------------------------------------------------------------------------------------------------------------------------------------------|--------------------------------------------------------------------------------------------------------------------------------------------------------|---------------------------------------------------------------------------------------------------------------------------------------------------------------------------------------------------------------------------------------------|------------------------------------------------------------------------------------------------------------------------------------------------------------------------------------------------------------------------------------------------------------------------------------------|---------------------------------------------------------------------------------------------------------------------------------------------------------------------------------------------------------------------------------------------------------------------------------------------------------------------------------------|------------------------------------------------------------------------------------------------------------------------------------------------------------------------------------------------------------------------------|----------------------------------------------------------------------------------------------------------------------------------------------------------------------------------------------------------------------------------------------------------------------------------------------------------------------------------------------------------------------------------------------------------------------------|--|--|
| 72.1                     | 26.7                                    | 100                                                                                                | 5.5                                                                                                                                                 | 53.0                                                                                                                                                   | 19.4                                                                                                                                                                                                                                        | 18.5                                                                                                                                                                                                                                                                                     | 8.6                                                                                                                                                                                                                                                                                                                                   | 26.2                                                                                                                                                                                                                         | 1.1                                                                                                                                                                                                                                                                                                                                                                                                                        |  |  |
| <b>71.4</b> <sup>*</sup> | 27.9                                    | <b>98</b> *                                                                                        | 5.5                                                                                                                                                 | 53.6                                                                                                                                                   | 20.2                                                                                                                                                                                                                                        | 18.9                                                                                                                                                                                                                                                                                     | 9.6                                                                                                                                                                                                                                                                                                                                   | 26.6                                                                                                                                                                                                                         | 0.97*                                                                                                                                                                                                                                                                                                                                                                                                                      |  |  |
| <b>72.6</b> *            | <b>26.3</b> *                           | 96.6**                                                                                             | 5.6*                                                                                                                                                | 53.7                                                                                                                                                   | 19.4                                                                                                                                                                                                                                        | 19.1                                                                                                                                                                                                                                                                                     | 9.5                                                                                                                                                                                                                                                                                                                                   | 27.9                                                                                                                                                                                                                         | 0.95*                                                                                                                                                                                                                                                                                                                                                                                                                      |  |  |
| <b>73.5</b> *            | 26.4*                                   | 96.5**                                                                                             | <b>5.8</b> *                                                                                                                                        | 55.6                                                                                                                                                   | 19.9                                                                                                                                                                                                                                        | 18.9                                                                                                                                                                                                                                                                                     | 9.4                                                                                                                                                                                                                                                                                                                                   | 28.9                                                                                                                                                                                                                         | 0.96**                                                                                                                                                                                                                                                                                                                                                                                                                     |  |  |
| 72.5                     | 26.3                                    | 95.7**                                                                                             | 5.8*                                                                                                                                                | 54.9                                                                                                                                                   | 19.9                                                                                                                                                                                                                                        | 19.5                                                                                                                                                                                                                                                                                     | 9.4                                                                                                                                                                                                                                                                                                                                   | 28.9                                                                                                                                                                                                                         | 0.96**                                                                                                                                                                                                                                                                                                                                                                                                                     |  |  |
|                          | 72.1<br>71.4*<br>72.6*<br>73.5*<br>72.5 | 72.1     26.7       71.4*     27.9       72.6*     26.3*       73.5*     26.4*       72.5     26.3 | 72.1     26.7     100       71.4*     27.9     98*       72.6*     26.3*     96.6**       73.5*     26.4*     96.5**       72.5     26.3     95.7** | 72.1     26.7     100     5.5       71.4°     27.9     98°     5.5       72.6°     26.3°     96.6°°     5.6°       73.5°     26.4°     96.5°*     5.8° | 72.1     26.7     100     5.5     53.0       71.4°     27.9     98°     5.5     53.6       72.6°     26.3°     96.6°°     5.6°     53.7       73.5°     26.4°     96.5°°     5.8°     55.6       72.5     26.3     95.7°°     5.8°     54.9 | 72.1     26.7     100     5.5     53.0     19.4       71.4°     27.9     98°     5.5     53.6     20.2       72.6°     26.3°     96.6°°     5.6°     53.7     19.4       73.5°     26.4°     96.5°°     5.8°     55.6     19.9       72.5     26.3     95.7°°     5.8°     54.9     19.9 | 72.1     26.7     100     5.5     53.0     19.4     18.5       71.4°     27.9     98°     5.5     53.6     20.2     18.9       72.6°     26.3°     96.6°°     5.6°     53.7     19.4     19.1       73.5°     26.4°     96.5°°     5.8°     55.6     19.9     18.9       72.5     26.3     95.7°°     5.8°     54.9     19.9     19.5 | 72.126.71005.553.019.418.58.671.4*27.9 $98^*$ 5.553.620.218.99.672.6* $26.3^*$ $96.6^{**}$ $5.6^*$ $53.7$ 19.419.19.573.5* $26.4^*$ $96.5^{**}$ $5.8^*$ $55.6$ 19.918.99.472.5 $26.3$ $95.7^{**}$ $5.8^*$ $54.9$ 19.919.59.4 | 72.1     26.7     100     5.5     53.0     19.4     18.5     8.6     26.2       71.4*     27.9     98*     5.5     53.6     20.2     18.9     9.6     26.6       72.6*     26.3*     96.6**     5.6*     53.7     19.4     19.1     9.5     27.9       73.5*     26.4*     96.5**     5.8*     55.6     19.9     18.9     9.4     28.9       72.5     26.3     95.7**     5.8*     54.9     19.9     19.5     9.4     28.9 |  |  |

| <b>T</b> 11 | 1 |
|-------------|---|
| Table       |   |
| I uore      |   |

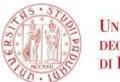
Student's t-test; \*p<0.05; \*\*p<0.0001

Table 2.

|                                         | Daily protein intake (g) |        |        | Daily BCAA protein intake (mg) |        |        | Daily Leucine intake (mg) |        |        |        | Breakfast protein intake (g) |        |        |        |        |        |
|-----------------------------------------|--------------------------|--------|--------|--------------------------------|--------|--------|---------------------------|--------|--------|--------|------------------------------|--------|--------|--------|--------|--------|
|                                         | 1 FU                     | 2 FU   | 3 FU   | 4 FU                           | 1 FU   | 2 FU   | 3 FU                      | 4 FU   | 1 FU   | 2 FU   | 3 FU                         | 4 FU   | 1 FU   | 2 FU   | 3 FU   | 4 FU   |
|                                         | (n=58)                   | (n=44) | (n=35) | (n=28)                         | (n=58) | (n=44) | (n=35)                    | (n=28) | (n=58) | (n=44) | (n=35)                       | (n=28) | (n=58) | (n=44) | (n=35) | (n=28) |
| FFM                                     | 0.31*                    | 0.35*  | 0.55*  | 0.13                           | 0.13   | 0.23   | 0.98                      | -0.17  | 0.23   | 0.30*  | 0.93                         | -0.18  | 0.18   | 0.24   | 0.36*  | 0.57   |
| FFMI                                    | 0.17                     | 0.29   | 0.58** | 0.06                           | 0.15   | 0.24   | 0.99                      | -0.19  | 0.33   | 0.18   | 0.96                         | -0.19  | 0.04   | 0.17   | 0.34   | -0.14  |
| ASM                                     | 0.04                     | 0.22   | 0.55** | 0.30                           | -0.70  | 0.14   | 0.98                      | -0.18  | -0.10  | 0.20   | 0.93                         | -0.18  | 0.09   | -0.31  | -0.12  | 0.04   |
| SMI                                     | 0.28                     | 0.08   | 0.61** | -0.14                          | 0.12   | 0.17   | 0.99                      | -0.14  | 0.29   | 0.07   | 0.99*                        | -0.04  | 0.10   | 0.37*  | 0.37*  | -0.29  |
| HG                                      | 0.29*                    | 0.37*  | 0.29   | 0.38                           | -0.20  | 0.35*  | 1.0*                      | 0.02   | 0.21   | 0.39*  | 0.98                         | -0.54  | 0.25   | 0.39*  | 0.53*  | 0.40*  |
| WS                                      | 0.23                     | 0.17   | 0.09   | 0.44*                          | 0.42   | 0.35*  | 0.02                      | 0.23   | 0.03   | 0.31*  | -0.54                        | 0.54   | 0.39** | -0.02  | 0.28   | 0.59*  |
| Dearcon coefficient: *n<0.05: **n<0.002 |                          |        |        |                                |        |        |                           |        |        |        |                              |        |        |        |        |        |

Pearson coefficient; \*p<0.05; \*\*p<0.002

(W=Weight (kg); BMI= Body Mass Index (kg/m<sup>2</sup>); WC= Waist circumference (cm); PA= Phase Angle (°); FFM=Free Fat Mass (kg); FFMI= Free Fat Mass Index (kg/m<sup>2</sup>); ASM=Appendicular Skeletal Muscle Mass (kg); SMI=Skeletal Muscle Index (kg/m<sup>2</sup>); HG= Handgrip (kg); WS= Walking Speed (cm); FU=follow up;)



Università degli Studi di Padova University of Padua PhD Courses Medical and Biomedical Sciences

## PhD COURSE "CLINICAL AND EXPERIMENTAL SCIENCES" COORDINATOR: PROF. ALBERTO FERLIN

## Curriculum "HEPATOLOGY AND TRANSPLANTATION SCIENCES"

#### MANAGING CIRCADIAN DISRUPTION DUE TO HOSPITALISATION: A RANDOMISED CONTROLLED TRIAL TESTING THE CIRCADIANCARE INPATIENT MANAGEMENT SYSTEM

Ph.D. Student: Dr. Chiara MANGINI TUTOR: Prof. Sara MONTAGNESE Ph.D. Course Clinical and Experimental Sciences Curriculum "Hepatology and Transplantation Sciences"

#### **Background and aim**

The objective of the present study was to test an inpatient management system (CircadianCare) aimed at limiting the negative impact of hospitalisation on sleep by enhancing circadian rhythmicity.

#### **Materials and Methods**

Fifty inpatients were randomised to either CircadianCare (n=25; 18 males,  $62.4\pm1.9$  yrs) or standard of care (n=25; 14 males,  $64.5\pm2.3$ ). On admission, all underwent a full sleep-wake evaluation; they then completed daily sleep diaries and wore an actigraph for the whole length of hospitalisation. On days 1 (T0), 7 (T1) and 14 (T2, if still hospitalised) salivary melatonin for dim light melatonin onset (DLMO) and 24-hour skin temperature were recorded. In addition, environmental noise, temperature and illuminance were monitored. Patients in the CircadianCare arm followed one of three schedules for light/dark, meal and physical activity timings, based on their diurnal preference/habits. They wore short-wavelength-enriched light-emitting glasses for 45 min after awakening, and short-wavelength light filter shades from 18:00 until sleep onset.

#### Results

Based on sleep diaries, there was a significant advance in bedtime for CircadianCare compared to standard of care patients between T0 and T1; similarly, DLMO time also significantly advanced. Patients sleeping near the window had significantly higher sleep efficiency, regardless of treatment arm. As noise fluctuation increased, so did the number of night awakenings, also regardless of treatment arm.

#### Conclusions

The CircadianCare management system showed positive results in terms of advancing sleep timing and the circadian rhythm of melatonin. Further, our study identified a combination of environmental noise and lighting indices, which could be easily modulated to prevent hospitalisation-related insomnia.



Università degli Studi di Padova University of Padua PhD Courses Medical and Biomedical Sciences

## PhD COURSE "CLINICAL AND EXPERIMENTAL SCIENCES" COORDINATOR: PROF. ALBERTO FERLIN

## Curriculum "MULTIDISCIPLINARY APPROACH TO RARE DISEASES"

#### POSSIBLE PREDICTORS OF TREATMENT RESPONSE TO BUROSUMAB IN ADULT PATIENTS WITH X-LINKED HYPOPHOSPHATEMIA (XLH)

Ph.D. Student: Dr. Gaetano Paride ARCIDIACONO TUTOR: Prof. Sandro GIANNINI Ph.D. Course Clinical and Experimental Sciences Curriculum "Multidisciplinary approach to rare diseases"

#### Background

X-linked hypophosphatemia (XLH) is a rare disease due to inherited mutations in the PHEX gene, characterized by excess circulating levels of Fibroblast Growth Factor 23 (FGF23), leading to lifelong renal phosphate wasting and hypophosphatemia, and thus to many musculoskeletal consequences, such as rickets/osteomalacia. XLH is conventionally treated with phosphate salts and active vitamin D to raise serum phosphate level; however, conventional treatment is burdened with adverse effects and possibly low adherence which may impair its effectiveness. In 2018, a monoclonal antibody neutralizing FGF23, burosumab, was approved by health authorities for the treatment of XLH.

#### **Material and Methods**

In this multicentric study we enrolled adult patients with a diagnosis of XLH, treated with burosumab, administered every 4 weeks for 24 weeks. Laboratory tests were performed at baseline, at midpoints and endpoints of dosing intervals (ie, 2 and 4 weeks after every dose). Patients were divided into two groups according to mean serum phosphate concentration across the midpoints: below (Group 1) or above (Group 2) the lower limit of normal (2.5 mg/dL).

#### Results

A total of 19 patients, aged 18-62 years, were included; 5 of them were classified in Group 1 and 14 in Group 2; their mean phosphate across the midpoints was respectively  $2.18\pm0.08$  and  $3.23\pm0.48$  mg/dL. We observed that patients in Group 1 compared to Group 2 had higher PTH (179.11±91.80 vs 73.93±23.60 ng/L; p = 0.001) and intact FGF23 (211.50 vs 99.31±36.60 pg/mL; p = 0.02) levels at baseline; no differences were observed in age, sex, body mass index, and baseline phosphate and TmP/GFR levels.

#### Conclusions

We hypothesize that high baseline PTH and FGF23 levels may predict a poorer response in XLH patients treated with burosumab; further studies are needed to understand if this hypothesis may lead to changes in suggested dosing schedule, targeted on patients' characteristics.

#### DEVELOPMENT OF A THREE-DIMENSIONAL *IN-VITRO* MODEL FOR THE STUDY OF EXTRA-PULMONARY GRANULOMATOUS INFLAMMATION

Ph.D. Student: Dr. Jessica CECCATO TUTOR: Prof. Carlo AGOSTINI – CO-TUTOR: Prof. Marcello RATTAZZI Ph.D. Course Clinical and Experimental Sciences Curriculum "Multidisciplinary approach to rare diseases"

#### Background

Sarcoidosis is a rare disease characterized by the formation of non-caseating granulomas, organized structures made up of macrophages, multinucleated giant cells (MGC), monocytes, lymphocytes and fibroblasts, which can potentially appear in every district of the body. Mechanisms which contribute to disease induction and maintenance are still unclear. Recent studies demonstrated the relevance of innate immunity, proving the formation of granulomas in patients with adaptive immunity defects. Therefore, a better understanding of the granuloma formation could be provided by the simultaneous dissection of the mechanisms occurring in immunodeficient patients with granuloma manifestations like Granulomatous Lymphocytic Interstitial Lung Disease (GLILD), a rare disease which occurs in patients with Common Variable Immunodeficiency (CVID). The *invitro* models currently present for sarcoidosis are not totally able to recapitulate the disease, mostly in extrapulmonary environment, and no *in-vitro* models are available for GLILD. Therefore, the aim of the project was to develop a model suitable for the study of those diseases and to investigate the mechanisms behind granuloma formation and persistence.

#### **Material and Methods**

Primary monocytes were isolated from untreated patients with sarcoidosis, CVID with or without GLILD and healthy donors, according to the local ethic committee. Cells were treated 7 days with GM-CSF and 7 days with IL-4 to be differentiated into macrophages and then fuses into MGC over a glass coverslip. Cells were then stained and analyzed by confocal microscopy. To generate the scaffold for the 3D model, human femoral bones were cut into sections approximately 2 mm thick and then subjected to decellularization to remove cellular components and maintain extracellular matrix. The effectiveness of the decellularization protocol was verified by DNA extraction and histological analysis. Seeding techniques were developed to recellularized the scaffold with primary cells. Immunofluorescence techniques were established to visualize the 3D model.

#### Results

Thanks to the techniques established to fragment and decellularize bone tissue, a ready to use physical and biological 3D support has been developed. We also established that primary monocytes were autonomously able to adhere to the 3D biological scaffold and to differentiate into MGC. At the same time, 2D analysis of the macrophage tendency to fuse into MGC has been done and the fusion index has been calculated as a ratio between the number of nuclei into MGC and the total number of nuclei. Preliminary results showed that in monocytes-derived macrophages isolated from granulomatous patients there was a higher intrinsic tendency to fuse into MGC, one of the main hallmarks of pathological granulomas (Fusion index – healthy: 6.6, n=4; non-granulomatous CVID: 8.8, n=3; GLILD: 13.1, n=1; sarcoidosis: 20.1, n=3). Samples recruiting is still ongoing.

#### Conclusions

The 3D ECM-based scaffold model we proposed represents the starting point for exploring cell-cell and cell-ECM interaction. By recreating *in-vitro* a 3D microenvironment, the model may help to clarify the role of the microenvironment during granuloma formation. Concurrently, 2D analysis highlighted a higher intrinsic tendency of pathological macrophages to form MGC. Preliminary data will be improved and then evaluated in the 3D contest.



Università degli Studi di Padova University of Padua PhD Courses Medical and Biomedical Sciences

## PhD COURSE "CLINICAL AND EXPERIMENTAL SCIENCES" COORDINATOR: PROF. ALBERTO FERLIN

## Curriculum "RHEUMATOLOGICAL AND LABORATORY SCIENCES"

#### THE CHARACTERIZATION OF CIRCULATING EXTRACELLULAR VESICLES AND MICRORNAS CARGO IN IDIOPATHIC INFLAMMATORY MYOPATHIES REVEALS DIFFERENCES ACROSS CLINICALLY DIAGNOSED MYOSITIS SUBSETS

Ph.D. Student: Dr. Michela GASPAROTTO TUTOR: Prof. Margherita ZEN - CO-TUTOR: Prof. Mariele GATTO Ph.D. Course Clinical and Experimental Sciences Curriculum "Rheumatological and Laboratory Sciences"

#### Background

Idiopathic inflammatory myopathies (IIM) are a rare group of heterogeneous autoimmuneassociated muscle disorders with a specific spectrum of muscular and extra-muscular involvement along, in most cases, with a serologic signature defined by specific and associated autoantibodies. Comprehension of the underlying pathogenesis is still partial but updated knowledge demonstrates differences for each disease subtype and involves inflammatory, innate, and adaptive immune abnormalities in association with non-immune mechanisms. Our study aims to explore the circulating EVs pool in patients with IIM and potential correlates with clinical and laboratory features of the disease.

#### **Material and Methods**

64 adult ( $\geq$ 18 years old) patients affected with IIM and followed-up at the Unit of Rheumatology of Padova University Hospital and 65 sex-matched healthy donors (HDs) were enrolled in the study. Intact EVs were isolated, through size exclusion chromatography and ultrafiltration, from plasma samples of each participant. A quantitative analysis of EVs concentration was then performed. Subsequent EVs microRNAs (mRNAs) extraction, amplification, and quantification was obtained through the next generation sequencing technology from samples of 47 patients and 49 HDs. 123 miRNA were selected for the comparison analysis based on an established expression cut-off (average read count cutoff of  $\geq$ 2,5/group and expressed in at least 30 subjects/group). The bioinformatic analysis allowed a comparative evaluation of the differential miRNA expression profile between HDs and IIM patients and in different clinical subsets.

**Results:** Patients with IIM had a significantly higher concentration of circulating EVs compared to HDs (p=0.0073). Among patients, those with a cancer-associated myopathy (CAM) had the highest level of circulating EVs (p=0.006). The EVs concentration was higher in disease remission compared to active disease (p=0.0087). Among treated patients, those who had received rituximab were characterized by a significantly lower circulating EVs concentration compared to other immunosuppressive therapies (p<0.0001). After miRNA bioinformatic analysis, six miRNA (miR-2223-3p, miR-15a-5p, miR-451a, miR-486-5p, miR32-5p, miR-222-3p) resulted significantly higher expressed in the group of patients compared to HDs while 3 miRNA (miR-141-3p, miR-142-3p e let-7a-5p) were significantly hyper expressed in HDs compared to patients. MiR451a and miR-486-5p were significantly higher in CAM compared to HDs. MiR-148a-3p and miR-335-5p were significantly increased in the dermatomyositis group with respect to anti-synthetase group. Treatment with corticosteroids induced a significant increase of miR-4433b-5p, miR-92a-3p, and let-7f-5p in comparison to corticosteroids plus immunosuppressants, while miR-27a-3p was significantly reduced.

**Conclusions:** This study provides evidence of EVs and miRNA implication in IIM pathogenesis and development. EVs and EVs-miRNA concentration and expression level were indeed influenced by disease phenotype, activity, duration, and treatment, suggesting their potential role as disease biomarkers.



University of Padua PhD Courses Medical and Biomedical Sciences

# PhD COURSE "DEVELOPMENTAL MEDICINE AND HEALTH PLANNING SCIENCES"

**COORDINATOR: PROF. GIANNI BISOGNO** 

Curriculum "ONCOHEMATOLOGY, MEDICAL GENETICS, RARE DISEASES AND PREDICTIVE MEDICINE"

#### IMPACT OF ANTIBIOTIC STEWARDSHIP PROGRAMS ON ANTIBIOTIC PRESCRIPTIONS IN PEDIATRIC SETTING

Ph.D. Student: Dr. Giulia BRIGADOI TUTOR: Prof. Liviana DA DALT – CO-TUTOR: Dr. Daniele DONA' Ph.D. Course Development Medicine and Health Planning Science Curriculum "Oncohematology, Medical Genetics, Rare Diseases and Predictive Medicine"

#### Background

Antibiotics are the most commonly prescribed drugs for children worldwide, both in hospital and community settings. However, it has been demonstrated that up to 30% of antibiotic prescriptions are unnecessary or inappropriate, and many children receive broad-spectrum antibiotics for viral infections. This overuse and misuse of antibiotics have led to an increase in antibiotic resistance.

Antimicrobial Stewardship Programs (ASPs) have proven effective in reducing inappropriate antimicrobial use and resistance, enhancing patient safety, and lowering drug costs. While ASPs are widely used in adult settings, they are not as frequently implemented in pediatric settings. Furthermore, Italy currently lacks a pediatric Stewardship plan or network. The primary objective of this study was to evaluate the impact of multistep ASP in a pediatric ward over eight years.

#### **Material and Methods**

This quasi-experimental study aims to assess variations in antibiotic prescriptions for various infectious syndromes in children admitted to the Pediatric Acute Care Unit (PACU) of Padua University from October 2014 to August 2022.

Starting from October 2015, a multistep stewardship program was introduced in our Department. Daily prescriptions were collected and analyzed, taking into account the type of antibiotics and their classification according to the AWaRe classification. Variations in antibiotic prescriptions were evaluated by considering the number of antibiotics prescribed and the Days of Therapy (DOT) per 1000 patient days. The results were visualized through p-control charts.

#### Results

From October 1st, 2014, to August 31st, 2022, 7,229 children were admitted to the PACU, with 3,216 included in our study. The number of patients receiving antibiotics decreased over time: 52.2% in the pre-implementation period, 44.6% in the post-implementation period, and 37.6% in the COVID-19 period (p < 0.001). The Days of Therapy (DOT) per 1000 patients day for Watch antibiotics was notably high during the pre-implementation period, surpassing twice the value of Access antibiotics. In the post-implementation period, the DOT/1000 patient days of Watch antibiotics started to decline, becoming more or less similar to Access antibiotics in the latter half. During the COVID-19 period, following an increase in DOT/1000 patient days of Watch antibiotics in the first trimester, there was a shift, and DOT/1000 patient days of Watch antibiotics became lower than that of Access antibiotics.

#### Conclusions

A multistep Antimicrobial Stewardship Program (ASP) has effectively transformed antibiotic usage for most infectious syndromes treated in our PACU. Given the favorable outcomes achieved through its implementation in a single setting, our future perspective involves extending these strategies to other environments.

Two distinct projects are prepared to commence in September 2023: CHOICE, a multicenter Italian study encompassing 12 different pediatric emergency departments, which focuses on implementing clinical pathways for pharyngitis, acute otitis media, and pneumonia; and TEAMCOACH, a European initiative involving a pediatric network in Italy, Greece, and Spain aiming to disseminate knowledge about ASP and Infection Prevention and Control practices within pediatric settings (pediatric wards and pediatric intensive care units).

#### DEVELOPMENT OF AN EX VIVO GENE THERAPY FOR INFANTILE GM1-GANGLIOSIDOSIS

Ph.D. Student: Dr. Linda BUCCIARELLI TUTOR: Prof. Alessandra BIFFI – CO-TUTOR: Dr. Valentina POLETTI Ph.D. Course Development Medicine and Health Planning Science Curriculum "Oncohematology, Medical Genetics, Rare Diseases and Predictive Medicine"

GM1-gangliosidosis (GM1, OMIM #230500) is a rare, genetic condition resulting from deficiency of the lysosomal enzyme  $\beta$ -Galactosidase ( $\beta$ -Gal). The subsequent accumulation of undegraded gangliosides and other metabolites in the lysosomal compartment, lead to cell and organ damage culminating in a fatal neurodegeneration. To date, there is no cure for GM1, and the rapid and severe progression of the disease would require a therapy providing a prompt and robust enzyme delivery in the central nervous system coupled to a systemic biodistribution of the therapeutic enzyme.

In this context, *ex vivo* Gene Therapy (GT), i.e. the autologous transplantation of Hematopoietic Stem/Progenitor Cell (HSPCs) genetically-corrected by lentiviral gene transfer, may represent a valuable therapeutic option for GM1, as proven for other LSDs in multiple preclinical and pivotal clinical studies. The replacement of dysfunctional microglia with metabolically competent myeloid progeny secreting the therapeutic enzyme offers the opportunity to restore lysosomal function, mitigate cellular and tissue damage, and ultimately alleviate the neurodegenerative effect of GM1.

With the aim of developing an innovative *ex vivo* GT strategy for GM1, we designed lentiviral vectors (LVs) expressing either a codon-optimized sequence of the human *GLB1* gene, or the murine *Glb1* cDNA, informed by published research testifying a higher enzyme activity of the murine enzyme with respect to the human counterpart. The two LV constructs were produced at a high titer, and were able to efficiently transduced multiple human cell lines and primary cells, providing a stable and lasting transgene expression.

The therapeutic potential of our LV constructs was firstly evaluated in GM1-patient primary fibroblasts, LV transduction resulted in a dose-dependent supraphysiological enzyme activity with an average VCN of  $\geq$  3, stable metabolic correction and enzyme secretion, proven by the rescue of storage material as early as two weeks post-transduction. Following the in vitro characterization of the two LVs constructs, we proceeded to an in vivo proof-of-concept of efficacy and feasibility study in the murine model of the disease, represented by GM1 mice. These mice are a valuable disease model as they show neurological symptoms by 18-20 weeks of age, and succumb to the disease by 40 weeks of age. The animal study included Busulfan-myeloablated 8-weeks old GM1 mice receiving *Glb1<sup>-/-</sup>* HSPCs transduced with the huβ-gal LV, muβ-gal LV, or a control LV expressing GFP, or wild-type (wt) cells to mimic allogeneic HSC transplantation. Control groups included wt mice receiving mock-transduced cells, or untreated wt and GM1 mice. The study is currently on-going. The interim results thus far suggest a significant reconstitution of the enzymatic activity, comparable to wild type levels, in the peripheral blood mononuclear cells of mice receiving HSPCs transduced with the mu\beta-gal LV (VCN ~ 2), and of about the ~50% of wild type when the huß-gal LV was used, despite a higher vector content was achieved with the latter vector as compared to the murine counterpart (VCN  $\sim$  6). This biochemical correction was associated to an amelioration of the neuromuscular phenotype of the treated versus control mice, as assessed by multiple behavioral tests, and to an extended survival of the former up to the end of the study (50 weeks of age).

In summary, our GT strategy hold the promise to significantly mitigate the phenotype of GM1 mice. Interestingly, the mu $\beta$ -gal LV provided an advantageous dose-effect profile suggesting novel direction for optimization of clinically translatable LVs.

These finding underscore the potential translational impact of our *ex vivo* GT approach to treat GM1-gangliosodosis but also the importance of further refinement.

#### INTESTINAL ORGANOIDS: A MODEL TO STUDY NECROTIZING ENTEROCOLITIS (NEC) MECHANISMS AND THE INFLUENCE OF MODULATING AGENTS ON THE INTESTINAL EPHITELIAL INJURY

#### Ph.D. Student: Dr. Miriam DUCI TUTOR: Dr. Francesco FASCETTI-LEON Ph.D. Course Development Medicine and Health Planning Science Curriculum "Oncohematology, Medical Genetics, Rare Diseases and Predictive Medicine"

#### Background

Necrotizing Enterocolitis (NEC) is a devastating neonatal disease, imposing an ever-increasing burden on both families and society. Despite the continuous strides in neonatal care and ongoing research endeavours, the mortality rates persist at around 30-50%. The intricate variability inherent in NEC's pathogenesis has rendered it a major unsolved clinical challenge, impervious to comprehensive solutions. To transcend the challenges posed by the variability in patients attributes and disease manifestations, the *in-vitro* models are being devised. These models seek to understand the intricate cellular mechanisms underpinning the disease, alongside the assessment of therapeutic interventions' efficacy. While various NEC models have been used, existing single-cell models fall short in capturing the intricate interplay between diverse intestinal cell types. Against this backdrop, intestinal organoids emerge as a promising paradigm, offering the potential to emulate native tissue architecture and function in a multicellular culture setting. Considering these developments, our goal is to establish an *ex-vivo* model employing human intestinal organoids to investigate cellular mechanisms in NEC development.

#### **Material and Methods**

Using an approved ethical protocol, we obtained biopsies from the small intestine of infants undergoing resection due to non-inflammatory conditions. Prior to analysis, the intestinal segments underwent thorough examination to confirm the absence of histological inflammation. Afterwards, the tissue underwent mechanical dissociation to release crypts, followed by filtration and centrifugation to isolate the crypts. The isolated crypts were suspended in Matrigel growth factor-reduced matrix. Organoids were then cultured in enteroid growth media that was replaced every 2 days. Once the organoids reached a state of maturity, the damage to simulate NEC was applied. The intestinal injury was investigated by assessing occludin expression.

#### Results

We developed a 3D-NEC model, based on intestinal organoids derived from biopsies of infants. The organoids have been obtained from both frozen and fresh samples demonstrating comparable robustness across the two sources. Employing this model, we performed a comprehensive characterization using phalloidin, occludin and proliferation marker (Ki67). Once organoids reached the maturity state, to reproduce NEC damage, we subjected the organoids to a 48-hour exposure to lipopolysaccharide (LPS). Tight junction marker showed an internal ring immunostaining pattern in the control organoids which was disrupted after exposure to LPS.

#### Conclusions

With this project, we have created a highly replicable *ex-vi*vo model capable of showing in depth the cellular mechanisms involved in NEC. The utilization of organoids within this context has yielded a powerful *ex-vivo* system that enables a comprehensive exploration of intestinal pathophysiology, particularly in the early intestinal disorders. In the future, hopefully this model's applicability extends beyond understanding pathogenesis, into testing potential therapeutic pharmaceuticals and gene- modulators ex vivo for validation prior to human trials.

#### THE MATURATION OF APERIODIC EEG ACTIVITY ACROSS DEVELOPMENT REVEALS A PROGRESSIVE DIFFERENTIATION OF WAKEFULNESS FROM SLEEP

Ph.D. Student: Dr. Jacopo FAVARO TUTOR: Prof. Irene TOLDO – CO-TUTOR: Prof. Stefano SARTORI Ph.D. Course Development Medicine and Health Planning Science Curriculum "Oncohematology, Medical Genetics, Rare Diseases and Predictive Medicine"

#### Background

During development, the brain undergoes radical structural and functional changes following a posterior-to-anterior gradient, associated with profound changes of cortical electrical activity during both wakefulness and sleep. However, a systematic assessment of the developmental effects on aperiodic EEG activity maturation across vigilance states is lacking, particularly regarding its topographical aspects.

#### **Material and Methods**

Here, in a population of 160 healthy infants, children and teenagers (from 2 to 17 years, 10 subjects for each year), we investigated the development of aperiodic EEG activity in wakefulness and sleep. Specifically, we parameterized the shape of the aperiodic background of the EEG Power Spectral Density (PSD) by means of the spectral exponent and offset; the exponent reflects the rate of exponential decay of power over increasing frequencies and the offset reflects an estimate of the y-intercept of the PSD.

#### Results

We found that sleep and development caused the EEG-PSD to rotate over opposite directions: during wakefulness the PSD showed a flatter decay and reduced offset over development, while during sleep it showed a steeper decay and a higher offset as sleep becomes deeper. During deep sleep (N2, N3) only the spectral offset decreased over age, indexing a broad-band voltage reduction. As a result, the difference between values in deep sleep and those in both light sleep (N1) and wakefulness increased with age, suggesting a progressive differentiation of wakefulness from sleep EEG activity, most prominent over the frontal regions, the latest to complete maturation. Notably, the broad-band spectral exponent values during deep sleep stages were entirely separated from wakefulness values, consistently across developmental ages and in line with previous findings in adults. Concerning topographical development, the location showing the steepest PSD decay and largest offset shifted from posterior to anterior regions with age. This shift, particularly evident during deep sleep, paralleled the migration of sleep slow wave activity and was consistent with neuroanatomical and cognitive development.

#### Conclusions

Overall, aperiodic EEG activity distinguishes wakefulness from sleep regardless of age; while, during development, it reveals a postero-anterior topographical maturation and a progressive differentiation of wakefulness from sleep. Our study could help to interpret changes due to pathological conditions and may elucidate the neurophysiological processes underlying the development of wakefulness and sleep.

#### PET/MR APPLICATION FOR LUNG NODULES IN PEDIATRIC SARCOMA AT STAGING: RESULTS OF A PRELIMINARY STUDY

Ph.D. Student: Dr. Giulia FICHERA TUTOR: Prof. Gianni BISOGNO – CO-TUTOR: Dr. Chiara GIRAUDO Ph.D. Course Development Medicine and Health Planning Science Curriculum "Oncohematology, Medical Genetics, Rare Diseases and Predictive Medicine"

#### Background

Lungs are the most common site of metastasis in children and adolescents with bone and soft tissue sarcomas and chest Computed Tomography (CT) is recommended for their detection. Hybrid imaging such as <sup>18</sup>F-FDG- PET/CT or PET/MR allowing simultaneous acquisition of diagnostic images and metabolic information are useful to evaluate loco-regional and distant metastases. PET/MR offers low radiation exposure and higher soft-tissue contrast allowing a better diagnostic performance for this group of tumors although it cannot be overlooked that the MR component is less accurate for pulmonary assessment. In the last years, the technical improvements improved the lung evaluation also by MR.

Thus, the aim of our study was to evaluate the diagnostic performance of PET/MR for pulmonary nodules in pediatric patients with sarcoma examined at staging.

#### **Material and Methods**

Pediatric patients (< 18 years) with histologically proven bone or soft tissue sarcoma who underwent a whole-body PET/MR and a chest CT scan for staging were included in this retrospective study. One radiologist with five years of experience in oncological imaging assessed lung nodules (size, location, and FDG-avidity) on PET/MR images, including chest MR sequences such as T1w CAIPIRINHA Water, TIRM, and inverted TIRM. Sensitivity and specificity were computed to evaluate the diagnostic performance of PET/MR using the contrast-enhanced chest CT performed at diagnosis as gold standard.

#### Results

Fifty-nine patients matched the inclusion criteria (28 females; mean age  $9\pm4.9$  years), 29 (74.6%) affected by rhabdomyosarcoma, and thirteen with lung metastasis at diagnosis. A total of 36 nodules (range size 2-15 mm) were detected. Left lower lobe was the most commonly affected area (8 nodules). TIRM and inverted TIRM showed same sensitivity of 84.62% (95%, CI: 54.55-98.08%, each), but TIRM demonstrated a higher specificity (86.96% and 89.13%, respectively). The T1w CAIPIRINHA showed low sensitivity (60%) but high specificity (100%). PET also showed similar results with a sensitivity of 30.77% (95%, CI: 9.09-61.43%) and specificity of 97.83% (95%, CI: 88.47-99.94%).

#### Conclusions

PET/MR demonstrated a good performance in the diagnosis of lung nodules for children with sarcoma at staging.

#### **Clinical relevance**

PET/MR is an excellent diagnostic tool for pediatric oncological imaging, combining the high soft tissue contrast of MR, the metabolic information of PET, and a low radiation dose.

#### MID TERM ELECTRICAL REMODELING AFTER PERCUTANEOUS ATRIAL SEPTAL DEFECT CLOSURE WITH GCO DEVICE IN A PEDIATRIC POPULATION

Ph.D. Student: Dr. Jennifer FUMANELLI TUTOR: Prof. Giovanni DI SALVO – CO-TUTOR: Dr. Loira LEONI Ph.D. Course Development Medicine and Health Planning Science Curriculum "Oncohematology, Medical Genetics, Rare Diseases and Predictive Medicine"

#### Background

Ostium secundum Atrial Septal Defect (ASD) is a common congenital heart defect, found in about 1.0/1.000 live births and leads to right chamber volume overload, pulmonary hypertension, systemic embolism, atrial arrhythmias and premature death over a long-term follow-up. Atrial arrhythmias are well known long-term complications of ASD, possibly due to chronic right atrial volume overload and resulting stretch. In addition, also in other congenital and acquired heart diseases, P-wave and QTc dispersion are well-known predictors of arrhythmias and are often considered as prognostic factors of morbidity and mortality. The GORE® CARDIOFORM septal occluder is an atrial septal defect/patent foramen ovale closure device with theoretical advantages over other commercialized devices thanks to its softness and anatomical compliance. Our aim was to evaluate the short and medium-term electrocardiographic changes after percutaneous ASD closure with GCO in a pediatric population.

#### **Material and Methods**

This was a prospective single-arm study performed at the Pediatric Cardiology and GUCH Unit of the Heart Hospital "G. Pasquinucci" of Massa and the Pediatric Cardiology Unit of the University of Padua. We enrolled 39 pediatric patients (age 5-18 years) with isolated ASD submitted to transcatheter closure with GCO from January 2020 to June 2021. The following patients were excluded from the study: (i) patients with sinus venosus or primum type ASD, (ii) patients with inadequate rims, (iii) patients with significant cardiac/extra-cardiac comorbidities. EKG was performed before, at 24 hours and 6 months after ASD transcatheter closure. P wave dispersion, QTc ed QTc dispersion were calculated. We performed EKG Holter recording at 6-months after device implantation.

#### Results

Patients' age and BSA were  $8.2\pm4.2$  years and  $1.0\pm0.3$  m2 respectively. At the baseline mean P wave dispersion was  $40\pm15$  msec and decreased at 24h (p<0.002), without any further change at 6 months. PR conduction significantly improved at 24 h from device implantation (p=0.018) and did not significantly change at 6 months. Absolute QTc value did not significantly changed at 24, but significantly improved at 6 months from the procedure (p=0.03). QTc dispersion decreased at 24 hours (p<0.02) and at 6 months (p<0.002) from device implantation. After device deployment, 2 pts developed transient, self-limited junctional rhythm. One of them needed a short course of Flecainide for supra-ventricular tachycardia. No tachy/brady-arrhythmias were recorded at the 6-months follow-up ever.

#### Conclusions

Percutaneous ASD closure with the GCO device results in significant, sudden improvement of intra-atrial, atrio-ventricular and intraventricular electrical homogeneity. These favorable electrical changes persist unaltered over a mid-term follow-up, possibly due to a positive right heart volumetric remodeling not hindered by the mechanical impact of the occluding device and could explain the low rate of cardiac arrhythmias found at the mid-term ambulatory ECG evaluation in this series.

#### NEOGLUCONTROL STUDY – NEONATAL BRAIN OXYGENATION AND GLUCOSE CONTROL: METABOLOMIC FINGERPRINTS OF HYPOGLYCEMIA

Ph.D. Student: Dr. Silvia GUIDUCCI TUTOR: Prof. Eugenio BARALDI – CO-TUTOR: Dr. Alfonso GALDERISI Ph.D. Course Development Medicine and Health Planning Science Curriculum "Oncohematology, Medical Genetics, Rare Diseases and Predictive Medicine"

#### Background

Preterm infants have high risk of glucose instability, a preventable cause of brain injury influencing long-term neurodevelopment outcomes. The aim of the project is to identify the impact of glycaemic fluctuation on neuronal functions combining simultaneous monitoring of glucose blood level by means of Continuous Glucose Monitoring (CGM) with two indicators of brain activity: the regional changes in cerebral blood volume and brain oxygenation, measured through Diffuse Optical Tomography (DOT) and the modification of metabolic pathways involved in cellular energy and neurotransmitters' regulation, detected with metabolomic analysis. All these results are then related to neurodevelopment outcome evaluated at 1 and 2 years of life.

#### **Material and Methods**

Participants were preterm infants born at  $\leq$ 32 weeks' gestation or with a birthweight <1500g. CGM sensor was placed within 48 hours from birth for 5 days. The euglycaemic range is set at 72-144mg/dL, values below 72mg/dL and above 144mg/dL are considered hypoglycaemia and hyperglycemia, respectively. Simultaneously to CGM, DOT was adopted to monitor changes in brain oxygenation of 5 areas: frontal, left and right temporal, central posterior, occipital. Urinary and blood sample were collected at baseline, then blood samples were collected after 48 hours and 120 hours. Neurodevelopment assessment was conducted at 12 and 24 months corrected age by the Bayley Scales of Infant and Toddler Development III and by two paradigms, gap-overlap task and simultaneous stream change detection task, for the investigation of precursors of executive function. **Results** 

We enrolled 60 patients with CGM data available for 52. 26 patients (50%) were females; the average gestational age and birth weight were respectively 29.6±3.1 weeks and 1281±367 g. The average CGM recording was 81.1±29.3 h. The average time spent in hypoglycaemia and hyperglycaemia was 9% and 15% respectively with an average coefficient of variation (CV) of 0.20±0.06. Currently, neurodevelopment assessment was available at 12 months corrected age for 29 participants, 12 (41%) females. Average Bayley-III scores were cognitive 98±15, communication 93±12, motor 92±12 and socioemotional 98±13. A simple regression analysis showed a negative correlation between hypoglycaemia, hyperglycaemia, CV and Bayley-III communication score, even if statistically significant only for CV ( $\beta$  -0.223; p-value 0.028). The analysis of DOT from a single participant showed changes in cerebral blood volume in case of hypoglycaemia, mainly in right hemisphere and more pronounced in case of severe hypoglycaemia. Based on data in adults, we hypothesized a neurotoxic pathway triggered by glycaemic instability: hypoglycaemia seems to increased 3-OH-kynurenine, a tryptophan metabolite that can be converted into quinolinic acid, a neurotoxic metabolite involved in neurodegenerative process. Urine and blood samples collected during the enrolment will be processed through untargeted and targeted metabolomic analysis focusing on this metabolic pathway.

#### Conclusion

We showed the impact of glycaemic variability on regional brain oxygenation and the effect on long-term neurological outcome; metabolome analysis could give more advice for identifying neonates at risk for neurodevelopmental impairment related to glycaemia. If these preliminary results will be confirmed, the integration of CGM, DOT and metabolome could be a new instrument for clinicians to individualize glucose intake and improve neurodevelopmental outcome of preterm infants.

#### ADVANCING LEUKEMIC NICHE MODELING: A FOCUS ON AML-3D MODELS AND AML-MSCs SECRETOME IN PEDIATRIC AML

#### Ph.D. Student: Dr. Giorgia LONGO TUTOR: Prof. Martina PIGAZZI – CO-TUTOR: Dr. Claudia TREGNAGO Ph.D. Course Development Medicine and Health Planning Science Curriculum "Oncohematology, Medical Genetics, Rare Diseases and Predictive Medicine"

**Background:** Acute myeloid leukemia (AML) is a life-threatening disease in childhood, and chemotherapy is still the cornerstone of treatment. One of major limitations in new drug development is the low predictivity of the pre-clinical models. Thus, it is urgent to develop three-dimensional (3D) models that recapitulate the AML microenvironment, which plays a pivotal role in regulating hematopoiesis, secreted molecules, and cell-cell interactions. In this study we aim investigating the role of the leukemia BM microenvironment by creating a model of the bone marrow (BM) niche, with the final goal to perform robust pharmacological and immunotherapeutic screenings to improve AML treatment strategies.

**Material and Methods:** We previously generated a niche by co-culturing Mesenchymal Stromal Cells (MSCs) and AML blasts in a scaffold made up of hydroxyapatite and collagen type I. We documented that the MSCs derived from patients with AML (AML-MSCs) undergo to a gene expression reprogramming that modify their functions and secretome (Borella G. et al Blood 2021). Here, to deep into the AML-MSCs secretome we used Mass Spectrometry and an induced pluripotent stem cells (iPSCs) model. To mimic the heterogeneous composition of the BM microenvironment we implemented the previous 3D model by adding endothelial cells (ECs), monocytes and Schwann cells. We tested the 3D bioprinting for generating a leukemic BM niche.

Results: By Mass Spectrometry we detected 17 new synthesized secreted factors by AML-MSCs with respect to healthy MSCs (h-MSCs) cultured in 3D. We focused on the most 3 upregulated factors. We co-cultured h-MSCs with CD34pos cells with or without the 3 factors in comparison with CD34pos cultured on a layer of AML-MSCs. We demonstrated that CD34pos cells, when cultured with AML-MSCs or with h-MSCs + 3 factors, exhibited a reduced proliferation (0.6 -fold decrease by Ki-67+, p<0.01), maintained the CD34 expression (1.9-fold and 1.5-fold increase, respectively), and increased colonies number (2.3-fold increase p<0.05) with respect to CD34 pos cultured with h-MSCs alone. We documented that the 3 factors supported the stemness of the CD34 pos cells like the AML-MSCs whole secretome, contributing to block the hematopoietic differentiation. Moreover, we induced iPSCs differentiation toward the myeloid lineage with or without the 3 factors. We observed that both, the addition of AML secretome or of the 3 factors triggered the maturation of part of CD34pos cells into macrophages observed by morphology (5.7 and 4-fold increase of number of macrophages) and by flow cvtometry (2 and 1.1-fold CD68 expression increase) suggesting that these 3 factors secreted by the AML-MSCs are key players in deregulating the healthy hematopoiesis during leukemia. To deep into the BM niche cell composition, we introduced different cell types in our 3D model testing various cell numbers, culture conditions, and timing. We established seeding 100.000 MSCs, 100.000 ECs and 5.000 Schwann on day-7, 12.500 monocytes on day-4, and 400.000 primary AML blasts on day0. We measured cell viability of the system from day0 to day+21 finding that the microenvironment reached the highest proliferation at day 7 and then lightly decreases (16%) up to day+21, whereas we assessed its supportive effects on AML blasts proliferation which gradually increased up to day+21 (n=3). This latter finding was confirmed by flow cytometry and immunofluorescence since all cell types were transduced with a fluorescent-reporter gene. A preliminary experiment by using the 3D bio-printing was also performed, but cellular viability decreased from day+7 of culture and dramatically drop out at day+14 suggesting this technology not suitable for liquid tumors.

**Conclusions:** We found 3 new factors supporting leukemia microenvironment. The improvement of the 3D model with different cell types will help to dissect how leukemic niche secretome supports AML and disadvantages the hematopoiesis. By elucidating leukemia progression key players in 3D we will identify novel targeted treatments to definitively clear AML blasts.

#### DECIPHERING METABOLIC ALTERATIONS IN CHEMORESISTANT MEDULLOBLASTOMA CELLS: THE INFLUENCE OF FATTY ACID METABOLISM

Ph.D. Student: Dr. Lorenzo MANFREDA TUTOR: Prof. Giampietro VIOLA – CO-TUTOR: Dr. Roberta BORTOLOZZI Ph.D. Course Development Medicine and Health Planning Science Curriculum "Oncohematology, Medical Genetics, Rare Diseases and Predictive Medicine"

#### Background

Medulloblastoma (MB) is a highly aggressive central nervous system tumor that primarily affects children under the age of 10. Despite multimodal treatment approaches, including surgery, chemotherapy, and radiotherapy, MB patients often experience tumor recurrence (20-30%), and the most aggressive cases have a very poor overall survival rate (40-50%).

The rarity of this tumor and the lack of matched samples of diagnosis and relapse make the study of recurrence a difficult challenge to overcome. In this context, we established an in vitro model of MB resistance to chemotherapy by weekly exposing MB cell lines to a cocktail of chemotherapeutics commonly used in MB treatment (Vincristine, Etoposide, Cisplatin, Cyclophosphamide – VECC).

#### Material and Methods

To evaluate mitochondrial morphology and the lipid content in the cells, both flow cytometry and confocal microscope analysis were carried out using MitotrackerGreen/DeepRed and the Bodipy493-503 respectively. The evaluation of the FAO rate and uptake of FA was measured through the use of the BodipyFL-C16 under confocal microscopy and flow cytometry respectively. The enzymatic activity of ETC complexes and citrate synthase (CS) was measured spectrophotometrically using a Cary UV 100 spectrophotometer (Varian). All these analyses were integrated by the use of Western Blot and Seahorse XFe96 Analyzer. Preliminary untargeted Metabolomics was performed using UHPLC-Q Exactive<sup>TM</sup> mass spectrometer with ESI source (Thermo Scientific).

#### Results

Multi-omics data analysis highlights metabolism as one of the most deregulated hallmarks in MBresistant cells, with enrichment in terms like fatty acid metabolism, amino acid metabolism, pyruvate metabolism, TCA cycle, mitochondrial biogenesis, and oxidative phosphorylation. Functional validation of these data reveals dramatic changes in mitochondrial morphology and function in chemotolerant cells, with enhanced activity of respiratory chain enzymes. Moreover, we demonstrated an increase in the uptake and beta-oxidation of long-chain fatty acids, such as palmitate. As a consequence, resistance cells acquired a heterogeneous accumulation of lipids within lipid droplets, both in terms of number and size. Those data are corroborated by preliminary untargeted metabolomics that reveals a clear and distinct metabolic and lipidomic profile.

These findings suggest potential avenues for further investigation into the metabolic mechanisms underlying cellular adaptation to chemotherapy. In this context, targeting fatty acid metabolism reveals a vulnerability to be exploited to overcome chemotherapy resistance in resistant medulloblastoma.

#### Conclusions

Recent studies highlight the relevance of the metabolic plasticity of cancer cells in chemotherapy adaptation and in the maintenance of high antioxidant power and macromolecule biosynthesis, to counteract the damage caused by chemotherapy. Our data suggest that MB-resistant cells change their metabolic behaviour and enhance their dependency on FAO required to sustain the increased OXPHOS, revealing a novel vulnerability to selectively target chemotolerant MB cells.

### EMERGING ROLE OF BAG6 AS CANCER CELL PLASTICITY REGULATOR IN MEDULLOBLASTOMA

Ph.D. Student: Dr.ssa Chiara MARCHIORO TUTOR: Prof. Giampietro VIOLA– CO-TUTOR: Dr. Elena MARIOTTO Ph.D. Course Development Medicine and Health Planning Science Curriculum "Oncohematology, Medical Genetics, Rare Diseases and Predictive Medicine"

#### Background

Medulloblastoma (MB) is the most common malignant brain tumor of childhood and, despite a multimodal therapeutic approach, approximately 30% of patients experience tumor relapse. Recurrences arise from resistant cells that are able to escape chemotherapy, through different mechanisms such as the overexpression of the antiapoptotic Bcl-2 associated-athanogene (BAGs) family proteins. BAGs proteins are mainly reported as Hsp70 co-chaperones, as well as regulators of apoptosis and autophagy, while their role in cancer cell differentiation has never been investigated. In particular, the most divergent member of the family, namely BAG6, is highly expressed in medulloblastoma (MB) resistant cells and it is upregulated in response to chemotherapy stress, thus suggesting possible role for BAG6 in chemotherapy resistance.

#### **Material and Methods**

In order to investigate the role of BAG6, a BAG6-depleted MB cell line was exploited for this project. RNA-seq data analysis was then performed to identify differential gene expression in BAG6 silenced cells, and then confirmed by Western Blot and Immunofluorescence analysis. In addition, through an Immunoprecipitation-Mass Spectrometry (IP-MS) approach, BAG6 interactome analysis was performed in order to understand the mechanisms by which BAG6 is able to drive MB cell fate.

#### Results

The depletion of BAG6 induces a drug tolerant phenotype to chemotherapeutic agents used for MB treatment. Transcriptomic analysis of BAG6-depleted MB cells reveals the downregulation of neuron differentiation program, in favor of the upregulation of muscle cell development gene ontology terms, especially *Mef2* and *MyoD1* muscle differentiation transcription factors. In particular, BAG6 depletion modulates the expression levels of both stemness and neural progenitor markers, hence possibly blocking MB cells into a transit-amplifying progenitor status. Accordingly, BAG6-depleted cells display a proliferative advantage *in vivo*, and increased c-Myc levels, a major driver oncogene in MB. A negative enrichment in genes involved in cell-cell and cell-substrate adhesion was also observed, underlying the acquisition of epithelial-to-mesenchymal transition (EMT) features. Accordingly, a peculiar spindle-shaped subpopulation was observed in BAG6-depleted MB cells expressing muscle specific proteins, such as Desmin and Myosin heavy chain (MyHC). Lastly, BAG6 interactome analysis reveals that the transcriptional repressor for myogenic and neural differentiation, OTX2, interacts with BAG6 thus strengthening an unprecedented role for BAG6 as a fundamental player for cells differentiation.

#### Conclusions

Collectively, these results demonstrate that BAG6 depletion is sufficient to reprogram MB cells to a muscle cell fate, typical of pre-somitic mesoderm progenitors. Future studies on the regulation of BAG6 gene during brain and muscle development will pave the way to recognize the role of the BAG6 protein as a master regulator of neuronal/muscle cell fate and its possible involvement in the pathogenesis of rare and particularly aggressive medullomyoblastoma.

#### BONE STATUS IN IUGR PRETERM NEWBORNS: POSSIBLE INFLUENCES OF NUTRITIONAL INTAKES

Ph.D. Student: Dr. Marta MENEGHELLI TUTOR: Prof. Eugenio BARALDI – CO-TUTOR: Dr. Giovanna VERLATO Ph.D. Course Development Medicine and Health Planning Science Curriculum "Oncohematology, Medical Genetics, Rare Diseases and Predictive Medicine"

**Background:** Intrauterine growth restriction (IUGR) refers to a condition in which a fetus is unable to achieve its genetically determined potential size. The combination of IUGR and preterm birth is especially harmful for bone health. In these preterm infants, special nutritional care is required to promote growth and bone development.

**Material and Methods:** We enrolled patients admitted to the Neonatal Intensive Care Unit (NICU) of University Hospital of Padova < 34 weeks of gestational age (GA) within 72 hours from birth, receiving total parenteral nutrition (TPN) within 48 hours of life, with informed consent for participation. Each IUGR newborn was matched with a non IUGR patient and anthropometry, biochemistry and bone quantitative ultrasound to assess bone status (metacarpus bone transmission time, mcBTT) were measured prospectively from birth till 36 weeks of GA together with nutritional data.

Results: 354 preterm infants were enrolled from January 2017 until May 2022. Among these, 75 IUGR were matched with 75 non IUGR infants with same GA, followed up until discharge. IUGR infants at birth and at 21 days of life presented a worse bone status (lower mc-BTT, metacarpal bone transmission time) than non IUGR (mcBTT mean±standard deviation at birth: 0.45±0.10 vs 0.51±0.09; p=0.0005; at 21 days: 0.43±0.08 vs 0.46±0.09; p=0.0401), while no significant difference was detected at 36 weeks of GA. Basal and 21 day mcBTT correlated with anthropometric parameters in particular with length of the tibia at birth (r=0,59, p=0,000). Lower plasmatic phosphate levels were found in IUGR infants at birth (p=0,0000) and at 21 days of life (p=0,050) and serum phosphate at 21 days positively correlated with mc-BTT at 36 weeks of GA (r=0.36, p=0.031). Concerning nutritional parameters, in IUGR infants mc-BTT at 36 weeks of GA positively correlated with mean total energy intake of the first week of life (r=0,29, p=0,040), while prolonged NPT and number of days needed to reach full enteral feeding (FEF) of 150 ml/kg/day negatively correlated with QUS values on day 21 and at 36 weeks of GA. In the same group of patients, parenteral vitamin D intake during the first week of life positively correlated with mc-BTT at 36 weeks of GA (r=0,69, p=0,000). Furthermore, we found cut-off values that could be used as markers of bone status at 36 weeks of GA: IUGR with lower limb length at 21 days < 91 mm, a mean energy intake in the first week < 76.9 Kcal/kg/die or in the first month of life < 105.6 Kcal/kg/die, a vitamin D intake in the first week < 36.6 UI/Kg/day or a prolonged NPT (days  $\geq 16$ ) showed a worse mc-BTT at 36 weeks of GA. Finally, with a multivariate analysis we found that NPT days, intravenously vitamin D intake in the first week of life and lower limb length at 21 days of life can predict bone status at 36 weeks of GA with the following model: BTT 36 weeks GA=0.4962+0.0569\*(NPT days)+0.0401\*(VitD iv 1week)+0.0421\*(lower limb length 21 day). Conclusions: IUGR infants have a worse bone status at birth. Serum phosphate level, reduced in

**Conclusions**: IUGR infants have a worse bone status at birth. Serum phosphate level, reduced in IUGR infants from birth and in the first weeks of life, correlates positively with BTT values and it can reflect bone status in preterm infants. Furthermore, shorter limb length, low vitamin D intakes in the first week and a long duration of parenteral nutrition are predictive for lower mcBTT values at 36 weeks of GA. Newborns with lower energy intakes have a worse bone status at 36 weeks of GA. Our study outlines that IUGR newborns need careful nutritional interventions to improve bone status, though further studies with a higher number of patients and comprehensive of metabolomic analysis will clarify the effects of early nutrition on bone growth.

#### LONG TERM EFFECTS OF DISEASE-MODIFYING AND DISEASE CURATIVE THERAPIES ON ORGAN DAMAGE IN SICKLE CELL DISEASE

#### Ph.D. Student: Dr. Giulia REGGIANI TUTOR: Prof. Raffaella COLOMBATTI Ph.D. Course Development Medicine and Health Planning Science Curriculum "Oncohematology, Medical Genetics, Rare Diseases and Predictive Medicine"

#### Background

Patients with sickle cell disease (SCD) progressively develop chronic organ injuries which limit their life expectancy. Standardized and systematic data collection in longitudinal observational studies allows to monitor the natural history of chronic organ damage in SCD. However, the effect of disease-modifying (chronic red blood cell transfusion regimen, hydroxyurea, and more recently crizanlizumab and voxelotor) and disease curative treatments (hematopoietic stem cell transplantation, HSCT) on the evolution of chronic organ damage has not been clearly defined yet. Moreover, biomarkers of organ damage and response to different therapies are lacking in SCD. Oxygenscan is a novel physiological assay of red blood cells' deformability at different oxygen tensions; it allows the measurement of parameters that could serve as SCD biomarkers. Early screening and prevention of SCD chronic complications could improve survival and quality of life. The aims of this project are: to analyze the prevalence of chronic damage in the mainly affected organs (brain, eye, heart, lung, kidney and liver) of pediatric SCD patients; to analyze the effect of disease-modifying and disease curative therapies on the development of chronic organ damage in children affected by SCD; to explore the role of oxygenscan parameters as possible biomarkers of organ damage and response to different treatments in SCD.

#### **Material and Methods**

SCD patients diagnosed between the prenatal period and the age of 20 years, with any genotype, are included in the study. Data on chronic organ injuries were prospectively collected in a dedicated SCD database since 2009 in the context of a natural history cohort of SCD patients followed in the Paediatric Haematology of Padova. Standardized programs of follow-up are adopted for every SCD patient to monitor the evolution of organ damage. Moreover, a specific protocol for post-HSCT follow-up has been created and applied. In the framework of the European project GenoMed4All, a standardized protocol for oxygenscan has been defined and tested. Blood samples of untreated and treated patients have been prospectively collected to measure oxygenscan parameters through a Laser-assisted Optical Rotational Red Cell Analyser (LLORCA).

#### Results

Every SCD patient in our Centre receives regular blood test and instrumental exams as part of a screening for organ damage. Specifically, a total of 25 patients submitted to HSCT are receiving instrumental follow-up; 18/25 have already undergone at least 1 brain MRI and Transcranial Doppler after HSCT. We are organizing controls for the remaining patients. From November 2021 to July 2023 we have collected steady state blood samples of 101 patients: 16 without disease-modifying therapies, 71 in monotherapy with hydroxyurea, 5 in combined therapy with hydroxyurea and crizanlizumab, 2 in combined therapy with hydroxyurea and chronic simple transfusion regimen, 4 in chronic exchange transfusion regimen, 3 submitted to allogeneic HSCT. Oxygenscan has been performed on each sample to determine specific parameters such as the point of sickling; the test has been repeated twice on every sample to verify reproducibility.

#### Conclusions

We have planned standardized post-HSCT organ damage monitoring for all patients. Oxygenscan is a feasible and reproducible test for children with SCD. After the completion of data collection, we will explore the eventual role of the point of sickling as a biomarker of the disease by looking for correlations between organ damage, response to different types of treatment and oxygenscan parameters.

#### BONE MARROW INFILTRATION IN HIGH-RISK NEUROBLASTOMA: CHARACTERISTICS OF INFILTRATING CELLS AND PROGNOSTIC IMPACT

Ph.D. Student: Dr. Bartolomeo ROSSI TUTOR: Prof. Alessandra BIFFI – CO-TUTOR: Dr. Elisabetta VISCARDI Ph.D. Course Development Medicine and Health Planning Science Curriculum "Oncohematology, Medical Genetics, Rare Diseases and Predictive Medicine"

#### Background

Neuroblastoma (NB) is the most common extracranial solid tumour in childhood. The bone marrow (BM) represents the most frequent NB metastatic sites (70% at diagnosis in high-risk patients) and is a place where disease recurrence often takes place. NB cells dissemination in BM is a negative prognostic marker in high-risk (HR) patients. Although long-term survival has improved over the past 25 years, particularly with the introduction of the immunotherapy, 50% of patients still relapse or have refractory disease. Therefore, it is essential to identify new prognostic factors for metastatic and recurrent NB. In this study we will evaluate the morphological pattern of BM involvement from NB cells at diagnosis evaluating the prognostic role in HR patients.

#### **Material and Methods**

Retrospective analysis of high risk neuroblastoma BM samples from 49 patients treated in Oncology-Hematology Unit of Padua University from January 2004 to December 2018. The main objective of the project encompassed the comprehensive characterization of BM specimens at morphology evaluation with optical microscopy. We described and characterized two different morphological pattern of BM invasion at diagnosis: clumps pattern (A pattern) and diffuse-type pattern with replacement of the normal hematopoietic component (B pattern). We assessed the correlation between morphological pattern of BM invasion and the clinical disease characteristics.

#### Results

BM involvement from NB cells was present at diagnosis in 43 of 49 patients (88%). Twenty-six (60%) of these presented with an A pattern, 17/43 (40%) with a B pattern. 5-year OS and PFS of the cohort were 48% and 38%, respectively. Considering the different pattern of BM invasion, B pattern appears to be associated with poor outcome (OS=35%; PFS=18%) in comparison to A pattern (OS=50%; PFS=42%) or to patients without BM infiltration (OS=80%; PFS=83%). In fact, patients with B pattern invasion relapsed more frequently (82%) than patients with A pattern (54%) or with negative BM (17%).

#### Conclusions

These are the first data on the prognostic role of the different BM infiltration in HR NB. B pattern invasion is associated with a less favourable outcome than A pattern, due to the higher relapse rate.

#### ALTERATIONS OF SURFACTANT LIPIDS COMPOSITION IN CHD CHILDREN UNDERGOING CPB DURING SURGERY

Ph.D. Student: Dr. Anna SARTORI TUTOR: Prof. Alfonso GALDERISI – CO-TUTOR: Prof. Paola COGO Ph.D. Course Development Medicine and Health Planning Science Curriculum "Oncohematology, Medical Genetics, Rare Diseases and Predictive Medicine"

#### Background

Pulmonary surfactant composition is essential for normal lung function. Significant changes in surfactant lipids have been documented in human lung diseases. Nowadays there is a lack of information in the surfactant lipid composition of children with congenital heart disease (CHD) both in the main lipid classes and in the less represented ones. In CHD children, pulmonary blood flow (Qp) contributes to alterations of pulmonary mechanics and gas exchange, while cardiopulmonary bypass (CPB) induces lung edema.

We aimed to determine the effect of hemodynamics and inflammation on surfactant lipids composition in CHD children undergoing CPB compared to controls.

#### **Material and Methods**

Comprehensive lipidomics profiles of bronchoalveolar lavage (BAL) fluid from children and controls were generated by electrospray ionization tandem mass spectrometry analysis. CHD children were classified as high Qp (n=10) or low Qp (n=12), according to preoperative cardiac morphology. Controls (n=14) were infants with no cardiorespiratory diseases at the time of endotracheal intubation for elective surgery.

#### Results

36 children were included in this study. Results showed that, despite the great inter-individual variability, the surfactant DSPC (desaturated phosphatidylcholine) content of CHD children tend to be lower compared to controls, probably due to the reduced synthesis of pulmonary surfactant or increased catabolism. CHD children before surgery had lower content of phosphatidylethanolmine (PE), lyso-phosphatidylcholine (LPC) and plasmalogens (PE-P and PC-P) compared to controls. No statistically significative differences were identified for phosphatidylcholine (PC), phosphatidylglycerol (PG), phosphatidylinositol (PI) and sphingomyelins (SM).

After surgery in the low Qp group LPC and plasmalogens (PE-P and PC-P) significantly increased probably due to inflammation whereas in the high Qp group remain unaltered, while myeloperoxidase activity (MPO) in tracheal aspirates increased after the CPB.

#### Conclusions

The surfactant lipidome is substantially altered in CHD children compared to controls before surgery. Pulmonary blood flow and CPB significantly affected the surfactant lipid composition.

#### MODELING A NOVEL CILIOPATHY IN C.ELEGANS

#### Ph.D. Student: Dr. Elena TACCHETTO TUTOR: Prof. Eva TREVISSON Ph.D. Course Development Medicine and Health Planning Science Curriculum "Oncohematology, Medical Genetics, Rare Diseases and Predictive Medicine"

#### Background

Cilia are evolutionary conserved organelles protruding from the surface of eukaryotic cells. There are two major types of cilia (primary and motile), consisting of a basal body and the axoneme. We have identified 2 novel heterozygous variants in KIF3B in a patient with a severe ciliopathy. Its protein product belongs to the kinesin superfamily (KIFs), a class of molecular motors that exploit ATP hydrolysis to transport intracellular cargo along MT. KIF3B is organized in a N-terminal motor domain (responsible for ATP and MT binding), a coiled-coiled domain, and a C-terminal globular domain, determining cargo specificity. KIF3B interacts with KIF3A and KAP, forming the heterotrimeric Kinesin-2: this complex, transports multimeric protein complexes (IFT particles) along the cilium MTs. KIF3B mutations have been identified as a cause for an autosomal-dominant ciliopathy, mainly characterized by retinitis pigmentosa. C.elegans is a leading model organism for cilia research. This nematode possesses 60 ciliated neurons that function in chemo-, thermo-, mechanosensation and proprioception that are mapped: the amphids are a pair of laterally located sensilla in the head that represent the largest chemosensory organs of C. elegans. In C. elegans the orthologue of KIF3B is klp-11, a motor subunit that interacts with klp-20 and kap-1 to form the heterotrimeric kinesin II. This complex drives the IFT along MTs cooperating with homodimeric OSM-3 motors. To investigate the molecular consequences of defects in KIF3B, we have proposed to generate and characterize a *C.elegans* model harboring the novel variants in KIF3B gene, to explore their consequences on cilia structure and function in vivo.

#### **Material and Methods**

We edited the worm genome by inserting through the CRISPR/Cas9 technology the truncating mutation and the missense mutation found in our patient. After genotyping, animals will be backcrossed twice to reduce off-target. We evaluated cilia-dependent behaviors in our mutants (chemosensation, osmotic avoidance, dye filling uptake). Different compounds have been used to assess chemosensory function of neurons in our *klp-11* mutant lines. Finally, we crossed our *klp-11* mutants with a reporter strain to measure amphid cilia length by confocal microscopy to check on possible effects of *klp-11* mutations on cilia structure.

#### Results

We performed chemotaxis assays using two different attractants: NaCl and sodium acetate, to test the functionality of different type of ciliated neurons. In both cases we observed a difference between wild-type and mutant worms. Moreover, we performed a dye-filling assay to check for morphological intactness of cilia and sensory neurons: we observed a significant decrease in dye uptake in *klp-11 C.elegans* mutant compared to control worms. Finally, observing and measuring cilia length in mutant and control reporter worms, we observed that *klp-11* knock-out worms have a reduced cilia length.

#### Conclusions

These results suggest that this gene is important for both cilia-dependent behaviours, as our mutant worms show an impaired chemotaxis and chemosensation; but also, in cilia structure and integrity as a close observation showed a decreased cilia length and an impaired capacity of lipophilic dye uptake. Further experiments are needed to elucidate the role of the other missense variant that we found, and also to better understand the role of this protein in different pathways where cilia have fundamental roles and functions.

#### TRAP1: THE CROSSROAD OF METABOLIC AND EPIGENETIC REMODELING OF AGGRESSIVE B CELL LYMPHOMAS

Ph.D. Student: Dr. Anna TOSATO TUTOR: Prof. Lara MUSSOLIN – CO-TUTOR: Prof. Katia BASSO Ph.D. Course Development Medicine and Health Planning Science Curriculum "Oncohematology, Medical Genetics, Rare Diseases and Predictive Medicine"

**Background:** Metabolic reprogramming and epigenetic remodeling interact in a bidirectional manner towards the sustainment of tumor growth as metabolic enzymes provide the "ink" for epigenetic modifications. Diffuse Large B Cell Lymphoma (DLBCL) arises from the clonal expansion of germinal center (GC) B cells that experience uncontrolled proliferation promoted by the dysregulation of epigenetic modifiers. The histone methyltransferase EZH2 is mutated in 21% of cases of Germinal Center-like DLBCL (GCB-DLBCL) and its enhanced enzymatic activity leads to increased deposition of the repressive trimethylation mark on histone 3 lysine 27 (H3K27me3) and silencing of differentiation and cell cycle repression genes. This favors the maintenance of an undifferentiated state of GC B cells leading to overgrowth and GC hyperplasia. We have previously shown that the mitochondrial chaperone TRAP1 prompts a pro-neoplastic succinate accumulation in different cancer cell models by inhibiting succinate dehydrogenase (SDH) enzymatic activity: when accumulated, succinate inhibits Jumonji-C (JMJC) domain-containing histone demethylases (JHDMs) causing epigenetic rearrangements that may further contribute to neoplastic growth. However, no TRAP1-dependent epigenetic change has ever been reported.

Materials and Methods: TRAP1 expression was tested by IHC in primary DLBCL and in reactive lymph nodes (RLNs). RT-qPCR analysis of n=12 RLNs and n=9 DLBCL cases was performed to validate TRAP1 mRNA expression. The NCI-DLBCL cohort [Schmitz R., *et al.* 2018] was used to analyse TRAP1 levels in n=385 DLBCL cases. *In vitro* experiments were carried out in three different DLBCL model cell lines: U2932 (ABC-DLBCL), SUDHL-4 (GCB-DLBCL) and Karpas-422 (GCB-DLBCL). TRAP1 KO cells were produced with the lentiCRISPRv2 system [Sanjana NE., *et al.* 2014]. SDH activity was measured using a spectrophotometric assay following the reduction of 2,6-dichlorophenolindophenol (DCPIP) at 600nm in the presence of succinate. Cell cycle analysis was performed by staining the cells with Annexin/PI and reading the samples on a BD Cytofluorimeter. Colony formation assays were performed by plating single cell suspensions in the presence of MethoCult<sup>TM</sup> and following colony growth for about 15 days.

**Results:** IHC analysis and RT-qPCR revealed that TRAP1 is upregulated in DLBCL patients compared to RLNs (unpaired t-test, \*p<0.05). Stratification of the NCI-DLBCL patient cohort based on TRAP1 expression identified two groups, a TRAP1-low and TRAP1-high group, the latter being associated with a worse prognosis (Gehan-Breslow-Wilcoxon test, \*p<0.05). Additionally, TRAP1 was upregulated in ABC-DLBCL cases and in the MCD and A53 genetic subgroups [Wright GW., et al. 2020], that largely correspond to ABC-DLBCL. Following TRAP1 KO in DLBCL cell lines, SDH activity was significantly increased in the KO cells, while K27me3 levels were drastically reduced in U2932 and SUDHL-4 but not in Karpas-422, carrying EZH<sup>Y641N</sup> gain-of-function mutation. Following K27me3 disruption in U2932 and SUHDL-4 KO cells, EZH2 target genes CDKN2A and PRDM1 were upregulated, respectively. Moreover, treatment of KO cells with succinate analogue DMS or with exogenous SDH inhibitor 3-NP led to increased K27me3 levels in the absence of TRAP1, confirming the effect of succinate accumulation on epigenetic remodelling. Ultimately, cell cycle analysis revealed that KO cells accumulate in G1 phase and colony formation assay demonstrated that TRAP1 KO cells are less capable of forming colonies compared to scramble cells.

**Conclusions:** TRAP1 is upregulated in ABC-DLBCL and ABC-like DLBCL patients (MCD and A53) and it negatively correlates with their prognosis. TRAP1 may, thus, represent a novel metabolic target for the treatment of DLBCL with innovative TRAP1 inhibitors.

For the third year of my PhD program I transferred to Columbia University in New York and, under the supervision of Dr. Katia Basso, I will be carrying on a parallel project aimed at characterizing the intra and inter-tumour heterogeneity of Burkitt's Lymphoma.

# STUDY OF HUMAN ADCK PROTEINS IN COQ SYNTHESIS AND CELLULAR METABOLISM

Ph.D. Student: Dr. Agata VALENTINO TUTOR: Prof. Leonardo SALVIATI – CO-TUTOR: Prof. Maria Andrea DESBATS Ph.D. Course Development Medicine and Health Planning Science Curriculum "Oncohematology, Medical Genetics, Rare Diseases and Predictive Medicine"

# Background

Coenzyme Q (CoQ), is a redox active lipid and an essential component of the mitochondrial respiratory chain. Even if CoQ was discovered more than 60 years ago the mechanism of CoQ biosynthesis, and especially its regulation, are not yet completely understood. Since then, it has become evident that CoQ has many other functions, not directly related to respiration. Indeed, it is a cofactor of several mitochondrial dehydrogenases involved in the metabolism of lipids, amino acids, nucleotides, and in sulphide detoxification. Furthermore, it is a powerful antioxidant, and it is involved in the control of programmed cell death by modulating both apoptosis and ferroptosis (Baschiera, 2021). The ADCK (AARF Domain-Containing Kinase) family of proteins is comprised by several evolutionarily conserved proteins that have been classified as atypical kinases, even though no formal proof of their kinase activity has ever been observed (Stefely 2015). Higher eukaryotes harbour five *ADCK* genes: *ADCK1*, *ADCK2*, *COQ8A*, *COQ8B* and *ADCK5*. Mutations in *COQ8A* and *COQ8B* have been associated to diseases in patients and CoQ deficiency in some tissues (Stefely, 2017). While the role of *ADCK1* and *ADCK5* in humans has never been studied.

#### Materials and methods

In this work, we aim to study the role of *ADCK* genes in human cells. To achieve this, we have generated six different HEK293 knockout cell lines by CRISPR-Cas9: *COQ8A<sup>-/-</sup>*, *COQ8B<sup>-/-</sup>*, *COQ8A<sup>-/-</sup>*, *ADCK1<sup>-/-</sup>*, *ADCK5<sup>-/-</sup>* and *ADCK1/5<sup>-/-</sup>*. We started by characterizing the mitochondrial function of COQ8A and COQ8B. We measured Coenzyme Q levels, mitochondrial respiration, respiratory chain complexes activity and organization in all cell lines.

# Results

We found a reduction on CoQ levels, respiration, activity of complex III and II+III, and respiratory chain super-complexes only in COQ8A/B<sup>-/-</sup> cells. At the transcriptomic level, COQ8A/B<sup>-/-</sup> cells showed higher expression of respiratory chain subunits and lower expression of genes related to TCA cycle, Urea cycle and Fatty Acids synthesis and degradation. Finally, metabolomics analysis showed a general metabolic shutdown in COQ8A/B<sup>-/-</sup> cells and some interesting differences related to TCA cycle and Proline cycle metabolites in COQ8A<sup>-/-</sup> and COQ8B<sup>-/-</sup> cells.

#### Conclusions

Overall, these findings indicate some overlapping and specific roles of COQ8A and COQ8B in human cell metabolism. We are planning to re-express the tagged versions of COQ8A and COQ8B and two hybrids versions (one harbouring the N-terminus of COQ8A and the rest of the molecule from COQ8B and the other harbouring the N-terminus of COQ8B and the rest of the molecule from COQ8A) in COQ8A/B<sup>-/-</sup> cells in order to understand if may have redundant function. Then we will perform the same functional characterization of ADCK1<sup>-/-</sup>, ADCK5<sup>-/-</sup>, ADCK1/5<sup>-/-</sup> cells.

#### References

- Baschiera et al., "The multiple roles of coenzyme Q in cellular homeostasis and their relevance for the pathogenesis of coenzyme Q deficiency". Free Radic Biol Med. 2021 Apr; 166:277-286
- Stefely et al., "Mitochondrial ADCK3 employs an atypical protein kinase-like fold to enable coenzyme Q biosynthesis". Mol Cell 57, 83-94 (2015).
- Stefely and Pagliarini, "Biochemistry of Mitochondrial Coenzyme Q Biosynthesis". Trends Biochem Sci. 2017 October; 42(10): 824–843.



University of Padua PhD Courses Medical and Biomedical Sciences

# PhD COURSE "DEVELOPMENTAL MEDICINE AND HEALTH PLANNING SCIENCES"

**COORDINATOR: PROF. GIANNI BISOGNO** 

# Curriculum "HEALTH PLANNING SCIENCES"

#### NATURAL SHEAR WAVES ELASTOGRAPHY IN FONTAN PATIENTS: A NEW TOOL FOR NON-INVASIVE ASSESSMENT OF DIASTOLIC FUNCTION?

Ph.D. Student: Dr. Irene CATTAPAN TUTOR: Prof. Jan D'HOOGE – CO-TUTOR: Prof. Giovanni DI SALVO Ph.D. Course Development Medicine and Health Planning Science Curriculum "Health Planning Sciences"

**Background:** Ventricular compliance is known to have a direct impact on ventricular filling and therefore on diastolic function. Chamber compliance, in turn, is directly related to myocardial stiffness. The operational stiffness of the myocardium can non-invasively be assessed using shear wave elastography (SWE), a promising new echocardiographic modality based on measuring the velocity of naturally occurring shear waves using high frame imaging. SWE thus offers a novel tool to study diastolic function. To date, non-invasive evaluation of diastolic function remains challenging, particularly in Fontan patients in which conventional approaches are not reliable.

**Aim of the Study:** i) to assess feasibility of shear waves elastography on univentricular hearts; ii) to document the observed natural shear wave speed after atrioventricular valve closure (AVVC) and outflow valve closure (OVC) in both paediatric and adult Fontan patients; iii) to consider whether SWE can provide additional information on diastolic function in these hearts.

**Materials and Methods:** this prospective cohort study was conducted between September 2022 and June 2023 at Gasthuisberg University Hospital, Leuven. We enrolled 47 consecutive Fontan patients: 15 children, 12 adolescents and 20 adults (mean age  $19 \pm 11$  years, range 3-46y). High frame rate parasternal long-axis views were acquired using an experimental scanner (1367  $\pm$  270 frame/s). Images were processed offline by extracting tissue Doppler acceleration coded M-modes drawn in the middle of the wall related to the main atrioventricular valve and the outflow valve. Conventional echocardiographic parameters of systolic and diastolic function were collected using a high-end clinical scanner. To test whether shear wave speed was related to filling pressures, we collected records of pressure in cavo-pulmonary conduit from recent heart catheterization or from peripheral intra-venous line that served as a surrogate for invasive measurements. Pressure measurements were available in 30 patients.

Results: 66% of the patients enrolled had left-dominant ventricles, while the remaining 34% was right-dominant (12 patients had tricuspid atresia, 13 DILV, 5 unbalanced AVSD, 8 HLHS, 2 DIRV, 4 pulmonary atresia with VSD, 3 pulmonary atresia with intact interventricular septum, 1 Ebstein anomaly). Shear waves (SW) speed measurements across the wall most similar to septum was feasible in 97% of patients both after AVVC and OVC. Average shear waves velocities were significatively higher than previously collected data from healthy volunteers in our laboratory  $(5,3 \pm$ 1,5 m/s after atrioventricular valve closure versus 3,54  $\pm$  0,93 m/s, p< 0,001; 5,1  $\pm$  1,93 m/s after outflow valve closure vs  $3,75 \pm 0,76$  m/s, p< 0,001). There was no correlation between shear waves velocities and age (r=0,092, p=0,54 for SW after AVVC; r=0,13, p=0,39 for SW after OVC) and no significant difference between age groups (p=0,69 for SW after AVVC; p=0,71 for SW after OVC). Ventricular dominance did not significantly influence shear waves velocities (p=0,68 for SW after AVVC; p=0,36 for SW after OVC). Shear waves velocities after AVVC showed a good correlation with pressure in the cavo-pulmonary conduit (r=0,55, p=0,002), while no other conventional echo parameter showed correlation with measured filling pressures (E/A r=-0,14, p=0,48; E/E' r=-0,15, p=0,41; Tei index r=-0,19, p=0,92; S/D ratio r=0,25, p=0,18; pulmonary a wave velocity r=0,14, p=0,53; pulmonary a wave duration – atrioventricular A wave duration r=-0,29, p=0,16).

**Conclusions:** Our findings show for the first time that measurements of natural shear waves are feasible in univentricular hearts with Fontan circulation. Their myocardium appears stiffer than normal. Whether this depends on an alteration of intrinsic myocardial properties (fibrosis) and/or on preload conditions, remains to be understood. Our data indicate that shear wave elastography may become a useful tool for non-invasive assessment of diastolic function in univentricular hearts.

# HEALTH DETERMINANTS INVOLVED IN CHILDHOOD OBESITY: EARLY-LIFE ANTIBIOTICS EXPOSURE – RELATED RISK, A POPULATION-BASED STUDY IN ITALY

# Ph.D. Student: Dr. Joaquin GUTIERREZ DE RUBALCAVA DOBLAS TUTOR: Prof. Carlo GIAQUINTO – CO-TUTOR: Prof. Silvia BRESSAN Ph.D. Course Development Medicine and Health Planning Science Curriculum "Health Planning Sciences"

#### Background

Childhood obesity is an increasing public health problem that is closely related to the development of noncommunicable diseases (heart disease, cancer, diabetes...). According to the World Health Organization (WHO) and its European Childhood Obesity Surveillance Initiative (COSI), in agreement with the last Italian Ministry of Health's report "OKkio alla Salute", 38% of Italian school-aged children have been found to be overweight, of which 16.5% obese, using the WHO Growth References.

#### **Material and Methods**

Our project aims at identifying health determinants involved in the development of childhood obesity, through a multi-step approach that combines "classic" modalities of data extraction and analysis from population databases, with "innovative" Artificial Intelligence (AI) Machine Learning (ML) methods, for data integration and subsequent comparison with such "classic" methods.

This is an observational, retrospective, non-interventional, population-based study, which objective is to examine the risk of developing obesity among children exposed to antibiotics early in life in a large population-based Italian birth cohort (Pedianet) with a detailed assessment of antibiotic use and long-term follow-up to assess the development of obesity.

#### Results

Among 121,540 children identified in the Pedianet network at birth, 45% were prescribed at least an antibiotic within the first year of life. The average follow-up period was approximately 5.5 years. Considering the total cohort of children, 22% were classified as obese during follow-up, with an incidence rate (IR) of 4.05 cases (95% CI 4.01 to 4.10) x100 person-year (PY). Among children without antibiotic prescription during their first year of life, 21% were observed to be obese, while 24% of those with antibiotic exposure were obese, with an IR of 3.82 x100 PY (95% CI 3.76 to 3.89) and 4.34 x100 PY (95% CI 4.26 to 4.41), respectively. The incidence of obesity was higher among antibiotic-exposed children than unexposed children across all baseline characteristics considered. As the number of antibiotics administered in the first year of life increased, the risk of obesity showed a significant rise (P for trend < 0.0001). The individual-specific-age analysis showed that starting antibiotic therapy very early (between 0-5 months) had the greatest impact (aHR 1.12, 95% CI 1.08 to 1.17) on childhood obesity with respect to what was observed among those who were first prescribed antibiotics between 5-8 months of life (aHR 1.08, 95% CI 1.04 to 1.12) and 8-12 months of life (aHR 1.03, 95% CI 0.99 to 1.06).

#### Conclusions

In this paediatric population-based cohort study of 121,540 children, we found a 6% increased risk of developing childhood obesity among children exposed to antibiotics within the first year of life compared to unexposed children. This relationship is stronger as the number of prescriptions increases and as the individual's age at the first prescription of antibiotics decreases. Results were consistent across all sensitivity and subgroup analyses conducted.

The results from this large population-based study support the association between early exposure to antibiotics and an increased risk of childhood obesity.



Medic

University of Padua PhD Courses Medical and Biomedical Sciences

# PhD COURSE "MOLECULAR MEDICINE" COORDINATOR: PROF. ARIANNA LOREGIAN

# Curriculum "BIOMEDICINE"

### ANALYSIS OF CHROMATIN ACCESSIBILITY OF OVARIES AND EARLY EMBRYOS OF AEDES AEGYPTI VIA ATAC-SEQUENCING

Ph.D. Student: Dr. Martina BADO TUTOR: Prof. Enrico LAVEZZO Ph.D. Course Molecular Medicine Curriculum "Biomedicine"

### Background

Aedes aegypti, commonly known as the yellow fever mosquito, is a vector of several arboviruses, including the yellow fever virus, Zika virus, dengue virus and chikungunya virus. The transmission of these pathogens is carried out exclusively by female mosquitoes, as they require a blood meal for the development of their eggs. Blood-feeding is a fundamental part of *Ae. aegypti* gonotrophic cycle since it provides the amino acids for the synthesis of vitellogenin, which is a protein essential for egg production. This study focuses on the analysis of the open chromatin regions in ovaries of blood-fed females (24h and 48h post-blood feeding) and in early embryos (3h and 5h post-oviposition) of *Ae. aegypti* using ATAC-sequencing. The main aim is to identify promoters of genes that are expressed during the development of eggs and early embryos.

This research is being conducted in collaboration with Polo GGB, within the scope of the PON PhD program.

#### **Material and Methods**

Raw ATAC-sequencing reads were generated and made publicly available on the European Nucleotide Archive (ENA) under accession ID: PRJEB55615, to specifically allow the herein described study. The dataset was downloaded from ENA and consists of 3 replicates for each sample: ovaries at 24h post blood meal (PBM), ovaries at 48h PBM, embryos at 3h post oviposition (PO), and embryos at 5h PO of *Ae. aegypti*. For data analysis, a bioinformatic pipeline was implemented and includes the following core steps: read parsing, trimming and filtering; alignment to the reference genome; post-alignment processing; peak calling and annotation.

#### Results

The results obtained thus far demonstrate a generally satisfactory quality of the dataset, with one exception: a sequencing failure occurred in one of the 24h PBM ovary samples. The number of identified peaks ranges from 128.331 in 3h PO embryos to 342.012 in 24h PBM ovaries. The most extensive fractions of peaks in all samples are situated in intergenic regions, likely corresponding to enhancers. Additionally, most of the peaks associated to the strongest signal are close to rRNA coding genes. However, further analyses are required to assess the validity of these outcomes.

#### Conclusions

The findings previously outlined are preliminary, and further analyses will be carried out to validate the results and characterize also weaker ATAC-seq peaks. Additionally, the ATAC-seq data will be integrated with RNA-seq data to explore the presence of a correlation between the ATAC signal and transcription. This comprehensive analysis has the potential to uncover regulatory sequences that allow transcription in developing eggs and early embryos, thereby shedding a light on the biology of *Ae. aegypti* mosquitoes. These insights could be leveraged to develop strategies for vector control.

# CC-VBD: MULTISECTORAL RESEARCH WITH A "ONE-HEALTH" AND "ECO-HEALTH" APPROACH TO REDUCE THE IMPACT OF CLIMATE CHANGE ON THE RISK OF VECTOR-BORNE DISEASES

Ph.D. Student: Dr. Emanuela DAL MOLIN TUTOR: Prof. Luisa BARZON Ph.D. Course Molecular Medicine Curriculum "Biomedicine"

#### Background

West Nile virus (WNV) is a mosquito-borne flavivirus, which every year causes outbreaks of encephalitis in humans and horses in Italy and other European countries. In 2022, a new WNV lineage 1 (WNV-1) strain emerged in the Veneto Region, where it co-circulated with an endemic WNV-2 strain and caused a large human outbreak (Barzon et al. Euro Surveill 2022). Epidemiological data suggested that the infection with the new WNV-1 strain was associated with an increased risk to develop neuroinvasive disease (Barzon et al. J Travel Med 2022). Aim of this study was to investigate and compare the replication and neuropathogenicity of this virus with other WNV strains. To this aim, we perfomed infection experiments in cortical neurons and brain organoids derived from human stem cells and applied reverse genetics to developed an infectious clone of WNV-2.

# Material and Methods

We followed a protocol developed by Molchanova et al. for generating hindbrain-like organoids from human pluripotent stem cell-derived pre-regionalized neuroepithelial stem cells.

Then we built an infectious clone of WNV-2, using a low copy plasmid vector with two introns inserted in NS1 and NS5 genes in order to avoid toxicity for bacteria. This plasmid contains a polymerase II-dependent CMV promoter, an ampicillin resistance gene to select the proper colonies, hepatitis delta virus ribozyme terminal site to permit a good processing and a termination of transcription (TT) to conclude the transcription process.

#### Results

Infection and replication of WNV in hindbrain organoids was confirmed by real time PCR and immunofluorescence. Preliminary data indicated that WNV-1 strains IT-22 and Ita09 infected and replicated in hindbrain organoids less efficiently than WNV-2 strains IT-22 and AUT/08.

With regard to reverse genetic system, we obtained different promising plasmids that we transfected in Vero E6 cells. The collected supernatant was used to infect new Vero E6 cells and recover the virus. The samples were tested positive in real time PCR and need to be confirmed by sequencing.

All analyses are still in progress and further replications and sequencings will be necessary to confirm that the infectious clone obtained is similar to the starting sequence and can, therefore, be used in future experiments.

#### Conclusions

In vitro models have proved to be an excellent system to evaluate the viral tropisms of different epidemic strains and their replication efficiency. Our in vitro experiments demonstrated that both WNV-1 and WNV-2 strains efficiently infected and replicated in human cortical neurons and brain organoids. These are preliminary analyses, which will need to be confirmed and investigated further.

Monitoring WNV genetic evolution and phenotypic characterization of new variants is crucial to early detect the emergence of new strains with epidemic potential, especially in the context of climate change that is affecting Europe in recent years.

#### SUSTAINABLE DEVELOPMENT: NEW TOOLS FOR SELECTION AND VALIDATION OF MACROMOLECULES FOR MEDICAL PURPOSES

# Ph.D. Student: Dr. Alice Cristina DONATO TUTOR: Prof. Paola BRUN Ph.D. Course Molecular Medicine Curriculum "Biomedicine"

**Background.** The biological role of hyaluronic acid (HA), along with its well-known antiinflammatory properties has recently stimulated the interest of pharmaceutical companies. The goal is to develop new HA-derived compounds capable of modulating the production of proinflammatory molecules, which are closely associated with the severity and progression of many inflammatory and fibrotic diseases. In irreversible pulmonary pathologies such as chronic obstructive pulmonary disease (COPD) and idiopathic pulmonary fibrosis (IPF), the presence of macrophages is enhanced, and related to elevated levels of pro-inflammatory cytokines and galectins (Gals). Recently, innovative tools such as computational simulations and *in silico* studies, have been employed to streamline the synthesis and *in vitro* and *in vivo* testing of new macromolecules.

The present study aims to:

- *in silico* test the ability of HA-based molecules functionalized with D-glucose and D-galactose (Hylach®) to bind to different inflammatory Gals, in particular to Gal-3;

- *in vitro* evaluate the capability of the selected Hylach polymers to reduce inflammation and fibrosis. Human primary pulmonary cells and *in vitro* models of inflammation and fibrosis are employed for this purpose.

**Materials and Methods.** To assess the binding affinity between Hylach polymers with different percentages of lactosylation and galectin, both molecular docking and dynamic simulations were used. The most effective Hylach ligands for Gal-3 were identified and subsequently tested *in vitro* for their anti-inflammatory and anti-fibrotic properties. In this study primary human bronchial fibroblasts obtained from smokers and human pulmonary fibroblasts were used. Mechanistically, the cells were either exposed to the conditioned medium (CM) derived from activated U937 monocytes to induce inflammation or treated with TGF- $\beta$  in order to promote fibrosis.

Changes in cell viability, ROS generation, pro-inflammatory mediators and extracellular matrix (ECM) molecules expression, at both gene and protein level, were analyzed.

**Results.** *In silico* analysis revealed that Hylach compounds exhibited higher docking scores compared to non-functionalized HA when interacting with Gal-3. Molecular dynamic simulations indicated that Hylach containing up to 30% lactose-derived residues exhibited the best ligand properties, forming stable protein-ligand complexes, with lower potential energy and binding free energy than HA. *In vitro* experiments demonstrated that Hylach polymers, administrated to bronchial fibroblasts from smokers exposed to the CM of activated monocytes, effectively counteracted the oxidative damage. As a result, gene and protein expression levels of IL-1 $\beta$ , TNF- $\alpha$ , IL-6, Gal-1, Gal-3 and MMP-3 were partially or fully restored towards baseline values.

Furthermore, these compounds exhibited significantly higher antifibrotic efficacy compared to HA when fibroblast cultures were treated with TGF- $\beta$ , reducing the expression of ECM molecules (Collagen type I, Collagen type III) at both gene and protein level.

**Conclusions.** This study demonstrates that Hylach molecules with up to 30% lactose-derived residues exert anti-inflammatory and antioxidant effects on *in vitro* inflamed human bronchial fibroblasts. Hylach downregulates pro-inflammatory molecules and MMP-3 expression, protecting against ECM degradation and lung damage. Additionally, Hyalch molecules exhibit antioxidant properties and induce antifibrotic effects in lung fibroblasts treated with TGF- $\beta$ . These findings highlight the importance of Hylach molecules as a potential therapeutic agent for smoking-related and fibrotic pulmonary diseases.

# FROM PROTEIN FUNCTION PREDICTION TO ANTIMICROBIAL RESISTANCE DETECTION THROUGH MACHINE LEARNING

Ph.D. Student: Dr. Emilio ISPANO TUTOR: Prof. Stefano TOPPO Ph.D. Course Molecular Medicine Curriculum "Biomedicine"

**Background:** Antimicrobial resistance (AMR) has emerged as a critical global health challenge, necessitating innovative approaches for its timely detection and prediction. Proteins play a crucial role in mediating various biological processes, including AMR mechanisms. Automated protein function prediction (APFP) methods have gained prominence in deciphering protein functions with computational tools, thereby facilitating drug discovery and enhancing disease understanding. This study focuses on leveraging APFP techniques to enhance AMR detection and prediction, contributing to the development of more effective strategies against antibiotic-resistant pathogens.

**Material and Methods:** In this PhD project, a comprehensive investigation of APFP techniques is undertaken to formulate an efficient approach for AMR prediction. The starting point is the development of a reliable general-purpose APFP tool, Argot3.0. This tool is an evolution of its predecessor version, Argot2.5, enhanced to extract information more effectively from protein sequences and incorporating machine learning for this task. Query proteins undergo a DIAMOND search against a database of previously annotated target proteins, and the former are categorized into three groups based on the quality of target protein hits. The Argot3.0 pipeline consists of three blocks, each running Argot2.5 with a different input. The first block derives its input from the raw DIAMOND search and is applied to all three protein groups. The second block comprises an embeddings-based recurrent neural network, generating input suitable for Argot2.5. This block is employed for the second and third protein groups. The last block incorporates FunSp, an in-house tool that performs functional enrichment using Argot2.5 output. FunSp is applied exclusively to the third and most challenging protein group.

**Results:** The novel Argot3.0 pipeline will be evaluated alongside various other tools with the same goal of performing APFP in the fifth edition of the CAFA challenge, which is currently ongoing on Kaggle. This evaluation will provide a comprehensive and unbiased assessment of the tool's performance and its comparison with other tools. Additionally, an in-house evaluation was conducted on proteins for which knowledge loss was simulated, as the waiting time for the CAFA challenge is not short. Evaluated in terms of precision and recall, Argot3.0 outperforms its predecessor, and notably, the neural network alone exhibits performance that is only slightly lower than Argot2.5 itself.

**Conclusions:** In conclusion, this project advances AMR detection by leveraging automated protein function prediction. The Argot3.0 pipeline, featuring an embeddings-based neural network, demonstrates improved predictive performance. Evaluation against benchmarks and in-house simulations underscores its enhanced precision and recall, surpassing its predecessor, Argot2.5. The link between Argot3.0 and AMR prediction is the embeddings-based recursive neural network: since it relies not only on the sequence but also on higher-level features, a dedicated version of it will serve as the foundation for building the novel AMR prediction and detection tool. This innovative approach holds promise for combating antibiotic-resistant pathogens and represents a pivotal step towards effectively addressing the global challenge of AMR. This study further confirms the scientific community's increasing reliance on machine learning for APFP, a trend that is believed to extend to AMR detection, the subsequent phase of this project.

### IDENTIFICATION OF NOVEL STRATEGIES FOR CFTR RESCUE IN CYSTIC FIBROSIS

# Ph.D. Student: Dr. Michela RUBIN TUTOR: Prof. Giorgio COZZA – CO-TUTOR: Dr. Ilaria ARTUSI Ph.D. Course Molecular Medicine Curriculum "Biomedicine"

# Background

Cystic fibrosis (CF) is a rare autosomal recessive disease caused by mutations on the cystic fibrosis transmembrane conductance regulator (CFTR) gene. F508del is the most common mutation, and it is responsible for the premature degradation of the chloride channel. Currently, approved treatments are based on VX445, VX661, VX809 (correctors), and VX770 (potentiator). Inefficient maturation and accumulation of F508delCFTR fragments by the proteasome system leads to ER stress, persistent inflammation, and oxidative imbalance caused by ROS overproduction. These are associated with a marked depletion of glutathione (GSH), which fosters oxidative damage of polyunsaturated fatty acids (PUFA) via lipid peroxidation (LPO). Similarly, low levels of NF-E2-related factor 2 (Nrf2), regulator of GSH synthesis, were observed in the CF cell lines. The project points to re-equilibrate redox homeostasis by testing Nrf2 activators to increase GSH levels, assuming that restoring the derailed CF intracellular environment might improve mutated CFTR proteostasis and its functional recovery.

# **Material and Methods**

CFBE410- were used as CF cell model. Cells have been treated with Nrf2 activators DMF and DXF for several time points between 3 and 48h; treatments with VX compounds lasted 24, 48 or 72h. Nrf2 levels and activity were assessed with WB and transfection with Nrf2 reporter plasmid, respectively. Moreover, GSH quantitative determination was assessed using the Tietze assay. Simultaneously, LPO levels were detected using C11-Bodipy. A protective role against erastin-induced ferroptosis was measured using a resazurin cell viability assay, and proteins involved in the anti-ferroptotic mechanism were studied using WB. CFTR channel activity was tested in Ussing chamber.

#### Results

Nrf2 activation induced by DMF and its derivative DXF has been characterized over time. DMF acted as a potentiator of CFTR when combined with a corrector. To optimize the combination, the potential antioxidant capabilities of the VX compounds was studied at different time points (24-72h). Surprisingly, VX770 decreased LPO already at 24h and preserved cells from erastin-induced ferroptosis at every time point. Moreover, it increased the amount of GPx4 and oxidized glutathione at 72h.

#### Conclusions

The data obtained suggest new therapeutic alternatives that could be used in clinical practice. As it is not directed against mutated CFTR, this proposal has the potential to be applied against orphan mutations in CF. Furthermore, the behaviour of VX770 resembles that of a canonical ferroptosis inhibitor. This promising compound has the potential to be translated into other disease models, whose pathogenesis is associated with ferroptosis.

#### GENETIC STRATEGIES TO CONTROL THE MALARIA VECTOR, ANOPHELES ARABIENSIS

#### Phd Student: Dr. Giuditta TANCREDI TUTOR: Prof. Ignazio CASTAGLIUOLO - CO-TUTOR: Dr. Federica BERNARDINI Ph.D. Course Molecular Medicine Curriculum "Biomedicine"

**Background** *An. arabiensis* and *An. gambiae*, sibling species of the *Anopheles gambiae complex*, are two of the most effective vectors for human malaria transmission and have the broadest and most sympatric species distribution among vectors in the African continent (Lanzaro & Lee, 2013). Many genetic control strategies developed in the past have shown their potential efficiency in lab setting for the suppression of mosquito population (Hammond et al., 2016; Kyrou et al., 2018; Simoni et al., 2020). Galizi et al., developed a self-limiting strategy, to bias the sex ratio towards males to collapse the population due to female absence in the progenies. The CRISPR-Cas construct, active in the early spermatogenesis during male meiosis, resulted in RNA-guided shredding of the X-chromosome by targeting the repetitive sequence of ribosomal genes, resulting in only viable Y chromosome-bearing sperm and in a male-biased sex ratio of >95% in the progeny. (Galizi et al., 2014, 2016) This strategy designed and tested in *An. gambiae* has been introgressed in the sibling species of *An. arabiensis* (Bernardini et al., 2019) resulting in sex bias toward males and confirming the conservation of the target sequence among the species of the *Anopheles gambiae complex*. An innovative strategy has been designed, in order to exploit sex distorter as potential species-specific strategy to target *An. arabiensis*.

**Material and Methods** To design a species-specific guideRNA to guide the cleavage of the Xchromosome, we looked for specific snips, occurring only in *An. arabiensis* coding sequence of the ribosomal genes, among genomic data gathered from our insectary colony and Anopheles gambiae 1000 genome project. To obtain the final CRISPR-Cas transformation construct we used a starting vector containing  $\beta 2::Cas9$  expression cassette, the U6::spacer cloning site and *piggyBac* inverted repeats to promote random genome insertion, and we cloned via Golden Gate the ribosomal DNA gRNA sequence GCTCCGGCATACACTGCCCC into the spacer cloning site. Embryos of the *An. arabiensis* wildtype strain were injected with the final CRISPR construct (200ng/µl) and a source of helper transposase (300ng/µl). Mosquitoes positive for the fluorescent marker were individually crossed to wild type to obtain transgenic lines then scored by the highest hatching rate, the inheritance marker pattern (expected 50% with a single autosomal integration) and sex bias. Ten strains were molecular characterized by inverse PCR and sequenced fragments were blasted using NCBI bioinformatic tool to identify the integration site. A fertility assay was performed to measure fertility and adult sex ratio.

**Result** Two potential candidates for sex distorter *An. arabiensis* specific strain were isolated. Line A integration site is in an intronic sequence of an autosomal translation regulator and line B integration site is in an intronic sequence of an autosomal trypsin enzyme. 30 Transgenic males from each line were crossed to 30 wild type females that were allowed to lay individually and fertility and sex distortion were measured and compared to a wildtype control cross. No significant difference has been highlighted in either clutch size or hatching rate (p value=0.0506, Kruskal-Wallis test). Whereas, when sexing a sample of pupae line A resulted in a sex bias of 72.9% (m=151, f=56) and line B of 99.3% (m=272, f=2).

**Conclusions** Sex distorter strategies can efficiently suppress caged wild-type populations, providing a powerful tool for vector control strategies. To further explore their potential, as a species-specific self-limiting control system, we are planning an introgression of the *An. arabiensis* transgenic line into *An. gambiae*, carrying out interspecific crosses able to escape hybrid incompatibility and measuring the capability of the distorter to target a sibling species and result in a reduction of the population.

# HIV-1 LATENCY: THE ROLE OF G-QUADRUPLEX STRUCTURE IN PROVIRAL TRANSCRIPTION OF LATENTLY INFECTED CELLS

# Ph.D. Student: Dr. Marianna TERRERI TUTOR: Prof. Sara RICHTER Ph.D. Course Molecular Medicine Curriculum "Biomedicine"

# Background

The Human Immunodeficiency virus (HIV) is the etiological agent of the Acquired immunodeficiency syndrome (AIDS). Although antiretroviral therapy reduces the viral load under detectable level, treatment interruption causes viral rebound because of virus persistence in latently infected cells. How HIV-1 establishes latency is not fully understood yet; however, it is well known that the long terminal repeat (LTR) promoter controls the expression of all viral genes. Given the reported presence of G-quadruplex (G4)-folding sequences in the LTR promoter of the HIV-1 provirus and their involvement in transcriptional activation *in vitro*, we here investigated the role of LTR G4s and its interactors in HIV-1 latency and reactivation.

#### **Material and Methods**

We employed J-Lat Tat-GFP and J-Lat full length cell lines, a valuable cell model for studying HIV-1 latency. The green fluorescent protein (GFP) gene downstream the LTR promoter and the use of latency reversing agents (LRAs) allowed us to isolate the transcriptionally silenced proviruses from those transcriptionally active by fluorescence-activated cell sorting (FACS). We next analysed the two cell populations (GFP-, GFP+) separately and compared LTR G4 folding and the presence of previously reported LTR interactors (nucleolin, SP1) in the two transcriptionally different cell populations by ChIP-qPCR. Next, we investigated the effect of nucleolin silencing on the activity of the LTR promoter.

#### Results

Through ChIP-qPCR experiments, herein for the first time we demonstrated that LTR G4s are folded when the promoter is in the latent state. We also showed that nucleolin, previously reported to stabilise LTR G4s and inhibit transcription, binds the LTR G4s in the latent state, whereas the transcription factor SP1 binds the LTR promoter in the active state, leading to transcription of the downstream genes. Since nucleolin was found to be an important player in the balance between active and inactive LTR promoter states, we evaluated the effect of nucleolin silencing on LTR promoter activity. At the highest concentration of anti-nucleolin siRNA, we observed an increase in GFP production, demonstrating that the reduction of nucleolin is associated with the reactivation of the LTR promoter. Finally, we investigated whether the results obtained in the cell models, were recapitulated also in vivo in Peripheral Blood Mononuclear Cells (PBMCs) isolated from patients. **Conclusions** 

# Conclusions

In conclusion, we uncovered a novel mechanism by which G4s stabilised by nucleolin inhibit HIV-1 transcription, whereas SP1 is mainly bound to the LTR in the active state. Furthermore, nucleolin depletion reactivated the LTR promoter. Taken together these results represent a step forward in the understanding of the HIV-1 latency mechanism and a possible target for the development of drug that could prevent virus reactivation from infected cells.

# A SIMULATION-BASED METHOD TO INFORM SEROSURVEY DESIGN TO ESTIMATE DENGUE FORCE OF INFECTION USING EXISTING BLOOD SAMPLES

# Ph.D. Student: Dr. Anna VICCO TUTOR: Dr. Claudia DEL VECCHIO – CO-TUTOR: Dr. Ilaria DORIGATTI Ph.D. Course Molecular Medicine Curriculum "Biomedicine"

# Background

Limited knowledge exists on the extent of dengue virus circulation in Africa. Cross-sectional serological surveys provide the ideal data to investigate historical dengue transmission, to reconstruct the age-dependent immunity profile of a population, and to estimate transmission intensity, as measured by the force of infection (FOI). However, owing to limitations in capacity for arboviral disease surveillance, only 17 dengue serosurveys have been conducted in the African region to date.

A convenient strategy to overcome this limitation is to leverage existing blood samples, e.g., from previous serosurveys, by secondary testing for anti-dengue antibodies. The aim of this study was to develop a simulation-based method for identifying the optimal testing strategy to estimate dengue FOI when leveraging existing blood samples.

#### **Material and Methods**

We developed a novel simulation-based method which reduces the number of samples to test and determines the optimal age-distribution for obtaining FOI estimates, which have comparable accuracy to those that would be obtained by testing all available samples. The method involves the use of dengue FOI estimates from the first global dengue FOI map and of catalytic models to simulate the age-dependent seroprevalence profile of a population, and identifies the optimal testing scenario, among a range of alternative sampling methods, by comparing the FOI estimates obtained under each scenario.

#### Results

We discuss an example of the method being used to inform dengue seroprevalence studies currently being conducted in three cities in Ghana, utilising blood samples previously collected for SARS-CoV-2 surveillance, and show that the method can be used to reduce the sample sizes required for testing, without affecting the accuracy of FOI estimates. We also present novel preliminary and final FOI estimates for this country.

#### Conclusions

This study highlights how existing blood samples from cross-sectional serosurveys can be leveraged for dengue surveillance and provides a framework for generating new serological data to better understand historical dengue circulation, while reducing resource requirements. The method can be adopted to investigate the transmission intensity of other endemic diseases across transmission settings.

# HSV-1 INFECTION IN MOUSE ENTERIC NERVOUS SISTEM: A TRIGGER FOR ALZHEIMER'S DISEASE-LIKE NEURODEGENERATION HALLMARKS

Ph.D. Student: Dr. Veronica ZATTA TUTOR: Prof. Ignazio CASTAGLIUOLO – CO-TUTOR: Prof. Paola BRUN Ph.D. Course Molecular Medicine Curriculum "Biomedicine"

# **Background:**

Alzheimer's disease (AD) is a neurodegenerative disease that induce progressive cognitive impairment in patients. A growing body of evidence supports the link between AD onset and infectious agents: in this context the neurotropic Herpes simplex virus type 1 (HSV-1) is extremely attractive for several experimental and clinical observations. Multiple HSV-1 reactivations from latency are thought to contribute to neuronal dysfunction, thus leading to neurodegeneration.

# **Material and Methods:**

Our group established and characterized a mouse model of persistent HSV-1 infection (up to 10 weeks) in the enteric nervous system. To detect APP (Amyloid Precursor Protein) and  $\beta$ -amyloid accumulation, immunohistochemical staining of ileal Longitudinal Muscle/Myenteric Plexus (LMMP) was performed. Moreover, the expression of secretase and cytokine genes was assessed by qPCR analysis. Acetylcholine levels in the myenteric plexus were measured via HPLC. Furthermore, primary enteric neurons were isolated from LMMP: the presence of APP,  $\beta$ -amyloid and the hyperphosphorylated form of Tau was detected by immunofluorescence, while neuronal redox homeostasis was analysed exploiting fluorescent probes.

#### **Results:**

We observed a progressive APP and  $\beta$ -amyloid accumulation in LMMP in response to HSV-1 infection, along with s significant decrease in acetylcholine levels. In addition, HSV-1 persistent infection induces the overexpression of secretase genes along with IFN $\alpha$ , IFN $\beta$ , IL-1 $\beta$  and IL-6. Moreover, we found APP and  $\beta$ -amyloid accumulation and Tau hyperphosphorylation in enteric neurons isolated from infected mice. HSV-1 persistent infection also determines lipid peroxidation and an increased mitochondrial production of free radicals.

#### **Conclusions:**

Overall these data suggest that persistent HSV-1 infection in the enteric nervous system leads to the accumulation of several neurodegeneration hallmarks, further supporting the infectious hypothesis of AD.



Università degli Studi di Padova University of Padua PhD Courses Medical and Biomedical Sciences

# PhD COURSE "MOLECULAR MEDICINE" COORDINATOR: PROF. ARIANNA LOREGIAN

# Curriculum "REGENERATIVE MEDICINE"

# LACK OF COLLAGEN VI ALTERS THE STRUCTURE OF MYOTENDINOUS JUNCTION

Ph.D. Student: Dr. Loris RUSSO TUTOR: Prof. Matilde CESCON Ph.D. Course Molecular Medicine Curriculum "Regenerative Medicine"

### Background

Collagen VI (ColVI) is a ubiquitous component of the extracellular matrix (ECM). Its role in the musculoskeletal apparatus is well-established, as mutations affecting its production or secretion in the ECM cause human myopathies with a broad spectrum of symptoms and severity, namely Bethlem myopathy (BM), Ullrich congenital muscular dystrophy (UCMD) and myosclerosis myopathy (MM). Individuals carrying mutations affecting ColVI assembly or secretion display muscle weakness and tendon contractures, as well as skin defects. In the context of ColVI-deficient ECM, very little is known about the site where myofibers connect to the tendon ECM, the myotendinous junction (MTJ). The MTJ has a crucial role in the musculoskeletal apparatus, as this site is subjected to high tensional forces and shear stress, making it susceptible to injury. Since ColVI is a key component of both skeletal muscle and tendon ECM, this project aims at revealing its role in muscle-tendon physiology with a focus on the MTJ.

#### **Material and Methods**

We used the previously generated and characterized  $Col6a1^{-/-}$  mouse model (hereafter called ColVI KO), lacking the  $\alpha 1$ (VI) chain of ColVI, thus preventing its assembly and deposition within the ECM, displaying the key features of BM. Mice were sacrificed at the age of 3 months for all the experiments. Proteomic analysis and western blots (WB) were carried out on an MTJ-enriched portion of the diaphragm, while imaging was performed on both diaphragm and tibialis anterior muscle sections. The tibialis anterior muscle was used to test the mechanical properties of the MTJ. The ultrastructure of the diaphragm MTJ was evaluated through TEM analysis. Cell proliferation was detected *ex vivo* subsequently to EdU injection.

#### Results

Proteomic analysis and WB showed significant changes in the matrisome of ColVI KO MTJ mice. The remodelling of collagen and proteoglycan composition or assembly might alter the mechanical properties of the MTJ. Indeed, mechanical testing performed on ColVI KO tibialis anterior muscle showed higher tenacity at their MTJ. Proteomic analysis also revealed a possible stabilization of the myofiber cytoskeleton, as the abundance of actin cross-linking proteins increased while actin depolymerizing proteins decreased. The use of a fluorescent F-actin probe also highlighted increased F-actin at the myofiber tip insertion into the tendon ECM. Sarcolemmal ultrastructure at the MTJ was also altered in ColVI KO mice, as highlighted by transmission electron microscopy. Additionally, the abundance of multiple nuclear components was increased in ColVI KO MTJ, indicating higher cell density. This was supported by the count of total and EdU<sup>+</sup> nuclei by fluorescence microscopy, showing increased proliferation.

#### Conclusions

We provide for the first time a characterization of MTJ-specific alterations in the gold standard mouse model for ColVI-related human diseases. The MTJ defects observed upon lack of ColVI are expected to contribute to both tendon and muscle pathology so far described in ColVI-related myopathies, as this site acts as a key mediator of force transmission from the muscle to the bone. Once completed, this study will provide a new step in the complete understanding of ColVI-related musculoskeletal defects, with relevance for both clinicians and patients.

#### MAIT CELLS PROMOTE TISSUE REPAIR THROUGH VEGF

# Ph.D. Student: Dr. Katia SAYAF TUTOR: Prof. Francesco Paolo RUSSO – CO-TUTOR: Prof. Paul KLENERMAN Ph.D. Course Molecular Medicine Curriculum "Regenerative Medicine"

#### Background

Tissue resident lymphocytes help maintaining homeostasis through different processes including antimicrobial defence and tissue repair. Mucosal-associated invariant T (MAIT) cells are a prominent subset of unconventional T cells in barrier tissues, respond to microbial derived antigens and are involved in both processes. Both murine and human MAIT cells express transcriptional signatures associated with tissue repair, including different elements such as matrix remodelling proteins, anti-inflammatory cytokines, and growth factors such as VEGFA and PDGFB. While the impact of MAIT cells on tissue repair has been demonstrated in different models in vitro and in vivo, which factors exactly endow MAIT cells to exert repair functions and how these are regulated is less clear. Previous transcriptomic studies indicate a particular dependency on TCR-mediated signals, however cytokine-mediated signals are likely to play a key role as well, at least in certain settings. Hence, the aim of our study is to better understand the role of MAIT cells in tissue repair upon combined stimulation of TCR and cytokines.

#### **Material and Methods**

PBMCs and MAIT cells were isolated from peripheral blood of healthy donors and stimulated via their TCR (5-OPRU or plate-bound anti-CD3) or cytokines alone or in combination for 72h. Supernatants resulting from these in vitro cultures were used to quantify the expression of different growth factors using the LEGENDplex<sup>TM</sup> growth factor kit. MAIT supernatants with or without VEGFR2 blocking antibodies were used in wound-healing assays in Caco2 epithelial monolayers to functionally validate the tissue repair function and the importance of this specific tissue repair associated growth factors.

#### Results

Our findings suggested that PBMCs and MAIT cells activated with TCR+cytokines produced GMCSF, VEGFA, PDGFAA, PDGFBB, TGF $\alpha$ , and MCSF. Interestingly, we found that VEGFA production was significantly higher in MAIT compared to conventional activated CD8 and CD4 T cells. From our wound healing assay, the percentage of recovered area was higher when Caco2 cells had been treated with supernatants from activated MAIT cells than the unstimulated ones. In addition, we observed that this effect could be blocked by anti-VEGFR2.

#### Conclusions

We found that TCR dependent (5-OPRU or plate-bound anti-CD3) and independent (cytokines) signals synergistically contribute to a massive production of growth factors in PBMCs and sorted MAIT cells. Supernatants of activated MAIT cells accelerated area recovery in *in vitro* Caco2 wound healing assays with MAIT-derived VEGF production standing out among T cells. Blocking VEGFR2 in our wound healing assays cells negatively impacted area recovery, pointing towards a key role of the VEGF-VEGFR2 signalling axis in MAIT-mediated tissue repair.

#### ROLE OF YAP AND TAZ IN METASTATIC BREAST CANCER

Ph.D. Student: Dr. Ambela SULI TUTOR: Prof. Francesca ZANCONATO – CO-TUTOR: Prof. Stefano PICCOLO Ph.D. Course Molecular Medicine Curriculum "Regenerative Medicine"

#### Background

The identification of the transcriptional mechanisms executing deranged transcriptional programs in cancer cells is a key and poorly understood issue in tumor biology. Moreover, the transcriptional features of the metastatic phenotype are still undefined. Recent studies have highlighted the involvement of the related transcriptional coactivators YAP (Yes-associated protein) and TAZ (transcriptional coactivator with PDZ-binding motif) in metastasis formation. These proteins are a source of interest because they are involved in the crosstalk between cancer cells and the surrounding tumor microenvironment (TME). They display a dual mechanism of action: on the one hand, they boost the tumorigenic abilities of cancer cells (cell-autonomously) and, on the other, they can impact the TME through modeling the extracellular-matrix (ECM) and cytokines and by interactions with the stromal cells, i.e., cancer associated fibroblasts or immune cells (non-cell autonomously). Here we investigate the role of YAP/TAZ in the development of Breast Cancer Metastasis (mBC), the main cause of lethality in breast cancer patients. The aim is to answer the medical need for both prognostic markers of metastasis to identify high-risk patients, and for a specific therapy to prevent metastasis development and relapse.

#### **Material and Methods**

To understand the mechanisms behind metastasis formation we generated genetically modified cell lines exploiting the CRISPR/Cas9 technology. We exploited a mouse triple negative breast cancer cell line in which we performed the knockout of either YAP or TAZ. The resulting cell lines were challenged for *in vivo* viability and ability to form metastases after tail vein injection in syngeneic immunocompetent mice. The use of syngeneic models would allow studying not only the cell-autonomous functions of YAP/TAZ in metastatic cells, but also the potential ability of these factors to control the evasion of tumor cells from immune recognition.

Moreover, to study the requirement of the two genes in metastasis maintenance, the cells were engineered to conditionally knockout TAZ, exploiting the Cre/loxP system, in an established metastatic microenvironment.

#### Results

Edited cell lines displayed full viability features both *in vitro* and *in vivo* and retained their ability to seed and form a tumor nodule in a syngeneic immunocompetent mouse. However, the edited cell lines displayed impaired metastatic capacity in preferential distal BC sites, such as the lungs, suggesting a non-redundant role of YAP and TAZ in the metastatic microenvironment.

#### Conclusions

This work suggests a function of YAP and TAZ in determining the metastatic proclivity of mammary tumor cells. Importantly, the two genes might have independent functions. Future work will investigate the cellular and molecular mechanisms of YAP and TAZ in metastasis formation, as well as their function in established BC metastases.



**University of Padua PhD Courses Medical and Biomedical Sciences** 

# **PhD COURSE** "PHARMACOLOGICAL SCIENCES" **COORDINATOR: PROF. NICOLA FERRI**

**Curriculum** 

# **"PHARMACOLOGY, TOXICOLOGY AND** THERAPY"

#### THIOL REACTIVE PEG LINKERS FOR HIGH LOADING ADCs

# Ph.D. Student: Dr. Benedetta CAMPARA TUTOR: Prof. Sara DE MARTIN – CO-TUTOR: Prof. Gianfranco PASUT Ph.D. Course Pharmacological Sciences Curriculum "Pharmacology, Toxicology and Therapy"

Background A high drug to antibody ratio (DAR) represents a highly demanded attribute for antibody-drug conjugates (ADCs), because it increases the *in vitro* potency of the entire platform. However, most anticancer drugs used in clinics (e.g., maytansinoids, auristatins, etc.) are unsuitable for high DAR ADCs owing to their high hydrophobicity. In fact, such issue might affect the stability of the ADC, inducing aggregation phenomena, and impact the pharmacokinetic profile, resulting in a short clearance of the ADC. To overcome this issue, it has been found that the detrimental effects of payload hydrophobicity can be modulated through linker design. In this work we exploited the hydrophilicity of polyethylene-glycol (PEG) based linkers to offset the hydrophobicity of eight molecules of auristatin E (MMAE) linked to the eight interchain native cysteines of trastuzumab, an anti-HER2 antibody. The linkers were based on two discrete PEG chains, of different length, branching out from a single point in the structure of a linker containing a ValCit dipeptide for enzymatic-controlled drug release. In fact, we have previously observed that this pendant PEG conformation is able to shield high drug loads in lysine-linked ADCs. Here, three linkers bearing two PEG chains each with 4, 8 or 12 ethylene oxide units (hereafter referred to as PEG4, PEG8, PEG12, respectively) were compared to each other in terms of stability under stress conditions, in vitro cytotoxicity, in vivo pharmacokinetic and antitumor activity of the whole ADCs. The parental antibody trastuzumab and an in-house synthesized low DAR ADC based on ValCitMMAE moiety were used as references.

**Material and Methods** Trastuzumab was treated with TCEP to reduce all the four interchain disulfide bonds. The thiol of reduced cysteines were alkylated with the linker-MMAE moiety. The homogeneity of the conjugates was studied by native HIC analysis. SEC-UPLC and SDS-PAGE demonstrated the ADCs' physical stability under stress conditions (40°C, 60%RH for 4 weeks). In *vitro* potency was evaluated in three cancer cell lines: SKOV3 and SKBR3 (HER2+) and MDA-MB-231 (HER2-). Pharmacokinetic studies were performed in female BALB/c mice, and total antibody concentration was monitored over 28 days by an ELISA kit. *In vivo* antitumor activity was evaluated in SKOV-3 xenografted SCID mice over 30 days. The animals (n=3) were treated with ADCs at the dose of 2.5 mg/kg injected twice (days 0 and 15) and sacrificed at the end of the study.

**Results** HIC analysis revealed the high homogeneity of the synthesized ADCs, eluting as a major peak corresponding to the fully conjugated species (DAR8). Remarkably, stability study under stress conditions highlighted that the aggregates content decreases as the PEG length increases. When tested for the *in vitro* cytotoxicity study, the ADCs exhibited a IC<sub>50</sub> in the order of nanomolar in HER2+ cell lines, which suggests that the PEG length does not interfere with the release of the free MMAE by lysosomal enzymes. Pharmacokinetics studies suggested a clear relationship between PEG length and clearance *in vivo*. In fact, the *in vivo* clearance resulted reduced for the ADCs bearing long PEG chains (PEG8 and PEG12) which can shield the burdensome hydrophobicity of eight MMAE molecules. *In vivo* antitumor activity results correlated with the *in vivo* clearance of the ADCs. In fact, the highest antitumor activity was observed for the ADCs bearing PEG sufficient long to maximize the *in vivo* exposure.

**Conclusion** In this work, three different linkers based on hydrophilic PEG were exploited to enable the construction of homogeneous highly drug loaded ADCs. We found that PEG length is important to control the stability and the *in vivo* pharmacokinetic and antitumor activity profile of the ADC.

# CHEMICAL CHARACTERIZATION AND EVALUATION OF THE POTENTIAL CHOLESTEROL-LOWERING PROPERTIES OF *CITRUS BERGAMIA*

# Ph.D. Student: Dr. Irene FERRARESE TUTOR: Prof. Nicola FERRI Ph.D. Course Pharmacological Sciences Curriculum "Pharmacology, Toxicology and Therapy"

**Background:** Bergamot (*Citrus bergamia* Risso et Poiteau) extracts have been studied for the management of hypercholesterolemia disorders. Up to now limited information is available concerning the activity of its main phytoconstituents towards the main targets of the cholesterol homeostasis. The effects peel extract and isolated constituents, namely glycosidic and non-glycosidic flavonoids, one coumarin and one limonoid on the low-density lipoprotein receptor (LDLR) and proprotein convertase subtilisin/kexin type 9 (PCSK9) were evaluated by using cultured HuH7 cell line. Furthermore, for the first time the effects of bergamot peel extract were studied to describe a potential hypolipidemic action.

**Material and Methods:** *In vitro* assays were performed using a Huh7 human hepatocarcinoma cell line, the experimental conditions used were 24h of incubation, MEM with 0.4% FBS. On the other hand, bergamot constituents were isolated extract using a preparative HPLC system. The extract was characterized by HPLC-DAD-MS analysis.

**Results:** Considering the thirteen isolated compounds, results revealed that naringenin-7-*O*-rutinoside (NA-rut) and apigenin-6,8-*C*-glicoside induced the expression of the LDLR while no effect was observed on PCSK9. However, hesperetin (HE) and its derivatives, hesperetin-7-*O*-glucoside and hesperetin-7-*O*-neohesperidoside (HE-glu, HE-neo) and eriodictyol (ER) showed a statin-like effect since a significant increase of both LDLR and PCSK9 expression were detected. Furthermore, bergamot peel extract (BE) firstly demonstrated a significant reduction of PCSK9 expression, indicating a potential adjuvant action to statins. BE, HE-neo, and NA-rut reduced intracellular sterols and the expression of PCSK9 transcription factor HNF1- $\alpha$ . BE also significantly improved the LDL uptake in Huh7 cells.

**Conclusions:** Based on the present data, bergamot peel constituents can play a role in the management of hypercholesterolemia, on one hand they may produce an adjuvant action in combination with statins, while on the other hand they may have a statin-like effect. Additionally, BE may be a good candidate as an adjuvant to statins action.

# REVIEW OF SOMATIC READ SIMULATORS: A COMBINATION OF THEIR ALGORITHMS GENERATES REALISTIC TUMORAL SAMPLES FOR SOMATIC VARIANT CALLING VALIDATION

# Ph.D. Student: Dr. Enidia HAZIZAJ TUTOR: Prof. Nicola FERRI Ph.D. Course Pharmacological Sciences Curriculum "Pharmacology, Toxicology and Therapy"

#### Background

In the past few years, remarkable progress has been made in developing and optimizing bioinformatic pipelines for variant calling. Improving mutation detection is crucial for personalized medicine both in terms of prevention and the development of therapies. While germline variant calling is almost clinically consolidated, somatic variant calling continues to be challenging due to many reasons: sparsity of somatic mutations, clonality and contamination of cancer samples, lack of matched normal samples, presence of complex mutational patterns, structural variants and chromosome-wide aneuploidies in tumoral genomes, are just some of the difficulties which are added to the technological limits of the main sequencing platforms. The optimization of variant calling in tumoral genomes is crucial for the correct detection of highly pathogenic driver mutations with low allele frequency. For these reasons, validation of somatic calling pipelines requires a reliable gold standard that should take into account tumoral variability in terms of interpatient variation intra-patient variation, inter-tumor variation, and intra-tumor variation. However, currently, such an extensive and fully characterized dataset of tumoral genomes for benchmarking of variant callers does not exist. Typical approaches used to create a validated truth set of somatic variants include variant calles confirmation through high-coverage NGS experiments, concordance of multiple variant callers, or generation of synthetic data. In this work, we focused on in silico data generation.

#### **Material and Methods**

Nine simulators have been deeply analyzed in terms of completeness and flexibility in parameters' control. We assessed their ability to control variant's features such as type, number, position, length, content and zygosity. We considered the following variant's types: Single Nucleotide Polymorphisms (SNPs), insertions (INS), deletions (DEL), duplications (DUP), inversions (INV) and translocations (TRA). Moreover, we ensured the user could somehow consider sample clonality and we checked whether the simulator could emulate sequencing error profiles or learn them from real samples. As no simulator, taken alone, was able to provide fully characterized tumoral samples, we combined the two best performing simulators: an improved version of SVEngine and Synggen. SVEngine is the most complete simulator from the biological point of view, while Synngen is the only simulator with an ad-hoc built-in read simulator that provides a reliable framework for the modeling of systematic sequencing errors. In order to obtain biologically realistic simulations, we mined statistical information about somatic variants' counts, lengths and positions from COSMIC and TCGA databases, focusing on the main types of mutations in order to create cancer-specific pre-sets for realistic and reliable cancer data generation.

#### Results

Each simulator has its strengths and weaknesses in mimicking technical and biological characteristics of real data. The above analysis showed that the simulator that mimic variant complexity more closely is SVEngine, as it allows the user to define each variant feature for each individual variant, together with the desired clonal tree architecture. While, the simulator that better simulates real data technical characteristics is Synggen as it overcomes the other read simulators by combining three different models for base qualities, systematic errors and read depth.

#### Conclusions

In this work, after performing an extensive analysis of nine somatic sample simulators, we built a simulation pipeline by combining two simulators and extending their functionalities, with the goal to generate both biologically and technically realistic tumoral genomes that can be used to validate variant calling pipelines. Also, we statistically characterized somatic variants from COSMIC and TCGA databases building customised pre-sets for biologically reliable simulations. Our simulation pipeline and presets allow the creation of fully characterized tumoral genomes that constitute an important resource for validation of somatic variant calling pipelines.

# SCHNIDER AND ELEVELD MODELS FOR PROPOFOL TARGET CONTROLLED INFUSION ANESTHESIA: A CLINICAL COMPARISON

Ph.D. Student: Dr. Federico LINASSI TUTOR: Prof. Michele CARRON Ph.D. Course Pharmacological Sciences Curriculum "Pharmacology, Toxicology and Therapy"

#### **Background:**

Various pharmacokinetic/pharmacodynamic (PK/PD) models have been developed to accurately dose propofol administration during Total Intravenous Anesthesia with Target Controlled Infusion (TIVA-TCI). We aim to clinically compare the performance of the Schnider and the new and general-purpose Eleveld PK/PD models during TIVA-TCI.

#### **Methods:**

We conducted an observational, prospective, single-center study enrolling 78 adult (<65 years) and elderly ( $\geq$ 65 years) women undergoing breast surgery with Propofol-remifentanil TIVA-TCI-guided by the bispectral index (BIS) for depth of anesthesia monitoring (target value 40–60) and surgical plethysmographic index (SPI) for antinociception monitoring (target value 20–50) without neuromuscular blockade. Concentration at the effect-site of propofol (CeP) at loss of responsiveness (LoR), during anesthesia maintenance (MA), and at return of responsiveness (RoR), duration of surgery and anesthesia (min), time to RoR (min), propofol total dose (mg), deepening of anesthesia events (DAEs), burst suppression events (BSEs), light anesthesia events (LAEs) and unwanted spontaneous responsiveness events (USREs) were considered to compare the 2 PK/PD models.

#### **Results:**

Patients undergoing BIS-SPI-guided TIVA-TCI with the Eleveld PK/PD model showed a lower CeP at LoR (1.7 [1.36–2.25] vs. 3.60 [3.00–4.18], p<0.001), higher CePMA (2.80 [2.55–3.40] vs. 2.30 [1.80–2.50], p<0.001) and at RoR (1.48 [1.08–1.80] vs. 0.64 [0.55–0.81], p<0.001) than with the Schnider PK/PD model. Anesthetic hysteresis was observed only in the Schnider PK/PD model group (p<0.001). DAEs (69.2% vs. 30.8%, p=0.001) and BSEs (28.2% vs 5.1%, p=0.013) were more frequent with the Eleveld PK/PD model than with the Schnider PK/PD model in the general patient population. DAEs (63.2% vs. 27.3%, p=0.030) and BSEs (31.6% vs 4.5%, p=0.036) were more frequent with the Eleveld PK/PD model than with the Schnider PK/PD model in the elderly.

#### **Conclusions:**

The Schnider and Eleveld PK/PD models impact CePs differently. A greater incidence of DAEs and BSEs in the elderly suggests more attention is necessary in this group of patients undergoing BIS-SPI-guided TIVA-TCI with the Eleveld PK/PD than with the Schnider model.



Università degli Studi di Padova University of Padua PhD Courses Medical and Biomedical Sciences

# PhD COURSE "TRANSLATIONAL SPECIALISTIC MEDICINE «G.B. MORGAGNI»"

**COORDINATOR: PROF. ANNALISA ANGELINI** 

Curriculum "BIOSTATISTICS AND CLINIC EPIDEMIOLOGY"

### MACHINE LEARNING FOR OMICS DATA ANALYSIS IN NEUROSCIENCE (GWAS FOR DMD)

Ph.D. Student: Dr. Sara AHSANI-NASAB TUTOR: Prof. Dario GREGORI - CO-TUTOR: Dr. Luca VEDOVELLI Ph.D. Course Translational Specialist Medicine "G. B. Morgagni" Curriculum "Biostatistics and Clinical Epidemiology"

#### Background

Duchenne Muscular Dystrophy (DMD) is a devastating genetic disorder characterized by progressive muscle degeneration and weakness, ultimately leading to loss of ambulation. The age at which ambulation is lost varies widely among DMD patients, suggesting a complex interplay of genetic factors influencing disease progression. Genome-Wide Association Studies (GWAS) have been valuable in identifying genetic variants associated to DMD. However, the complex nature of DMD necessitates advanced analytical methods to unravel its underlying genetic architecture. In this research project, we aim to benchmark machine learning techniques and employ them to enhance the detection of genetic variants associated with age-at-loss of ambulation in DMD patients.

In this research, we also employ multilevel modelling techniques to recognise genetic associations with age-at-loss of ambulation in DMD patients while considering the influence of multiple neuromuscular centres.

#### **Material and Methods**

We employed a collective GWAS dataset comprising genetic data including single nucleotide variants (SNVs) from a large cohort of approximately 680 DMD patients with diverse clinical profiles, from 14 academic neuromuscular centres across Italy.

Leveraging state-of-the-art machine learning algorithms, including random forests, support vector machines, and ensemble methods, we constructed predictive models to identify genetic markers that correlate with the age of ambulation loss. These models integrated genetic variants, clinical data, and potentially relevant covariates, offering a comprehensive perspective on the determinants of disease progression. Our goal was to determine if there were some SNVs associated with the time of loss of ambulation (i.e., the time to which the patient stopped walking).

To explain hierarchical and longitudinal structure of our dataset and account for the potential random effect of centres, we developed a 2-level mixed-effects survival model considering the SNV-based genetic relationship among patients of each individual centre.

#### **Results and Conclusions**

The fusion of advanced machine learning methods with GWAS data offers a powerful tool for unravelling complex genetic associations, thereby advancing our understanding of DMD pathogenesis. We found that among the millions of SNVs analysed, only a few of them were longitudinally associated with the outcome (loss of ambulation) and the results are being validated with wet-lab techniques. The findings of this research project will shed light on the genetic variants governing the timing of ambulation loss in DMD patients.

# DETERMINANTS OF PFOA SERUM HALF-LIFE AFTER END OF EXPOSURE: A LONGITUDINAL STUDY ON HIGHLY EXPOSED SUBJECTS IN THE VENETO REGION

# Ph.D. Student: Dr. Erich BATZELLA TUTOR: Prof. Cristina CANOVA – CO-TUTOR: Prof. Dolores CATELAN Ph.D. Course Translational Specialist Medicine "G. B. Morgagni" Curriculum "Biostatistics and Clinical Epidemiology"

#### Background

Perfluoroalkyl substances (PFAS) are widely used, ubiquitous and highly persistent man-made chemicals. Groundwater of a vast area of the Veneto Region (North-Eastern Italy) was found to be contaminated by PFAS from a manufacturing plant active since the late 1960s. As a result, residents were exposed to PFAS through drinking water until autumn 2013, mainly to perfluorooctanoic acid (PFOA). The aim of the present study was to estimate the rates of decline in serum PFOA, and their corresponding serum half-lives, while characterizing their determinants.

#### **Material and Methods**

We investigated 5,860 subjects aged more than 14 years who enrolled in the second surveillance wave of the Regional health surveillance program. Two blood samples were collected between January 2017 and December 2022 (average time between measurements 4 years). Serum PFOA excretion rates and half-lives were estimated based on linear mixed effect models, modelling subject-specific serum PFOA concentrations over time and correcting for background concentrations. For modelling determinants of half-life (age, sex, BMI, smoking-habit, alcohol consumption, and eGFR), we added interaction terms between each covariate and the elapsed time between the two measurements. PFOS and PFHxS apparent half-lives were also estimated. All analyses were stratified by sex.

#### Results

Median initial serum concentrations of PFOA was 49 ng/mL (range 0.5-1090), with a median reduction of 62.45%. The mean estimated PFOA half-life was 2.42 years (95%CI: 2.38;2.45), shorter in women (2.09, 95%CI: 2.06;2.13) compared to men (2.88, 95%CI: 2.81;2.94). Half-lives varied when stratified by some contributing factors, with faster excretion rates in non-smokers and non-alcohol drinkers (especially in males).

#### Conclusions

This study, the largest on PFOA half-life, provides precise estimates in young adults whose exposure via drinking water has largely ceased. For other PFAS longer half-lives than reported in other studies can be explained by some ongoing exposure to PFAS via other routes.

#### SOCIAL MEDIA MINING FOR FOOD SAFETY SURVEILLANCE

Ph.D. Student: Dr. Silvano SALARIS TUTOR: Prof. Dario GREGORI – CO-TUTOR: Prof. Corrado LANERA Ph.D. Course Translational Specialist Medicine "G. B. Morgagni" Curriculum "Biostatistics and Clinical Epidemiology"

#### Background

Foodborne diseases are a significant health concern, impacting millions globally each year. The effects of these diseases can vary from mild symptoms to critical health issues, leading to hospital stays and sometimes fatalities. Conventional approaches to identifying and addressing these illnesses typically involve official reporting systems, lab analyses, and occasional checks, but these methods can have limitations in their spread, speed, and efficacy.

However, the rise of online platforms, social media, and sophisticated computational methods in recent years has paved the way for innovative strategies to monitor and handle foodborne diseases. These modern techniques could fundamentally change how we spot outbreaks, measure public reactions, and implement preventive actions. The project aims to develop an automatic system for early signaling issues related to food safety in the food chain, using an integrated approach of big social media data mining and machine learning.

#### **Material and Methods**

In the first phase, Twitter data were retrieved and analyzed using the Twitter API for R as a coding language. Parameters were set in order to fetch tweets for a time period concerning the last 6 years (from 01/01/2017 to 01/07/2022), written in the Italian language, with keywords related to the 7 main foodborne pathogens (*campylobacter, listeria, staphylococcus, trichinella, E. coli, norovirus, salmonella*). For each pathogen keyword, we generated a frequency distribution of the associated tweets. Any data from peaks that exceeded the determined upper threshold value were then analyzed. This involved preprocessing the data, removing non-analytical characters from the text, and subsequently creating a word cloud. In the second phase data will be organized in a relational database using the SQL technology in order to achieve: data accuracy, easy access, data integrity, flexibility and feasibility for future modifications. An R based pipeline is designed to automatically retrieve new data and populate the database. Next steps will involve NLP (Natural Language Processing) models and possibly fine-tuned LLMs (Large Language Models) like GPT (Generative Pre-trained Transformer), which will be tested for the identification of a social media text related to a foodborne event. Finally, an online web application will be developed to provide access to the system and to provide summary insights.

#### Results

A total amount of 92.092 tweets were retrieved and 133 peaks were observed. Text mining techniques applied to the tweets included in each peak frequency returned specific information such as geographic areas, the vehicle of infection and food industries, allowing us to link the data to an alleged contamination or foodborne outbreak. 76 (~60%) generated word clouds were associated with well-documented cases of outbreaks or food contamination, 55 word-clouds returned confused or not related information to foodborne diseases, and in 2 cases possible events were not found through online research.

#### Conclusions

Social media are becoming a valuable source to retrieve information even for health surveillance. Monitoring social data can be an alternative approach to detect and prevent foodborne hazards.

# COMPARISON OF BORROWING METHODS FOR THE INCORPORATION OF HISTORICAL DATA IN SINGLE ARM PHASE II CLINICAL TRIALS

Ph.D. Student: Dr. Sara URRU TUTOR: Prof. Paola BERCHIALLA – CO-TUTOR: Prof. Ileana BALDI Ph.D. Course Translational Specialist Medicine "G. B. Morgagni" Curriculum "Biostatistics and Clinical Epidemiology"

# Background

Over the last years, many efforts have been made in leveraging historical information in clinical trials. Bringing historical data into current trials allows for a more efficient design, smaller-sized studies or shorter duration and may potentially increase the relative amount of information on efficacy and safety. Several methods for combining historical information with current data were developed.

# Material and Methods

This work aims to illustrate and compare the latest methods of borrowing historical data through the simulation of a single arm phase II clinical trial in terms of power and type I error implications.

Specifically, we examined static and dynamic versions of the power prior method, incorporating overlapping coefficient and loss functions, and meta-analytic predictive priors. These methods were compared with standard and pooling approaches, in which none or all historical data are used, respectively. For the power prior integrated with overlapping coefficient two scenarios were considered: Scenario I, where historical and current covariates are generated from distributions with the same parameters and Scenario II, where the distribution parameters of current covariates are slightly different.

# Results

Standard and pooling approaches are the extreme cases, the former has the lowest type I error but the highest power, vice versa the latter has the highest power but the lowest type I error. Power prior and MAP had been the focus of this work. Different versions of power priors were considered to find a suitable value of  $\alpha$ . The dynamic approach with the discounting function offers a more precise  $\alpha$  estimate than the static approach; it does not require prior knowledge of the researcher about the data. The power prior integrated with propensity score allows to take into account differences both in the outcome and baseline covariates. The performances are better for Scenario I where baseline characteristics of current data are coming from the same distribution of those of historical data. The situation changes when applying the discounting function; it flats the differences between the two scenarios and results in a more conservatives operating characteristics which overlapped those of the power prior without the propensity score integration. MAP approach confirmed these results, in fact it showed comparable power and type I error with the power prior approach with the loss function.

# Conclusions

Overall, dynamic borrowing methods achieve lower type I error inflation than pooling. The power prior integrated with the overlapping coefficients allowed to measure the similarity of the subjects also considering their baseline characteristics and not only the event rate. The use of the discounting function to estimate  $\alpha$  allows to guarantee the similarity of historical information and current trial data. Bayesian and dynamic approaches are suitable for the incorporation of historical data in current trial and their integration with propensity score and discounting functions could pave the way for making borrowing a standard practice in clinical trials design and analysis.



University of Padua PhD Courses Medical and Biomedical Sciences

# PhD COURSE "TRANSLATIONAL SPECIALISTIC MEDICINE «G.B. MORGAGNI»" COORDINATOR: PROF. ANNALISA ANGELINI

COORDINATOR: PROF. ANNALISA ANGELINI

Curriculum "CARDIOVASCULAR SCIENCES"

# MEMBRANE-SENSING-PEPTIDE APPLICATION IN MULTIPARAMETRIC FLOW CYTOMETRY ASSAY: NEW DIAGNOSTIC PLATFORM FOR CARDIAC ALLOGRAFT REJECTION MONITORING

Ph.D. Student: Dr. Ilaria BARISON

TUTOR: Prof. Annalisa ANGELINI– CO-TUTOR: Prof. Lucio BARILE Cotutelle between Università degli Studi di Padova and Università della Svizzera Italiana Ph.D. Course Translational Specialistic Medicine "G.B. Morgagni" Curriculum "Cardiovascular Sciences" and Ph.D. Course Biomedical Sciences Curriculum "Cardiovascular Sciences"

#### Background

Acute cardiac allograft rejection is the main threat for patients in the first year post-transplantation. Therefore, during first-year follow-up, endomyocardial biopsies (EMBs) are routinely performed to monitor the graft status. In the last decades, many efforts were made to identify new biomarkers as companion tools for EMBs, to increase the ability to predict rejections. Several groups investigated the role of Extracellular Vesicles (EVs) in post-cardiac transplant follow-up, demonstrating that EV surface antigens and cargo differ in patients with rejection compared to patients with no rejection. However, due to high variability in isolation, characterization, and lack of standardized methods, it is challenging to compare results across studies and apply research findings to clinical practice. This study aimed to examine the feasibility of incorporating membrane sensing peptide (MSP) into the flow-cytometer workflow for unbiased capture and surface antigen profiling of EVs and validate the diagnostic platform using blood samples from heart-transplanted patients.

#### **Material and Methods**

We conjugated MSP on Ni-NTA beads to perform EV capture in 136 transplanted patients' plasma samples. EVs were analyzed using multiparametric flow cytometry, evaluating the expression of different inflammatory markers known to be upregulated in subjects experiencing acute cellular rejection (ACR).

# Results

We evaluated the efficiency of EV isolation by measuring the level of expression and distribution trend of tetraspanins (CD9, CD63, and CD81) and verified that these results were consistently congruent between MSP technology and state-of-the-art bead-based assay (p-value <0.001). Furthermore, we found that specific antigens, such as CD2, CD49e, HLA-I, CD3, and CD8, were overexpressed onto EVs' surface derived from rejecting patients compared to control subjects. Among these markers, the assay was able to distinguish no rejection from different grades of ACR: CD3 can discriminate between R0 vs R1 and R0 vs R3 (p< 0.001), and R0 vs R2 (p<0.01); CD8 to discriminate between R0 vs R1 and R0 vs R2 (p<0.01), and R0 vs R3 (p<0.001).

# Conclusions

Our data show that MSP functionalized beads can be used to capture and isolate EVs from the serum and plasma of transplanted patients with high specificity, minimizing the co-precipitation of contaminants. Moreover, this technology can be implemented in high-throughput multiparametric flow cytometry, resulting in a cost-effective and highly efficient diagnostic tool. Such assay represents a concrete and plausible diagnostic platform adaptable to different clinically relevant contexts, not only in heart-transplant monitoring.

# CRISES IN ANCIENT HUMAN POPULATIONS: PALAEOPATHOLOGICAL AND PALAEONUTRITIONAL STUDIES ON CLIMATIC, ENVIRONMENTAL, AND ECONOMIC CHANGES FOR FUTURE SUSTAINABLE FOOD MODELS

Ph.D. Student: Dr. Michael Allen BECK DE LOTTO TUTOR: Prof. Fabio ZAMPIERI – CO-TUTOR: Prof. Alberto ZANATTA Ph.D. Course Translational Specialistic Medicine "G.B. Morgagni" Curriculum "Cardiovascular Sciences"

#### Background

Through an interdisciplinary scientific study involving medicine, bioarchaeology and geochemistry, this PhD project aims to contribute to the development of a sustainable dietary model by analysing the diet and health status of an ancient skeletal sample.

#### **Material and Methods**

The project analyses individuals from the Picene necropolis of Matelica (MC), contemporary and related to North-Picene societies that underwent a significant socio-economic crisis in the 6<sup>th</sup> century BC. Their resilient response prompts us to study their traditional diet and health status as a potential key to understanding sustainable dietary patterns.

The initial phase of the research involves reconstructing the ancient diet using stable isotope ratios of C and N. Bone collagen reflects the isotopes of food during life, and carbon ratios  $({}^{13}C/{}^{12}C)$  could reveal plant sources and distinguish marine, freshwater, and terrestrial foods, while nitrogen ratios  $({}^{15}N/{}^{14}N)$  indicate protein sources and trophic levels. Collagen extraction occurs at the Institute for the Study of Mummies - EURAC Research in Bolzano, a partner in the project. Subsequently, mass spectrometry analyses are carried out at the Department of Geosciences of the University of Padua.

The second phase involves detailed histological and geochemical studies of tooth enamel. These techniques offer insights into maternal health and weaning methods. The thin sections are obtained at the Department of Geosciences of the University of Padua, while the analyses are in collaboration with the Department of Odontostomatological and Maxillofacial Sciences of the Sapienza University of Rome, within the framework of the ERC Starting Grant project 'MOTHERS'.

#### Results

A total of 145 human and 17 fauna samples were chosen for analysis. All of these samples were powdered, and, to date, collagen has been successfully extracted from 98 human samples. Of these, only two samples failed to meet the minimum required threshold for validation of analysis by mass spectrometry.

At the same time, a series of 17 thin sections of sub-adult teeth, both deciduous and permanent, was prepared.

# Conclusions

Regarding the project schedule, the collagen extraction is scheduled to be completed in the last quarter of this year, and then analysis by mass spectrometry will begin. Subsequently, in the first months of next year, the complete examination of the thin sections is planned.

Currently, the selected samples show good potential to achieve the expected results, while the project is increasing the Humanistic Medicine group's collaborations with other research institutes.

### A HUMAN CARDIAC BIOELETRONICS MODEL: AN ALTERNATIVE TO ANIMAL MODELS FOR CARDIOTOXICITY RISK PREDICTION

Ph.D. Student: Dr. Giacomo BERNAVA TUTOR: Prof. Laura IOP – CO-TUTOR: Prof. Emanuele COZZI Ph.D. Course Translational Specialistic Medicine "G.B. Morgagni" Curriculum "Cardiovascular Sciences"

# Background

A considerable number of drugs, including chemotherapics, antibiotics and antidepressants, was removed from the pharmaceutical market due to cardiotoxicity. Moreover, adverse drug reactions are a significant cause of morbidity and mortality worldwide and are often associated with various cardiovascular side effects, including disturbances in ventricular repolarization and QT interval, arrhythmias, bradycardia, tachycardia, decreases in left ventricular ejection fraction, and congestive heart failure. Preclinical evaluation of drug cardiotoxicity has used animal models, which tend to be expensive, low throughput, and have limitations as not ever faithfully reflect the human pathophysiology, while current two-dimensional cellular models revealed to be not sufficient and specific. The aim of this study is to develop an efficient predictive model for drug cardiotoxicity, able to mimic the morphological, cellular, and electrophysiological complexity of the intact adult human heart, in order to study cardiotoxicity effect at both molecular and physiological levels.

#### **Material and Methods**

In order to advance a robust biolectronic model, an automated platform was developed to generate a three-dimensional, bioengineered replica of human myocardial tissue. Starting from fresh porcine hearts, cardiac specimens were isolated from left atrium and ventricle using biopsy puncher and sectioned with vibratome. Then, these tissue samples were decellularized through a novel, serial decellularization treatment based on osmotic shock and detergents. For a standardized removal of cardiac cells and non-ECM proteins, tissue specimens were submitted to an automated, dynamic decellularization with different perfusion devices. Such differently obtained scaffolds were analyzed for decellularization effectiveness by DNA quantification, histology, histochemistry, and immunofluorescence to evaluate cell removal and extracellular matrix integrity. Moreover, they were tested for cytocompatibility with human mesenchymal stem cells to assess possible proliferative or apoptotic effects.

#### Results

With respect to the standard decellularization protocol characterized by mild agitation, results based on the automated, dynamic treatments have shown a superior ability to obtain acellular, biocompatible scaffolds in terms of cell elements' removal and extracellular matrix preservation, as well as time- and cost-effectiveness. Indeed, these decellularized scaffolds allow for cell penetration, adhesion, and survival, thanks ECM microstructure integrity and preservation.

#### Conclusions

Further experiments will be focused on generating functional bioengineered myocardial tissues with cardiovascular progenitors derived from the differentiation of human induced pluripotent stem cells. The validation of these bioelectronic platforms will be performed with drugs with known cardiotoxic effect.

#### PROSTHESIS-PATIENT MISMATCH AFTER SURGICAL AORTIC VALVE REPLACEMENT WITH THREE DIFFERENT BIOPROSTHESES

Ph.D. Student: Dr. Giorgia CIBIN TUTOR: Prof. Augusto D'ONOFRIO – CO-TUTOR: Dr. Chiara TESSARI Ph.D. Course Translational Specialistic Medicine "G.B. Morgagni" Curriculum "Cardiovascular Sciences"

# Background

Aim of this retrospective single-center study was to compare incidence and clinical impact of measured prosthesis-patient mismatch (PPMm) versus predicted PPM (PPMp) after surgical aortic valve replacement (SAVR) with three different bioprostheses. Furthermore, we aimed at evaluating reliability of PPMp in identifying patients with postoperative actual PPM.

#### **Material and Methods**

We analyzed data of all consecutive patients who underwent SAVR with Magna Ease, Inspiris Resilia and Intuity bioprostheses (Edwards Lifesciences, Irvine, CA) at our institution from 2016 until 2022. PPM was defined if EOAi  $\leq$ 0.85 cm2/m2. PPMm was determined by institutional echo lab measured EOAi on discharge day echocardiogram. PPMp was assessed using reference values for each valve model and size indexed to BSA based on height, weight, prosthesis type and size. For the overall population and for the three valve types we also evaluated sensitivity, specificity, positive predicted value, negative predicted value and accuracy of PPMp. Furthermore, consistency between PPMm and PPMp were evaluated according to prosthesis type, size, stent internal diameter (ID) and true ID. The clinical impact of PPMm and PPMp was evaluated calculating odds ratio (OR) for 30-day mortality by means of univariable logistic regression.

#### Results

During the study period a total of 1323 consecutive patients underwent SAVR at our institution. Complete hemodynamic data were available for 872 patients who represent the population of our study. Magna Ease, Inspiris Resilia and Intuity were implanted in: 446 (51.1%), 85 (9.7%) and 341 (39.1%) patients, respectively. The incidence of PPMp was 15.5%, 16.5% and 24% in Magna Ease, Inspiris Resilia and Intuity, respectively (p < 0.001). The incidence of PPMm was 22%, 20% and 10.3% in Magna Ease, Inspiris Resilia and Intuity, respectively (p < 0.001). The incidence of PPMm was 22%, 20% and 10.3% in Magna Ease, Inspiris Resilia and Intuity, respectively (p < 0.001) (Fig. 1). In 635 out of 872 cases (72.8%) PPMp was consistent with PPMm (Magna Ease: 321/446, 72%; Inspiris Resilia: 58/85, 68.2%; Intuity: 256/341, 75%). Overall, sensitivity, specificity, positive predicted value, negative predicted value and accuracy of PPMp were: 0.26, 0.83, 0.24, 0.84 and 0.73, respectively (Magna Ease: 0.21, 0.82, 0.3, 0.8 and 0.72; Inspiris Resilia: 0.11, 0.82, 0.14, 0.79 and 0.68; Intuity: 0.45, 0.78, 0.19, 0.93 and 0.75). Table 1 shows consistency and discordance between PPMp and PPMm according to prosthesis type, size, stent ID and true ID. PPMm was significantly associated with 30-day mortality (OR: 1.89; 95%CI: 1-13-3.07; p=0.012) while PPMp was not (OR: 1.01; 95%CI: 0.57-1.71; p=0.96).

# Conclusions

The incidence of PPMm and of PPMp was different among the three valve types. In particular, Intuity shows a significantly lower PPMm. Consistency between PPMp and PPMm was suboptimal especially in terms of sensitivity. Discordance between PPMp ad PPMm was more evident in smaller valve sizes. PPMm (but not PPMp) is significantly associated with 30-day mortality. A thorough knowledge of each valve type's hemodynamics and of the reliability of predicting PPM especially in patients receiving small valves is crucial in order to select the most appropriate valve substitute and surgical technique (e.g., annular enlargement).

#### LEFT VENTRICULAR ENDOMYOCARDIAL BIOPSY IN THE DIAGNOSTIC WORK-UP OF CARDIOMYOPATHIES

#### Ph.D. Student: Dr. Monica DE GASPARI TUTOR: Prof. Cristina BASSO – CO-TUTOR: Prof. Martina PERAZZOLO MARRA Ph.D. Course Translational Specialistic Medicine "G.B. Morgagni" Curriculum "Cardiovascular Sciences"

**Background**: Endomyocardial biopsy (EMB) is an invasive technique used to diagnose heart muscle diseases. It can be performed both on the right (RV) and left ventricle (LV). LV EMB is less common than RV EMB and data are scanty on its additional diagnostic value.

**Scope**: To evaluate the usefulness of LV EMB and biventricular (BIV) EMB and the correlations between the clinical features and the histologic alterations in patients from two referral cardiological centres performing a high number of LV EMB procedures.

**Material and Methods**: Patients who underwent either electroanatomic voltage mapping (EVM) or cardiac magnetic resonance (CMR) and LV EMB, with a clinical diagnosis of myocarditis, LV isolated scar, arrhythmogenic cardiomyopathy - ACM and dilated cardiomyopathy - DCM). Of each patient, a set of clinical data and histological features were collected and analysed to search for clinical and pathological correlations.

**Results**: Among the 116 consecutive patients (74.1% males, mean 43.7 years, range 16-74 years) who underwent LV EMBs, 2 (1.7%) did not present any alteration and 15 (12.9%) manifested only alterations of unclear significance. Fibrosis was identified in 76 (65.5%), fibro-fatty replacement in 11 (9.5%), endocardial fibrous thickening in 99 (85.3%), cardiomyopathic changes in 78 (67.2%). Myocarditis (corresponding to presence of inflammation and necrosis) was diagnosed in 4 (3.4%).

The presence of fibrosis correlated significantly with repolarisation changes (odds ratio 3.26) and LV dilation (odds ratio 3.10). Fibro-fatty substitution correlated significantly with episodes of VT or VF (odds ratio 5.77). The presence of cardiomyopathic changes correlated significantly with ejection fraction (EF) reduction (odds ratio 3.71), LV dilation (odds ratio 2.76), episodes of ventricular tachycardia (VT) or fibrillation (VF) (odds ratio 2.66) and positive EVM (odds ratio 2.56). The presence of cardiomyocyte vacuolisations correlated significantly with EF reduction (odds ratio 3.59), LV dilation (odds ratio 2.32) and episodes of VT or VF (odds ratio 2.65). Endocardial fibrous thickening correlated significantly with premature ventricular beats (PVB) at ECG Holter analysis (odds ratio 2.95) and with a positive EVM (5.94). There was no correlation between the presence of fibrosis on LV EMB and a positive EVM or LGE. When evaluating patients with fibrosis on LV EMB, the percentage of fibrosis was higher in those with a positive subendocardial or transmural LGE and in those with a positive unipolar EVM. All patients with histologically-confirmed myocarditis (n. 4, 3.4%) had a clinical suspicion of myocarditis. In patients with a diagnosis of ACM or DCM, histological changes were more prevalent (fibrosis, cardiomyopathic alterations and vacuolisations) than in patients with a diagnosis of myocarditis or LV isolated scar (for fibrosis p value=0.05; for cardiomyopathic alterations p value=0.1; for vacuolisations p value=0.26, cardiomyocytes mean diameter in patients with DCM significantly higher than in patients belonging to other clinical categories (22.9 µm vs 20.3 µm, p=0.008).

A specific histological diagnosis was achieved in 6 (2 lymphocytic myocarditis, 2 eosinophilic myocarditis, and 2 ACM). In 25 patients who underwent both RV and LV EMB, the latter showed histological changes not evident on RV EMB in 12 cases (48%), whereas in 8 (32% the same histological alterations were visible on both RV and LV EMB.

**Conclusions**: LV EMB can be useful to confirm the clinical diagnosis. The absence of correlation between fibrosis and EVM and between fibrosis and LGE might suggest that guided EMB does not increase the diagnostic yield due to the uncommon presence of transmural LGE. Clinicopathological correlations must be further investigated, especially regarding the impact of endocardial thickening and the presence of cardiomyopathic changes. According to our data, LV EMB is usually not specific for clinical categories but might help in the diagnostic work up.



University of Padua PhD Courses Medical and Biomedical Sciences

# PhD COURSE "TRANSLATIONAL SPECIALISTIC MEDICINE «G.B. MORGAGNI»"

**COORDINATOR: PROF. ANNALISA ANGELINI** 

Curriculum "CLINICAL AND TRANSLATIONAL NEUROSCIENCES"

# NATURAL HISTORY OF BECKER MUSCULAR DYSTROPHY: A RETROSPECTIVE MULTICENTER STUDY

Ph.D. Student: Dr. Domenico GORGOGLIONE TUTOR: Prof. Elena PEGORARO – CO-TUTOR: Prof. Luca BELLO Ph.D. Course Translational Specialistic Medicine "G.B. Morgagni" Curriculum "Clinical and Translational Neurosciences"

# Background

Becker muscular dystrophy (BMD) is an X-linked muscle disease caused by mutations in the *DMD* gene, encoding the dystrophin protein. The clinical picture of this progressive neuromuscular disease is variable, including myalgias, limb-girdle weakness leading to wheelchair dependency usually after the age of 16 years or isolated elevation of serum creatine kinase without overt muscle weakness.

To overcome the rarity of the disease an Italian Multicentre BMD study group has been established under the aegis of Telethon. The overarching goals of the project include the collection of retrospective and longitudinal data and DNA samples to describe the natural history of the disease. Leveraging on the collected clinical data in the first two years of the project will allow to perform a Whole Genome Association Study (GWAS) for the identification and characterization of genetic modifiers in BMD.

#### **Materials And Methods**

Retrospective data were collected from 948 patients followed by 18 Italian Neuromuscular Centres. Statistical methods were used to describe the cohort of patients by examining patients' demographics, main signs and symptoms at BMD onset, neuropsychiatric comorbidities, age at loss of ambulation (LoA), cardiac left ventricular ejection fraction (LVEF), pulmonary forced vital capacity (FVC) and the effect of glucocorticoid (GC) therapy. DMD mutations were collected, and disease milestones were analysed in specific DMD mutational groups.

#### Results

At the last assessment, 15.6% of patients had lost the ability to walk at a mean age of 32.33 years. The estimated median age at LoA was 69 years. The patients were further grouped according to the reading frame retention and mutational subtypes of DMD gene. Out-of-frame mutations (10%) (p<0.0001) and deletions in the exons 45-49 (p<0.0001) associated with earlier LoA, instead deletions in the exons 45-55 (p=0.029) correlated with later LoA. On average, LVEF% was 55.85% and FVC% was 91.73% in the entire cohort. Using LVEF%<55% and FVC%<50% as threshold measures, 29.97% and 2.93% of patients presented left ventricular impairment and respiratory involvement. Deletions in the exons 45-47 (p=0.023), 45-48 (p=0.013) or in the N-terminal domain (p=0.042) were linked to decreased left ventricular systolic function. Moreover, deletions in the exons 45-55 (p=0.023) were identified to induce a lowered risk of developing a pathological LVEF%.

#### Conclusion

Our results contribute to better describing the natural history of BMD. The knowledge of the natural history in subsets of BMD patients carrying homogenous *DMD* mutation will serve as an *in vivo* model for the identification of successful therapies in Duchenne muscular dystrophy.



University of Padua PhD Courses Medical and Biomedical Sciences

# PhD COURSE "TRANSLATIONAL SPECIALISTIC MEDICINE «G.B. MORGAGNI»"

**COORDINATOR: PROF. ANNALISA ANGELINI** 

Curriculum "ENDOCRINE AND METABOLIC SCIENCES"

#### CELL-SPECIFIC ORIGIN OF ONCOSTATIN M AND REGULATION OF HEMATOPOIETIC STEM/PROGENITOR CELL TRAFFIC

Ph.D. Student: Dr. Anna RODELLA TUTOR: Prof. Gian Paolo FADINI – CO-TUTOR: Prof. Angelo AVOGARO Ph.D. Course Translational Specialistic Medicine "G.B. Morgagni" Curriculum "Endocrine and Metabolic Sciences"

**Background**: Hematopoietic stem/progenitor cells (HSPCs) reside in the bone marrow (BM) niche where are released continuously into the circulation following a circadian rhythm. Circulating stem cells have a role in angiogenesis, vascular repair; in the treatment of cardiac and peripheral ischemia; they represent also a diagnostic and prognostic biomarker. The mobilization of HSPCs in the bloodstream is regulated by neural system, non-hematopoietic stromal compartment of BM and innate immune system. It was discovered that BM macrophages retain HSPCs in the BM by producing Oncostatin M (OSM) which acts as a molecular brake by inducing the mesenchymal stem cells (MSCs)-derived chemoattractant CXCL12. Moreover, it has been found that clearance of aged neutrophils decreases the production of CXCL12, increasing the release of HSPCs in the blood. However, we found that *in vitro* senescent neutrophils express more OSM than other immune cells, therefore we want to investigate if neutrophil-derived OSM may be implicated in the regulation of BM niche.

**Material and Methods**: We take blood and BM samples from wild-type and total body Osm<sup>-/-</sup> mice to analyse gene expression through real-time pcr and cytokines production through ELISA test. We make adoptive transfers of neutrophils through intravenously injection of aged wild-type neutrophils into Osm<sup>-/-</sup> recipients at Zt5 and then quantify HSPCs at Zt13. We deplete BM macrophages through intravenously injection of clodronate liposomes to eliminate the macrophages interference in the BM.

Results: Circadian rhythm of HSPCs has analysed and it has found that Osm<sup>-/-</sup> mice have a persistent elevated level of HSPCs during the entire day/night cycle due to the loss of OSM. So, we have investigated what is the principal source of HSPCs braking OSM since neutrophils have higher expression of Osm. Osm<sup>-/-</sup> mice have a preserved oscillation of aged neutrophils in the circulation and in the BM compartment. Both Osm<sup>-/-</sup> and wild-type neutrophils have the conserved molecular clock machinery. Moreover, we confirm that aged neutrophils can be engulfed by BM macrophages, but this phenomenon occurs rarely. We make adoptive transfer of wild-type aged neutrophils in wild-type mice but it doesn't increase the blood level of HSPCs, suggesting aged neutrophils clearance might not be the primary mechanism whereby neutrophils regulate BM niche. To test the role of neutrophil-derived OSM in regulating HSPCs level, we make adoptive transfer of OSM-producing wild-type aged neutrophils in Osm<sup>-/-</sup> mice: the neutrophils transfer doesn't blunt the elevated HSPCs level. So, to rule out that the phagocytosis of neutrophils don't interfere with the effect of neutrophil-derived OSM, we deplete BM macrophages. Treatment with clodronate liposomes suppress BM macrophages successfully but don't modify the HSPCs blood level, according to the fact that macrophage-derived OSM is the major regulator of HSPCs. Injection of wild-type neutrophils in macrophage-depleted Osm<sup>-/-</sup> recipients again fails to reduce circulating HSPCs.

**Conclusions**: The replenishment of OSM-producing neutrophils is insufficient to rescue the elevated HSPCs levels of Osm<sup>-/-</sup> mice, so we can suppose that, despite neutrophils are the major expressing immune cells of Osm, they are not the major source of OSM in the regulation of HSPCs niche. Not all OSM produced by immune cells regulating the BM niche is equal: not all OSM is capable to stimulate the production of CXCL12, retaining the HSPCs in the BM. Eventually, future therapies should turn to macrophages rather than neutrophils in the goal of targeting OSM to modulate HSPCs mobilization.



University of Padua PhD Courses Medical and Biomedical Sciences

# PhD COURSE "TRANSLATIONAL SPECIALISTIC MEDICINE «G.B. MORGAGNI»"

**COORDINATOR: PROF. ANNALISA ANGELINI** 

Curriculum "THORACIC AND PULMONARY SCIENCES"

#### MACROPHAGES-DERIVED FACTOR XIII LINKS COAGULATION TO INFLAMMATION IN COPD

#### Ph.D. Student: Dr Alvise CASARA TUTOR: Prof. Graziella TURATO – CO-TUTOR: Prof. Erica BAZZAN Ph.D. Course Translational Specialistic Medicine "G.B. Morgagni" Curriculum "Thoracic and Pulmonary Sciences"

**Background**: Chronic Obstructive Pulmonary Disease (COPD) is a chronic lung disease characterized by limitation of airflow that is not fully reversible, an abnormal inflammatory process and a subsequent adaptive immune response in the small airways and in the lung parenchyma that worsens with the progression of the disease. The coagulation system could be involved in the inflammatory process in the disease. Coagulation Factor XIII (FXIIIA), besides its role in haemostasis, is also expressed in immune-inflammatory cells such as macrophages and dendritic cells, modifying their activity in wound healing and inflammation. Therefore, FXIIIA found in alveolar macrophages (AM) and dendritic cells (DC) might be an inflammatory modifier in COPD. Aim of the present study is to investigate the expression of FXIIIA in AM and Langerin+ DC (DC-1) and their relation to the inflammatory response and disease progression in COPD.

**Materials and Methods:** In 47 surgical lungs, 36 from smokers (22 COPD and 14 no-COPD) and 11 from non-smokers we quantified by immunohistochemistry FXIIIA expression in AM and DC-1. To assess its possible relation with the inflammatory response we quantified CD8+Tcells and the expression of CXCR3, a marker of inflammatory infiltrate activation, in lung parenchyma and airways. Lung function was measured prior to surgery. In three cases from each group, confocal microscopy was performed to study the expression of FXIIIA in DC and the possible co-expression of FXIIIA and CXCR3 in AM.

**Results:** The percentage of AM expressing FXIII (%FXIII+AM) was higher in COPD than no-COPD [median(range) 75.5(27-98)% vs 45(22-97)%; p=0.05] and non-smokers [median(range) 75.5(27-98)% vs 20(0-50)%; p=0.001]. %FXIII+AM positively correlated with the number of DC-1 in peripheral airways (r=0.43; p<0.018). Of interest, the number of DC-1 in peripheral airways was higher in COPD than in no-COPD and non-smokers (p<0.05). Confocal microscopy showed that FXIIIA was abundantly expressed in DC-1 in COPD, but not in non-smokers, a finding not previously reported. Both %FXIII+AM and number of DC-1 in peripheral airways were positively correlated with the numbers of CD8+Tcells (r=0.49; p<0.001 and r=0.61; p<0.001, respectively) and CXCR3+ cells (r=0.32; p<0.05 and r=0.44; p<0.05, respectively) in alveolar walls. CD8+Tcells infiltration and CXCR3 expression in the lung were higher in COPD than in no-COPD. Both %FXIII+AM (r=-0.6; p=0.001) and DC-1 (r=-0.7; p=0.001) correlated inversely with FEV1.

**Conclusion:** FXIIIA, an important link between the extravascular coagulation cascade and inflammatory response, is significantly expressed in alveolar macrophages and dendritic cells of smokers with COPD, suggesting that it could play an important role in the adaptive inflammatory reaction characteristic of the disease.

**Other Projects**: During this second year of my PhD project I focalized on the study of the molecular basis of lung diseases, addressing the role of different pathogenetic mechanisms including the analysis of extracellular vesicles as possible modulators of the inflammatory response in the lung of COPD patients and in particular the possible role of Suppressor of Cytokine Signaling (SOCS) 3. A new upcoming project will investigate the possible role of FXIII in the modulation of the immune-inflammation in Idiopathic Pulmonary Fibrosis.

# **AUTHORS' INDEX**

| SURNAME AND NAME            | Tutor-Co-Tutor                                     | PAGE     |
|-----------------------------|----------------------------------------------------|----------|
| AHSANI-NASAB Sara           | Prof D GREGORI - CO-TUTOR: Dr L VEDOVELLI          | Page 105 |
| ARCIDIACONO Gaetano Paride  | Prof S GIANNINI                                    | page 49  |
| BADO Martina                | Prof E LAVEZZO                                     | page 81  |
| BARISON Ilaria              | Prof A ANGELINI- CO-TUTOR: Prof L BARILE           | page 111 |
| BATZELLA Erich              | Prof C CANOVA – CO-TUTOR: Prof D CATELAN           | page 106 |
| BECK DE LOTTO Michael Allen | Prof F ZAMPIERI – CO-TUTOR: Prof A ZANATTA         | page 112 |
| BERNAVA Giacomo             | Prof L IOP – CO-TUTOR: Prof E COZZI                | page 113 |
| BORTOLETTO Alessandro       | Prof. Marco BERGAMIN                               | page 33  |
| BRIGADOI Giulia             | Prof L DA DALT – CO-TUTOR: Dr D DONA'              | page 57  |
| BUCCIARELLI Linda           | Prof A BIFFI – CO-TUTOR: Dr V POLETTI              | page 58  |
| CAMPARA Benedetta           | Prof S DE MARTIN – CO-TUTOR: Prof G PASUT          | page 99  |
| CASARA Alvise               | Prof G TURATO – CO-TUTOR: Prof E BAZZAN            | page 127 |
| CASARIN Martina             | Prof F DAL MORO – CO-TUTOR: Dr A MORLACCO          | page 21  |
| CATTAPAN Irene              | Prof J D'HOOGE – CO-TUTOR: Prof G DI SALVO         | page 77  |
| CECCATO Jessica             | Prof C AGOSTINI – CO-TUTOR: Prof M RATTAZZI        | page 50  |
| CIBIN Giorgia               | Prof A D'ONOFRIO – CO-TUTOR: Dr C TESSARI          | page 114 |
| D'ACCARDIO Giulia           | Prof A ROSATO – CO-TUTOR: Dr E VIGOLO              | page 22  |
| DAL MOLIN Emanuela          | Prof L BARZON                                      | page 82  |
| DE GASPARI Monica           | Prof C BASSO – CO-TUTOR: Prof M PERAZZOLO<br>MARRA | page 115 |
| DEBIASI Giulia              | Dr G LOMBARDI – CO-TUTOR: Prof A BERTOLDO          | page 23  |
| DONATO Alice Cristina       | Prof P BRUN                                        | page 83  |
| DUCI Miriam                 | Dr F FASCETTI-LEON                                 | page 59  |
| FAGGIAN Sara                | Prof A ERMOLAO                                     | page 34  |
| FAVARO Jacopo               | Prof I TOLDO – CO-TUTOR: Prof S SARTORI            | page 60  |
| FERRARESE Irene             | Prof N Ferri                                       | page 100 |
| FICHERA Giulia              | Prof G BISOGNO - CO-TUTOR: Dr C GIRAUDO            | page 61  |
| FIETTA Anna                 | Prof E CIMETTA – CO-TUTOR: Prof B MOLON            | page 13  |
| FRIGO Elena                 | Prof P BERNARDI – CO-TUTOR: Dr M<br>BRISCHIGLIARO  | page 14  |
| FUMANELLI Jennifer          | Prof G DI SALVO – CO-TUTOR: Dr L LEONI             | page 62  |
| GASPAROTTO Michela          | Prof M ZEN - CO-TUTOR: Prof M GATTO                | page 53  |
| GENOVA Beatrice             | Prof A ROSATO – CO-TUTOR: Dr A DALLA PIETA'        | page 24  |
| GIACCHIN Giacomo            | Prof CF VISCOMI                                    | page 15  |

| GORGOGLIONE Domenico                     | Prof E PEGORARO – CO-TUTOR: Prof L BELLO    | page 119 |
|------------------------------------------|---------------------------------------------|----------|
| GUIDUCCI Silvia                          | Prof E BARALDI – CO-TUTOR: Dr A GALDERISI   | page 63  |
| GUTIERREZ DE RUBALCAVA<br>DOBLAS Joaquin | Prof C GIAQUINTO – CO-TUTOR: Prof S BRESSAN | page 78  |
| HAZIZAJ Enidia                           | Prof N FERRI                                | page 101 |
| ISPANO Emilio                            | Prof S TOPPO                                | page 84  |
| JAFARNEZHAD ANSARIHA                     | Prof D BASSO                                | page 25  |
| Fahimeh<br>KOHLSCHEEN Eva                | Prof GP ROSSI – CO-TUTOR: Prof T SECCIA     | page 9   |
| LIEVORE Nicole                           | Prof V TIKHONOFF                            | page 35  |
| LINASSI Federico                         | Prof M CARRON                               | page 102 |
| LONGO Giorgia                            | Prof M PIGAZZI – CO-TUTOR: Dr C TREGNAGO    | page 64  |
| MADDALENA Giulia                         | Dr S LONARDI - CO TUTOR Dr S KOPETZ         | page 26  |
| MANFREDA Lorenzo                         | Prof G VIOLA – CO-TUTOR: Dr R BORTOLOZZI    | page 65  |
| MANGINI Chiara                           | Prof S MONTAGNESE                           | page 45  |
| MARANGIO Asia                            | Prof M AGOSTINI                             | page 27  |
| MARCHIORO Chiara                         | Prof G VIOLA- CO-TUTOR: Dr E MARIOTTO       | page 66  |
| MENEGHELLI Marta                         | Prof E BARALDI – CO-TUTOR: Dr G VERLATO     | page 67  |
| MORBIDELLI Maria                         | Prof E PAPINI- CO-TUTOR: Prof R TAVANO      | page 16  |
| MORO Nicola                              | Prof M MONGILLO – CO-TUTOR: Prof T ZAGLIA   | page 17  |
| PADOVAN Marta                            | Dr G LOMBARDI                               | page 28  |
| PINTUS Giovanni                          | Prof GP ROSSI – CO-TUTOR: Prof T SECCIA     | page 10  |
| QUINTO Giulia                            | Prof R VETTOR – CO-TUTOR: Prof A ERMOLAO    | page 36  |
| REGGIANI Giulia                          | Prof R COLOMBATTI                           | page 68  |
| RODELLA Anna                             | Prof GP FADINI – CO-TUTOR: Prof A AVOGARO   | page 123 |
| ROSSI Bartolomeo                         | Prof A BIFFI – CO-TUTOR: Dr E VISCARDI      | page 69  |
| RUBIN Michela                            | Prof G COZZA – CO-TUTOR: Dr I ARTUSI        | page 85  |
| RUSSO Loris                              | Prof M CESCON                               | page 93  |
| SACCHI Diana                             | Prof M FASSAN – CO-TUTOR: Prof M GUIDO      | page 29  |
| SALARIS Silvano                          | Prof D GREGORI – CO-TUTOR: Prof C LANERA    | page 107 |
| SARTORI Anna                             | Prof A GALDERISI – CO-TUTOR: Prof P COGO    | page 70  |
| SAYAF Katia                              | Prof FP RUSSO – CO-TUTOR: Prof P KLENERMAN  | Page 94  |
| SULI Ambela                              | Prof F ZANCONATO – CO-TUTOR: Prof S PICCOLO | page 95  |
| TACCHETTO Elena                          | Prof E TREVISSON                            | page 71  |
| TANCREDI Giuditta                        | Prof I CASTAGLIUOLO - CO-TUTOR: Dr F        | page 86  |
| TERRERI Marianna                         | BERNARDINI<br>Prof S RICHTER                | page 87  |
|                                          |                                             |          |

| TOMMASIN Ludovica | Prof P BERNARDI – CO-TUTOR: Dr M CARRARO    | page 18  |
|-------------------|---------------------------------------------|----------|
| TONIAZZO Silvia   | Prof P SPINELLA                             | page 41  |
| TOSATO Anna       | Prof L MUSSOLIN – CO-TUTOR: Prof K BASSO    | page 72  |
| URRU Sara         | Prof P BERCHIALLA – CO-TUTOR: Prof I BALDI  | page 108 |
| VALENTINO Agata   | Prof L SALVIATI – CO-TUTOR: Prof MA DESBATS | page 73  |
| VECCHIATO Marco   | Prof A ERMOLAO                              | page 37  |
| VICCO Anna        | Dr C DEL VECCHIO – CO-TUTOR: Dr I DORIGATTI | page 88  |
| ZATTA Veronica    | Prof I CASTAGLIUOLO – CO-TUTOR: Prof P BRUN | page 89  |